OsloMet – Oslo Metropolitan University

Department of Civil Engineering & Energy Technology
Section of Civil Engineering

Master Program in Structural Engineering & Building Technology

MASTER THESIS

Effect of high dosage of steel fibers on mechanical properties of UHPFRC: Application of Response Surface Method	DATE:25-05-2022
	PAGES / ATTACHMENTS :103
AUTHOR(S) Aswathy Babu	SUPERVISOR(S) Mahdi Kioumarsi Katalin Vertes

IN COLLABORATION WITH	CONTACT PERSON

SUMMARY / SYNOPSIS

The master thesis herein described mainly focused on developing a statistical model using Response Surface Methodology (RSM) to predict the performance of ultra-high performance fiber reinforced concrete (UHPFRC). Furthermore, the mechanical properties of UHPFRC containing higher fiber dosage (2.5-4%) were also investigated through an experimental program. An accumulation of the results indicated that the addition of fibers has the potential to improve the compressive strength of UHPFRC, and it depends on fiber content. The influence of increased fiber content in flexural strength merits further research. The statistical model developed with RSM showed an excellent correlation between the factors and responses. This mathematical model can predict the compressive strength of UHPFRC. Therefore, this study establishes the efficiency of RSM as a statistical tool that enables early decision-making during practical applications.

KEYWORDS
UHPFRC
Response Surface Methodology
Mechanical properties

Acknowledgment

Abstract

Ultra-High-Performance Fiber Reinforced Concrete (UHPFRC) is a highly advanced cementitious composite material with improved mechanical properties and durability than conventional concrete. The development of UHPFRC has been considered one of the remarkable milestones in the construction field. This material enables structural engineers to design lightweight structures with self-compacting ability, excellent mechanical properties, and high durability.

There are several factors and design principles such as lower water to binder ratio (less than 0.2), size of aggregates (coarse aggregates are avoided), higher binder content, the addition of high range water reducing admixtures (HRWRA), and the presence of fibers that keeps UHPFRC with a denser packing order that results in excellent mechanical properties, durability, and enhanced ductility. Though several factors contribute to these superior qualities, the effect of each parameter or their interactions on the mechanical properties has not been studied extensively. There are several papers available that investigated the effect of individual parameters. Still, the multi-factor interaction effects and the relationship between the factors and the mechanical properties were not developed fully yet.

Considering this research gap, we considered investigating the effects of multiple factors on the compressive strength of UHPFRC and determining the most significant factors and the influence of multi-factor interaction based on experimental results and predictive models. Therefore, this master thesis has mainly focused on analyzing the effect of the factors; steel fiber content (F_v), silica fume content (S_f), and water to binder ratio(w/b) on the compressive strength (28th day) of UHPFRC with the application of the statistical tool, Response Surface Methodology (RSM). The experimental results of the compressive strength tested on 45 specimens were used as input data for the RSM analysis. Using the software Minitab, a statistical predictive model connecting the input parameters and the compressive strength (response) was developed through RSM analysis. This predictive model can predict the response for any combination of the factors considered. Moreover, the effect of each variable on the response and the effects due to multi-variable interactions could be justified using the graphs and 3D plots.

The thesis also explored the effects of a higher dosage of steel fiber reinforcement on the mechanical properties of UHPFRC by estimating the compressive and flexural strength through experimental work. The results showed that the higher dosages significantly contribute to the mechanical properties of UHPFRC. However, some of the properties need to be investigated further for more reliable conclusions.

Abstract...

Abbreviations

UHPC   =   Ultra high-performance Concrete

UHPFRC   =   Ultra high-performance fiber reinforced concrete

SFRC   =   Steel fiber reinforced concrete

HPC   =   High Performance Concrete

SCC   =   Self compacting Concrete

ACI   =   American Concrete Institute

ASTM   =   American Standard Test Method

RSM   =   Response Surface Methodology

DOE   =   Design of Experiments

CCD   =   Central Composite Design

BBD   =   Box-Behnken Design

SF   =   Silica Fume

SP   =   Superplasticizer

HRWRA   =   High range water reducing admixture

ITZ   =   Inter Transition Zone

FA   =   Fly ash

GGBFS   =   Ground granulated blast furnace slag

e-CO_2 =   Embodied CO_2

SCM   =   Supplementary cementitious material

w/b   =   Water to binder ratio

Contents

List Of figures

List of Tables

1 Introduction

Concrete has been considered one of the most widely used materials on earth, mainly due to its availability, low cost, long durability, and ability to sustain extreme weather conditions. Concrete became one of the most popular building materials since Portland cement was invented in 1824; concrete is essential to our communities because it is the only building material that cost-effectively delivers resilience, energy efficiency, strength, durability, and low maintenance. Moreover, it facilitates local production and is recyclable [1].

Concrete has played a vital role in building our civilization since before the Romans built the Pantheon, which is almost 2000 years old and still exists as a unique heritage, making the construction industry proud. Even though we live in the 21st century now, concrete unquestionably dominates the building industry by playing an essential role in building the communities, from residential buildings to public transport, dams, powerhouses, from unfathomably massive structures to stepping stones [1].

Concrete comprises four primary ingredients: water, sand (fine aggregate), gravel (coarse aggregate), and cement. The volumetric proportions of the normal concrete mixture are appropriately 15-25% water,10-20% cement, and 60-70% sand and gravel. The mix of these ingredients forms a paste that solidifies and hardens due to the reaction called 'hydration,' which occurs by reacting cement with water. The rate of hydration is dependent on the w/c ratio. The concrete is then shipped to the worksite, compacted, placed, and cured [2].

41% Gravel or Crushed Stone (Coarse Aggregate)

26% Sand (Fine aggregate)

16% Water

11% Portland cement

6% Air
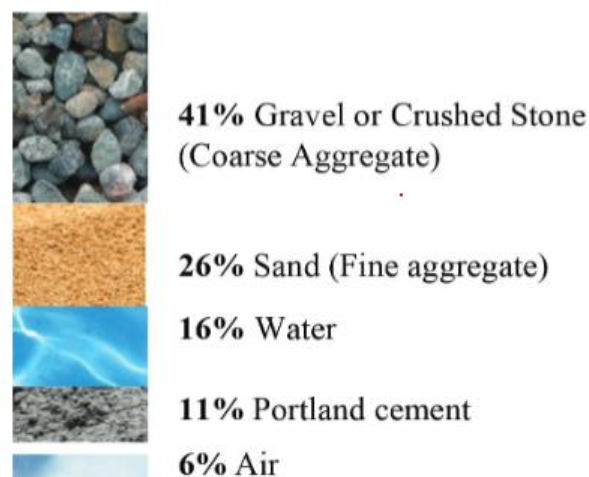
Figure 1.1:Typical volumetric proportions of basic ingredients of conventional concrete [[3]

As we discussed earlier, versatility is one of the significant characteristics of concrete; it allows for innovations. There are situations where conventional concrete's performance, in terms of its compressive strength or durability, is insufficient to meet the structural system's requirements to

ensure safety and comfort; the need to improve the ductility and compressive strength of concrete was an essential requirement. Thus, high-performance concrete was developed. According to American Concrete Institute(ACI), high-performance concrete can be defined as 'concrete meeting special combinations of performances and uniformity requirements that cannot always be accomplished routinely using conventional constituents of concrete and regular mixing, placing, and curing practices [4].

As now the construction industry faces many challenges in satisfying the needs of a changing world, they continue to work to evolve the production and use of cement and concrete to serve an even more significant contribution to development. UHPC (Ultra-High-Performance concrete) is considered one of the most significant and innovative concrete developed during the last two decades.

Ultra-high-performance concrete (UHPC) can be classified as a new class of concrete developed in the 1990s in France. UHPC possesses high compressive strength, usually 3-4 times the compressive strength of conventional concrete, and high durability due to the dense microstructure and fine materials. Ultra-High-Performance concrete permits the construction of light, strong, durable structures using less concrete and more efficiently. As the material has superior compressive and flexural properties, the need for passive reinforcement can be eliminated or reduced to a greater extent. UHPC can contribute to higher levels of durability and longer service life for buildings and structures. It is also regarded as self-healing concrete containing enormous cement [5].

The compressive strength of UHPC is greater than >150 MPa and sustained post cracking tensile strength is greater than 5 MPa. UHPC has a higher packing density and minimum voids. The high durability of UHPC is due to the dense microstructure and fine materials. The denser packing of ingredients in UHPC contributes to low porosity, high mechanical strength, im-permeability, and high durability. These superior characteristics of UHPC can contribute to durable structures and buildings with longer service life [6]. Extensive research has been conducted to develop advanced construction materials with outstanding mechanical properties. The high packing density of a particle is one of the key characteristic values to achieve a very dense microstructure of UHPC; thus, carefully adapting the measures for mixing the size of particles and gradation of the ingredients is highly important [7]. A denser mix always requires less water resulting in superior compressive strength and exceptional durability.

UHPC is often composed of cement, silica fume, quartz flour, fine quartz sand, and high range water reducing admixture (known as superplasticizer). A higher amount of cementitious material, fine sands, and very low water/cementitious material rate are the key strategies to be adopted while mixing

UHPC. A high dosage of HRWRA is used to achieve adequate rheological properties. The microscale silica fumes act as a filler between cement and fine sand to improve hydration and contribute to the increased density of the mix. Coarse aggregates are fully eliminated from the UHPC mixes to facilitate the microstructure and avoid forming voids. This provides homogeneity of the mixture. The water binder ratio for UHPC is generally lower than 0.25 and typically ranges between 0.16 and 0.20 [6].

UHPFRC is the Ultra-High-Performance Concrete with fiber reinforcement. As for the normal concrete, UHPC also exhibits a brittle failure mechanism during tension. Thus, the addition of steel fibers enhances the ductile behavior and bridges the cracking during the application of tensile loads. UHPC without fibers exhibits a direct tensile strength in the range of 7-10 MPa, which can be doubled with the addition of fibers in the mix [8]. The steel fibers contribute to enhanced tension and bonding strength, which provides enhanced post-cracking ductility instead of the usual brittle behavior. The fibers improve the tensile and flexural strength of concrete, while the contribution of fibers to the compressive strength is rather modest. The mix design of UHPFRC stands out with the key factors such as water binder ratio, size of aggregates, amount of cement, and the most significant difference from the UHPC is undoubtedly the presence of fibers. This design provides the UHPFRC with a denser packing order that contributes to the excellent mechanical properties, durability, and resistance to environmental impacts and enhanced ductility and reduction in brittleness [8].

Response Surface Methodology (RSM)is an effective experimental design technique popular in the research field over the last two decades for modeling and analyzing problems that have a response of interest influenced by several variables[9]. Even though RSM has been widely used to optimize several experimental processes, the concrete industry has not fully explored its applications. Previous research used RSM to optimize high-performance concrete mixtures for maximizing the compressive strength and minimum chloride permeability simultaneously. The feasibility of producing self-compacting UHPC mixtures with high flexural strength was also studied in previous studies [9]. However, limited papers analyzed the effect of influential parameters on the compressive strength of UHPFRC. Therefore, we intended to explore the impact of the three parameters such as 'steel fiber content (F_v)', 'silica fume content (S_f)' and 'water-binder ratio(w/b)' in optimizing the compressive strength of UHPFRC in this study.

As we intend to study the influence of the parameters for optimizing the response using Response surface Methodology in UHPFRC, several papers regarding UHPFRC and its material properties were reviewed. Some review papers included the mechanical properties of UHPFRC, but none specifically focused on the effects of higher steel fiber reinforcement on compressive and tensile strength[10].

Therefore, estimating the mechanical properties, such as compressive strength and flexural strength of UHPFRC with higher steel fiber dosages range (2.5 to 4 % by volume) is also included in the thesis.

The method adopted for conducting the study thesis was primarily literature review followed by experimental design, experiment execution, and analysis of the results. The research and experimental design were accomplished with the statistical software called Minitab. The experimental program was divided into two; i) application of Response Surface Methodology and ii) mechanical properties of UHPFRC with higher steel fiber dosage.

1.1 Research Objectives

This master thesis aims to provide a thorough study of Ultra-High-Performance Fiber Reinforced Concrete. As the field of UHPFRC is very extensive, this thesis attempts to investigate the methods for modeling and optimizing UHPFRC for maximum compressive strength. In addition to this primary objective, we also attempt to study the mechanical properties of UHPFRC with a higher dosage of steel fibers. This thesis is in continuity with our work last semester within UHPC material properties. This previous work is the basis for further progression within this focus area.

The thesis can be insightful for the development of UHPFRC and can additionally contribute to the research in the application of Response Surface Methodology (RSM) in UHPFRC.

Even though RSM has been used in numerous research regarding cement and concrete, its application to Ultra high-performance concrete (UHPC) is minimal. Therefore, this study focuses on bridging the research gap. Furthermore, several studies have investigated the mechanical properties of ultra-high-performance concrete; however, a few are available in the open literature regarding the effect of a higher dosage of steel fibers on the mechanical properties of UHPFRC. Most of the papers dealt with the addition of fibers up to 2% by volume. Thus, we intend to include the analysis of mechanical properties of UHPFRC with higher steel fiber dosage as a part of the thesis.

Therefore, our main research question is;

"How to develop a predictive model for maximum compressive strength of Ultra-High-Performance fiber reinforced concrete (UHPFRC) and how the higher dosage of steel fibers influences its mechanical properties?**"**.

The secondary objectives of the research are to.

- establish a predictive model that can provide a good correlation between the independent variables; water-binder ratio(w/b), steel fiber volume (F_v), and silica fume content (S_f) and the response; maximum compressive strength
- evaluate the individual and interactive effects of the variables on compressive strength (response) of UHPFRC

- to understand the influence of higher dosage of steel fibers on the compressive and tensile strength.
- evaluate how higher fiber dosage can affect the flowability of UHPFRC

1.2 Limitations

There were some limitations experienced during the course of the thesis with regard to materials, procedures, and time that altered the plans and goals. Those are enumerated in this section.

We initially planned to perform pull-out tests so as to consider the pull-out resistance as the response. However, this plan was later withdrawn, considering the availability of suitable machines in the laboratory.

Regarding the experiments with RSM, we initially planned to perform the experiments with fly ash or other supplementary cementitious material as one variable to explore the options to produce a greener UHPC. But there was an inordinate delay in procuring the materials due to the pandemic. Therefore, those plans were withdrawn later.

Besides, the analyses conducted are based on one single type of fiber, i,e short straight steel fiber. The efforts to procure different types of fibers also met with undue delay. Regarding time and materials, limitations in the laboratory had to be considered in planning the experiments.

There is no specific standard for testing the flexural test for UHPC. The ASTM C1609 is the most frequently used one which is the standard for fiber reinforced concrete. Standardised procedures for conventional or fiber reinforced concrete (the European standards [11, 12])is adopted for the thesis, in spite of emergence of an exclusive UHPC standard.

Afterall, it was challenging to execute the experiments, being alone in the group. The work would have been done more efficiently within a group.

1.3 Outline of the thesis

This thesis contains six chapters and is organized as follows:

Chapter 1 presents the background, problem statements, research objectives, significance, limitations, and thesis outline.

Chapter 2 reviews the studies related to UHPFRC's essential characteristics, composition, advantages over normal concrete, and development over the decades. The chapter also includes the environmental impacts of UHPFRC and the application of steel fibers in UHPFRC to improve mechanical properties. This chapter is the literature review on UHPFRC.

Chapter 3 outlines the theory of Response Surface Methodology, Design OF Experiments (DoE), different types of RSM designs, and applications of RSM in the Civil Engineering field.

Chapter 4 demonstrates the method adopted to achieve the research objectives. The method used is mainly an experimental program and application of RSM for the modeling and analysis. The materials used for the experiment and the testing apparatus; procedures are explained in this chapter.

Chapter 5 provides the results of the experiments and the analysis. These results include the regression equation developed using RSM. The results of the multi-factor interactions are illustrated with graphs and 3D plots. These results are discussed and explained in this chapter.

Chapter 6 summarises the findings from the experimental as well as RSM study and arrives at conclusions to propose recommendations for future research related to the subject of the study.

Chapter 7 indicates the limitations in interpreting the obtained results, which need to be studied deeply in future research. Also, some of the aspects that could not be included in this thesis due to the availability of time and materials that merit further research are recommended for future research.

2 Ultra-High-Performance fiber reinforced Concrete (UHPFRC)

Ultra-High Performance fiber reinforced concrete is a material that has a unique combination of excellent technical characteristics, including strength and durability.

The essential characteristics of UHPFRC are elaborated in chapter 2.1.

2.1 Basic characteristics of UHPFRC

2.1.1 Durability

One of the major objectives of developing UHPC is to have excellent durability. This quality keeps the concrete existing for a long term under the various conditions of the external environment, without significant deterioration in the quality, which enables the engineers to build safer structures with longer service life. In general, concrete structures might be exposed to severe environmental conditions that cannot be avoided, such as water penetration, chemical attacks, corrosion of reinforcement, chemical attacks, Alkali-Silica reaction, freeze-thaw cycles, chloride ingress, and carbonation. The exposure of the concrete structures to these severe conditions can lead to deterioration of the structures and increase the demand and cost of maintenance. The key factor that regulates the durability of the concrete mix is permeability. The concrete becomes more durable if it is less permeable. The main factors that influence the permeability are the density, microstructure, and the porosity of the mix. This can be achieved by excluding the coarse aggregate, including fine and ultrafine particles such as quartz powder, fine sand, and silica fume, lowering the water/binder ratio by adding an appropriate amount of superplasticizer. These measures enable the mix to be homogeneous and substantially reduce the pores. The water absorption capacity o UHPC is its permeability coefficient, which can indicate its high durability. A decrease in the water absorption capacity indicates a considerable reduction in porosity. As the water to binder ratio of UHPC is much lower than normal concrete, the water absorption capacity of UHPC is five times slower than that of normal concrete. Thus, the matrix of UHPC is impermeable as the pores are less than one-tenth of those in normal concrete. Many researchers have studied the behavior of UHPC during different environments and weather actions such as freeze-thaw cycles and observed that the deterioration happened in UHPC after several hundreds of cycles (up to 800 cycles) of freeze-thaw cycles was negligible [13].

2.1.2 Mechanical properties

Many experimental investigations established that UHPC possesses excellent mechanical properties that make it a superior construction material in the construction industry. Compressive strength is one of the major mechanical properties considered, which is significant in carrying the loads. In fact,

superior compressive in UHPC is achieved through adopting two major design criteria: i) close packing of the material particles without voids and ii) lower w/b ratio. For the compressive strength value, some papers stated that the compressive strength is usually greater than 120 MPa, while others stated that the compressive strength starts from 150 MPa. However, in either case, the compressive strength of UHPC is several times (3-4 times) greater than that of normal concrete [14].

The tensile properties of UHPFRC are different from normal concrete. Though they do not significantly impact compressive strength, steel fibers enhance the tensile strength of the UHPFRC. The tensile strength of the UHPFRC is usually within the range of 15-20 MPa, which is almost double the value of the tensile strength of UHPC without steel fibers. The flexural strength of UHPC is in the range of 30 - 35 MPa(from various experimental studies), which is achieved either in a high temperature curing regime or prolonged 28 days under a normal regime [13, 15]. The split tensile strength of UHPC from the many referred papers is in the range of 15-20 MPa [13, 16]. In general, the tensile strength of UHPC can be considered as one-tenth of its compressive strength; for example, if the compressive strength is 50MPa, then the tensile strength is 15 MPa.

UHPC has an increased tensile cracking capacity with its cementitious composite matrix, and bridging the cracks is possible with fiber reinforcement. In contrast to fiber-reinforced normal concrete, UHPFRC can exhibit significantly higher sustained post- cracking tensile capacity before crack localization, fiber pull out, and improved tensile behavior during loading. As the popularity of UHPC in the construction industry is rising, experimental investigations and determining compressive strength, tensile strength, and flexural strength are essential to understand the structural behavior, optimize the mix designs, and carry out numerical analyses of fracture mechanics [13].

2.2 UHPFRC composition

The general mix design of proprietary UHPFRC often contains a high binder content, including Portland cement as the major binder and silica fume, quartz flour or fly ash as supplementary cementitious materials. Coarse aggregate is usually removed from UHPC mixes to avoid the development of high voids and also to form a densified interfacial transitional zone around the aggregates, thus, eliminating the weakest region within the matrix. To confirm a high packing order, the coarse aggregate is replaced by well-graded fine sand. High range water reducing admixtures (HRWRA) are added to regulate the water to binder ratio of UHPC. Steel fibers improve the tensile strength and ductility of the mix by bridging the cracks during failures [5].

The basic components of UHPFRC are illustrated in Figure 2.1.
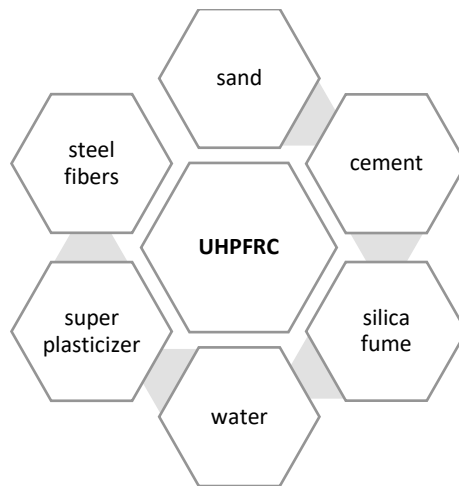
Figure 2.1:Basic components of UHPFRC

The major factor in producing UHPC is improving its ingredients' macro and micro properties to ensure mechanical homogeneity, maximum particle density, and minimizing voids' size [6]. The basic design principles for obtaining UHPFRC are i) elimination of coarse aggregates to increase the homogeneity)maximum packing of particles to increase the density by improving grain size distribution)reduce the water binder ratio iv) improving the ductility by adding steel fiber in appropriate quantity [17].

The major components and mixing ratios of UHPFRC are explained in the following.

2.2.1 Water to binder ratio

The water binder ratio for concrete mixing is the ratio of the weight of water to cement. The concept of a water-cement ratio(w/c) and water-binder ratios (w/b) are considered the bases of concrete technology. The lower these ratios, the stronger, more durable, and more sustainable the concrete. The w/b controls the initial network of capillaries of the cement paste. A low water-binder ratio is a key strategy for UHPC mixing. An optimum water binder ratio suggested in the previous studies ranges from 0.1 to 0.2 for achieving relatively higher compressive strength, packing density, and flowability. However, researchers have also achieved a compressive strength of 150 MPa using 0.25 w/b. Thus, it cannot be argued that the w/b alone regulates the strength properties. The curing regime and other parameters such as mixing procedure and mixer type also play major roles in producing a good mix with adequate flowability and strength [18].

2.2.2 Binders

A relatively high amount of cement is used in UHPC compared to that of conventional concrete. As it was observed that increasing the cement content improves the compressive strength, but after reaching an optimum cement content, around 1700 kg/m3, the compressive strength decreased, likely

due to the limited involvement of the aggregates. Although we largely use ordinary Portland cement to produce UHPC, special microfine cement with particle sizes smaller than OPC was also used to produce UHPC. As lower w/b is one of the key principles in designing the UHPC mix, only a part of the cement involves in hydration. Thus, the un-hydrated cement can be replaced with the suppletory cementitious materials such as blast furnace slag, fly ash, or silica fume in certain proportions without compromising the compressive strength [19]. The part of the cement that is not participated in hydration due to the small proportion of water will be used with other aggregates for packing optimization [13]. Figure 2.2 illustrates that the compressive strength and fluidity of UHPC improve with higher binder content.
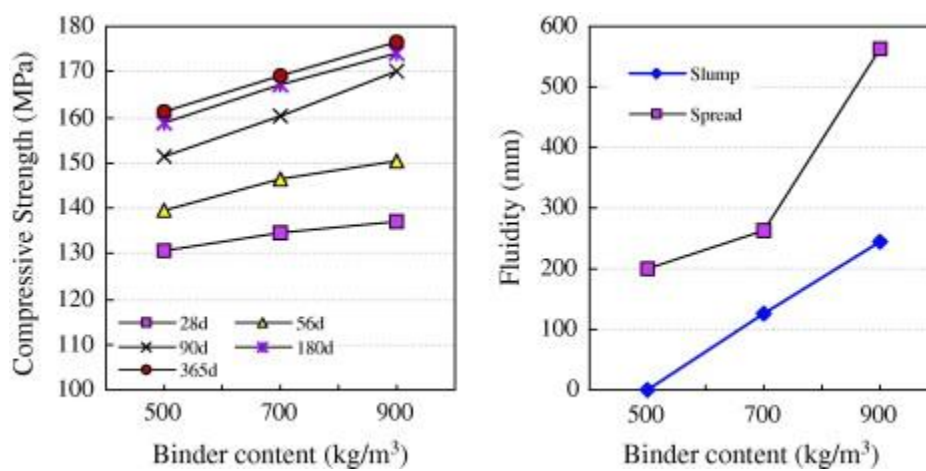
Figure 2.2:Influence of binder content on strength and fluidity of UHPC[20]

2.2.3 Superplasticizers

The superplasticizers, also known as high range water reducers (HRWRA), enable concrete production with lesser water content. The ability of superplasticizers to lower the w/c or w/b ratio in modern concrete is the significant factor that has resulted in the development of self-consolidating and high-performance concrete [21]. In UHPC, the reduced workability due to its lower w/b ratio is managed by adding superplasticizers (SP). Superplasticizers are generally used to produce flowable concrete with higher strength. Superplasticizers are organic polyelectrolytes; that belong to the category of polymeric dispersants. Some of the plasticizers are synthetic, while some are derived from natural products. Superplasticizers can be used at a higher dosage than conventional plasticizers, usually in the range of 0.5% to 3% by weight of cement [22].

2.2.4 Silica fume

Silica fume (SF) or micro silica is a powdery byproduct obtained during the manufacture of silicon Ferro silica from quartz, limestone, and iron. This dust from the electric furnace was collected in electrostatic

filters. Silica fume comprises very fine spherical particles (maximum particle size less 1 μm), with a great percentage of amorphous SiO_2(82-96%). The relative density of silica fume is 2200 Kg/m^3, and the specific surface of SF is between 15 and 30 m^2/g [19]. The SF added to the UHPC has two functions; primarily, it acts as a plasticizer due to its fineness and spherical shape. It reacts with the calcium hydroxide in cement to generate hydrated calcium silicates (C-S-H) gel.

Moreover, it improves the packing density and adhesion of the paste to the aggregates. The addition of SF makes the concrete highly resistant to chloride penetration because of its micro filling and pozzolanic effect, densifying the structure of the concrete's paste and interfacial transition zone (ITZ) [19]. Furthermore, the addition of silica fume as a binder improves the workability of UHPC by filling the voids between the coarser particles because of its finer size particle size and optimum spherical shape. Several previous studies recommended that silica fume dosages of 20%-30% of the total binder material achieve denser particle packing and pozzolanic activity in UHPC, leading to higher durability and strength [18][10][16].

Silica fume can be added to UHPC mixtures within a specific range; 150-250 Kg (10-30% of the cement mass). Figure 2.3 shows the relationship between silica fume content in UHPC and compressive strength. As we understand from the figure, concrete up to a strength of 81 MPa can be obtained without silica fume; it increases rapidly with the addition of silica fume [13].
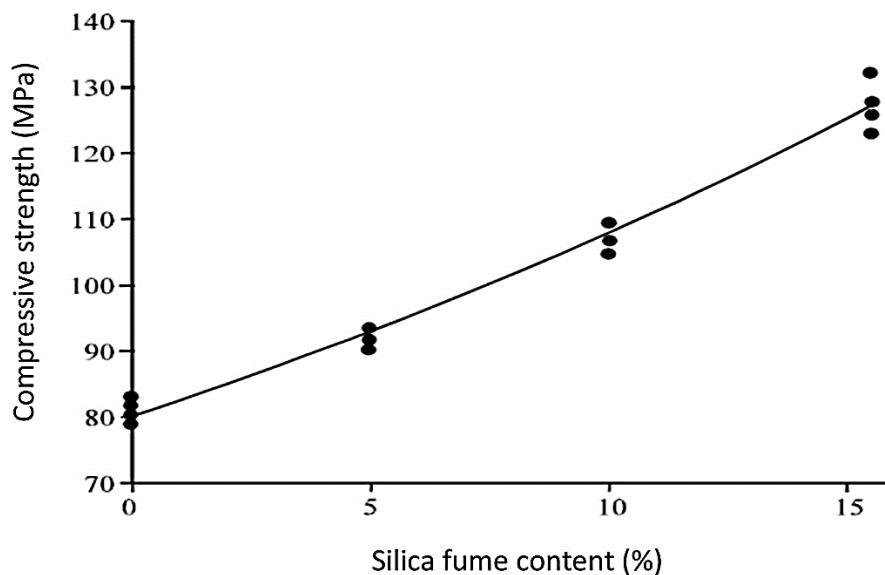
Figure 2.3:The relationship between compressive strength and silica fume content [10],[19]

One of the disadvantages of this material is its requirement for more water due to its significantly finer particles, but this can be managed by the addition of superplasticizers in UHPC. Another disadvantage is the limited availability and high cost of SF.

2.2.5 Aggregates

Coarse aggregates are generally avoided in UHPC mixes. As the size of aggregates is a major parameter deciding the mechanical properties, the average size of the aggregate particles is usually between 1 and 2 mm. As in conventional concrete, the failure mechanism is normally initiated by the failure of the ITZ (inter transition zone) between the cementitious matrix and aggregates. Therefore, removing coarse aggregates in UHPC eliminates such weakness induced by the ITZ as well as mitigating the ITZ flaws enables a reduction in porosity, leading to improved mechanical strength. The fine aggregates such as quartz sand play a key role in reducing the maximum paste thickness (MPT), which is also a significant parameter in the mix design of UHPC. Several papers found an optimum sand-to-cement ratio of 1.4 for a quartz particle size of 0.8mm [18, 19].

2.2.6 Water

Water is an important material in the manufacturing of concrete. The water should not contain any substances that might affect the chemical reaction between cement and water to produce good quality concrete. The quantity of water should be enough to complete the hydration process and maintain workability. The minimum w/c ratio for the normal concrete ranges from 0.4 to 0.5, including water for workability. The relationship between water in the concrete and its compressive strength is inversely proportional. If water is increased, strength will be decreased. The excess water remaining after the hydration would develop voids in the mix, leading to increased permeability and reduced strength. As in UHPC technology, superplasticizers are added to maintain workability without the need for excess water. Accordingly, the water to cement ratio (w/c) can be lowered to a range of 0.14-0.22, leading to increased compressive strength and enhancing all other properties of the concrete [13].

2.2.7 Steel fiber

Though UHPC is characterized by its high compressive strength, its fragile and exhibits a sudden fall in the load-bearing capacity after the crack initiation. UHPFRC makes this defect up by the presence of steel fibers, with improved ductility and tenacity to fracture as the fibers can bypass the cracks and delay the propagation of cracks. Thus, the addition of fibers improves the behavior of UHPC under flexure and tensile stress. The most commonly adopted fibers are short steel fibers, although glass, carbon, and polypropylene fibers are also used [19]. Steel fibers are characterized by their length, diameter, volume, orientation, and strength. The mechanical properties of steel fibers are shown in Table 2.1.

Table 2.1:Mechanical properties of steel fibers [8].

Length(mm)	Diameter(mm)	Volume(%)	Strength(MPa)
10-20	0.10-0.25	2	>2000

2.2.8 Typical UHPC mix design

A typical proprietary UHPC mix, designed and provided by Lafarge for Ductal[6], owing to the most widely used proprietary UHPC product in the United States, is shown in Table 2.2 [6].

Table 2.2:Typical composition of UHPC mixture

Typical composition of proprietary UHPC mix (Ductal)		
Material	Kg/m^3	Percentage (by weight)
Portland cement	712	28.5
Fine sand	1020	70.8
Silica fume	231	9.3
Ground Quartz	211	8.4
High Range Water Reducer (HRWR)	30.7	1.2
Accelerator	30	1.2
Steel fiber	156	6.2
Water	109	4.4

2.2.9 Comparison of conventional concrete and UHPC

Generally, the basic conventional concrete is made with ordinary Portland cement, fine aggregates, coarse aggregates, and water with or without admixtures. In contrast, UHPC is prepared by removing the coarse aggregates, replacing a portion of cement with SCMs such as fly ash or micro silica, and adding superplasticizers to be able to attain low w/c ratios [23]. Figure 2.4 compares the two-dimensional schematic particle packing of conventional concrete and UHPC. UHPC has a higher packing density and minimum voids. This contributes to low porosity, high mechanical strength, im-permeability, and high durability.

Conventional concrete   UHPC

● Coarse aggregate (4.75mm to 20mm)   ● Cement (1μm to 100 μm)   ● Pores in concrete
● Quartz sand (150μm to 600μm)   ● Quartz powder (1 to 100μm)   ● Silica fume (0.1μm to 1μm)
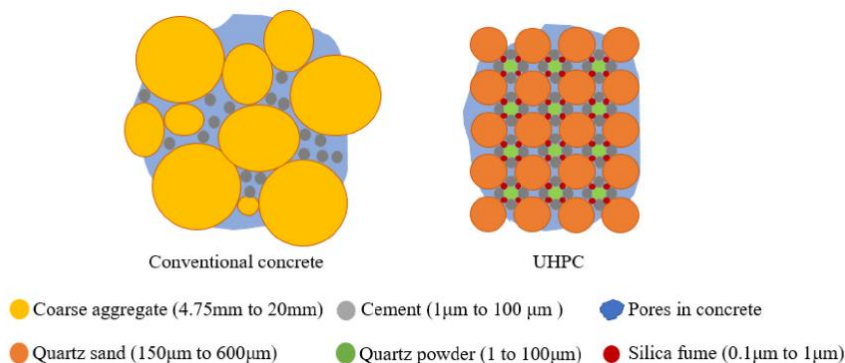
Fig. 2. Two-dimensional schematic particle packing of conventional concrete and UHPC. The UHPC has a higher particle packing density [20].

Figure 2.4:A comparison of 2D schematic particle packing of conventional concrete and UHPC [4]

Figure 2.5 represents the stress-strain responses of compressive and tensile behaviour of UHPC compared to conventional concrete, which explains the higher strength exhibited by UHPC during compressive and tensile behavior.
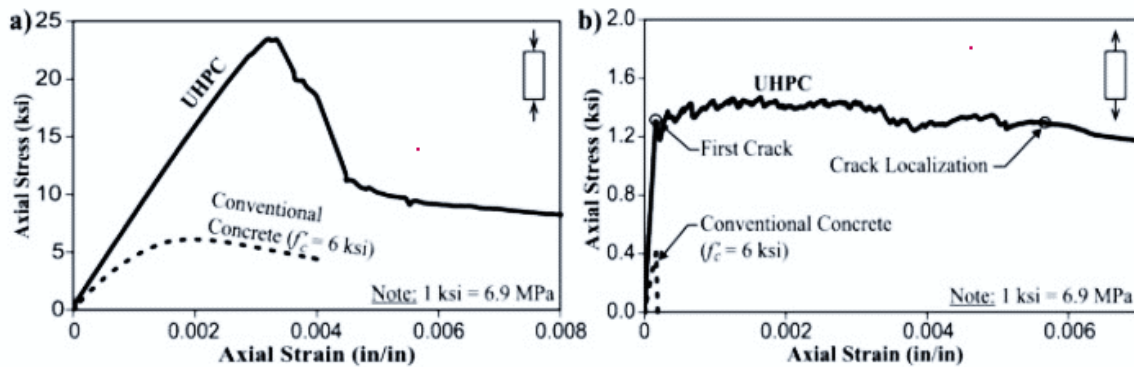
Figure 2.5:Stress-strain behavior of UHPC compared to normal concrete in a)compression and b)tension[24]

Table 2.3 represents the comparison of typical conventional concrete and UHPC, which reveals that the mechanical properties of UHPC are superior to that of conventional concrete; For instance, the ultimate compressive strength of UHPC is 3-4 times that of conventional concrete, which was already mentioned in the previous chapters. Further, the other mechanical properties are also extremely higher than those of conventional concrete.

Table 2.3:Comparison of mechanical properties of UHPC and conventional concrete [8]

	Normal concrete	UHPC
Compressive strength	20-40 MPa	120-200MPa
Split Tensile strength	< 5MPa	Up to 20MPa
Flexural Strength	< 6 MPa	Up to 30 MPa
Durability	Weak	Extremely high
Ductility	Weak	Extremely ductile
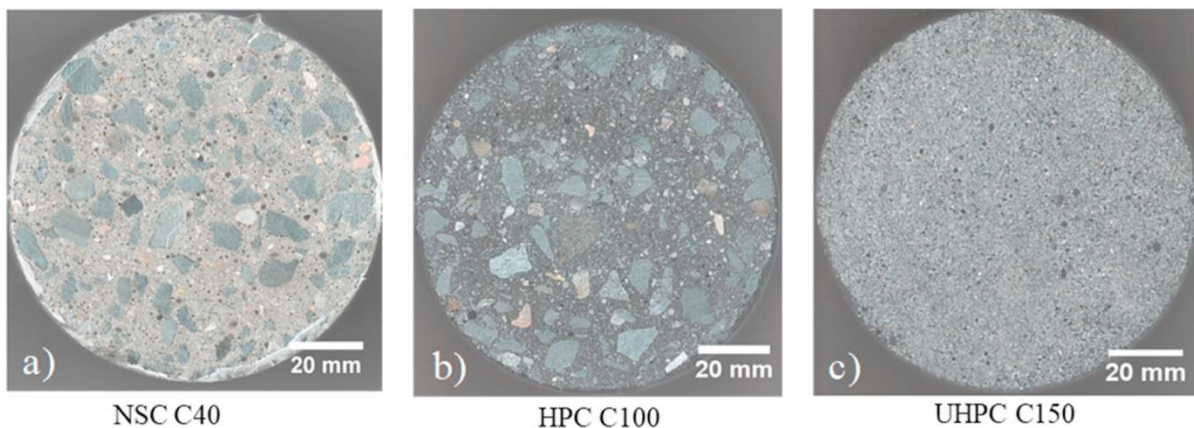
Figure 2.6:Cross-sectional views of cylindrical specimen a) conventional concrete, b) High-performance, and c)UHPC [21]

Figure 2.5 shows the cross-sectional views of normal concrete, HPC, and UHPC sample in the hardened state. These views highlight the denser packing structure of UHPC as it doesn't contain coarse aggregates. Table 2.4 shows the comparison of mix designs of UHPC and conventional concrete. UHPC has SCM as slag powder and silica fume, and superplasticizers are added to reduce the water-cement ratio. These fine particles contribute to the high durability of UHPC.

Table 2.4:A comparison chart of UHPC mix and conventional concrete mix

UHPC and normal concrete mix design		
	Qty .Kg/m3	
Material	UHPFRC	Qty .
Coarse aggregate	612	1080
Coarser silica sand	500	960
Finer silica sand	500	-
Cement	604	360
Silica fume	268	-
Slag powder	120	-
Limestone powder	216	-
Water	144	1512
Superplasticizer	57.6	-
Steel fiber	148	-

2.2.10 Advantages of UHPC over conventional concrete

There are several advantages to choosing UHPC over conventional concrete. Those are elaborated on in the following.

Workability: UHPC is mixed with the lowest possible w/c ratio (w/c <0.2), which reduces the porosity and im-permeability, increasing the strength and durability without compromising adequate flow as superplasticizers are added to the UHPC mix. To summarize, UHPC is a self-compacting concrete (SCC) that makes it possible to cast slender structural elements conveniently [25].

Strength: The strength of UHPC is higher than conventional concrete; it helps reduce the structural load and overall weight of the structural design. This feature indirectly helps in reducing the use of material [25].

Durability: Several papers have studied the exceptional durability characteristics of UHPC. As the aggregates are chosen in the UHPC mix, voids are minimized, and particle density is maximized. This provides superior durability to UHPC. UHPC has enhanced resistance to corrosion and other environmental actions [26].

Ductility: UHPFRC can be effectively used to withstand the tensile loads and reduce the cracks and crack propagation, and strain hardening, which have been observed in UHPFRC specimens. Unlike conventional concrete, microcracks in UHPC allow greater ductility [25].

Sustainability: UHPC, when used with fewer cement proportions, as the powdered SCMs could effectively substitute cement. It implies that the use of UHPC can reduce cement manufacturing and significantly reduce global warming, which indirectly promotes the sustainable development of the infrastructure [25].

2.3 UHPC Development

The plain concrete was made of Portland cement, and aggregates were generally considered first-generation concrete. This conventional concrete was associated with a lack of tensile strength and ductility, which led to structures' failure. Accordingly, this showed a path for the development of the second generation of concrete, in which reinforcement with steel bars was introduced as a solution. After the middle of the 20th century, increasing the strength of concrete to carry more loads or more advanced constructions was a challenge, possibly achieved through careful selection of aggregates and decreasing the water to binder ratio. The reduction in water content was made possible with the invention of water-reducing admixtures that facilitated the engineers to increase the strength of compromising without compromising the workability [13].

There has been a substantial number of research done in the field of materials development for developing concrete with high strength. Superplasticizers were developed in the late 1970s to reduce the water/cement and water/binder ratio as it was then found that concrete with low w/c w/b ratios could provide higher compressive strength. Besides those, concretes showed improved characteristics such as higher flexural strength, lower permeability, improved abrasion resistance, and better durability. It has been then understood from the experiments and research studies that the most significant factor influencing the concrete strength is the water/cement or water/binder ratio [27]. Figure 2.7 is a graphical representation of the relationship between the compressive strength of concrete and the water to binder ratio, which indicates that the compressive strength of concrete is higher for lower w/b .
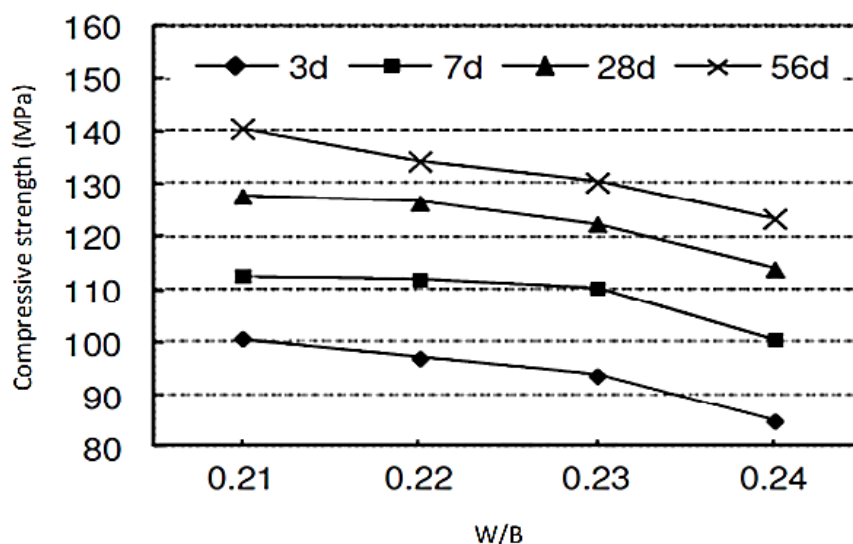
Figure 2.7:The relationship between compressive strength of concrete and water binder ratio at different ages [10, 24]

The traces of development of UHPC started back in the early 1980s when macro-defect free (MDF) cement was proposed. The development of what is now being characterized as UHPFRC was started

in the 1970s by Brunauer, Older, and Yudefrund. They have done research in in high strength cement pastes with w/c as low as 0.2-0.3, and these low w/c ratios gave concrete with low porosities led to compressive strength up to 200MPa and low dimensional change. The use of superplasticizers and pozzolanic admixtures was significant in the development of UHPFRC. In the 1980s, there were two new approaches used for the development of UHPFRC as a result of the development of SP and admixtures [8].

- The first approach was called Densified Small Particles (DSP), where the mix was granular that could provide a compressive strength between 150 and 400 MPa. For the concrete that was used in DSP, extremely hard aggregates were used, for instance, calcined bauxite or granite. In addition, it consisted of very high SP and silica fume content, which decreases the porosity and thereby increases the material strength.

- The second approach was called Macro Defect Free (MDF) concrete. That was a polymer-modified cementitious material, where polymerization fields the concrete's pores, leading to a highly compact and strong matrix. However, MDFs had demanding manufacturing conditions that were water susceptible and experienced excessive creep [8].

In 1994 Larrad first proposed the idea of UHPC, which was later defined as a cementitious composite with superior mechanical properties. These properties include compressive strength of over 150 MPa, superior durability, extremely low porosity, high packing density, and low permeability [28].

2.3.1 Definition of UHPC

There is no universal definition so far to define UHPC. However, different definitions have been used to define UHPC that we evaluate in the following.

In the United States, the Federal Highway Administration (FHWA) defines UHPFRCC as a cementitious composite material consisting of an optimized gradation of granular constituents; the ratio of a water-to-cementitious material below0.25, and a high amount of discontinuous internal fiber reinforcement. The mechanical properties of UHPC include compressive strength greater than 150 MPa and sustained post cracking tensile strength greater than 5 MPa. UHPC has a discontinuous pore structure, which minimizes liquid ingress and remarkably increases the durability compared to conventional concrete [5, 29].

The Association Francaise de Genie Civil (AGFC) Interim recommendations define UHPC as a material with a cement matrix and a characteristic compressive strength over 150 MPa and steel fibers to achieve a ductile behavior. According to AFGC, the main differences between UHPC and other types of concrete are 1) UHPC has higher compressive strength, 2) UHPC contains random steel fibers in the mix that ensures non-brittle behavior and alters the conventional requirements for passive or active

requirements, 3) UHPC mix design is characterized by high binder content and judicious selection of aggregates.

The Japan Society of Civil Engineers (JSCE) recommendations for the design and construction of Ultra-high strength fiber reinforced concrete define the UHPC 'as a type of cementitious composite reinforced by fibers, with characteristic values greater than 150 MPa in compressive strength, a minimum cracking strength of 4 MPa [6].

ASTM C1856 defines UHPC as a cementitious composite with a stipulated compressive strength of at least 120 MPa and specified durability, ductility, and toughness requirements [14].

Considering the above definitions, we could develop a definition for UHPC that includes major components, superior qualities, and basic design strategies. We may define UHPC as the new generation cementitious composite material designed for very high compressive strength, high durability and high ductility, and high sustainability, established with the microscale optimization of fine and ultrafine aggregates(silica fume and fine sand) , very low water-to- binder ratio(less than 0.2) and lower w/c ratio with added superplasticizers and reinforced with high strength steel fibers [13]. Generally, the mix proportion of UHPC characterizes by a very lower w/b ratio and high cementitious content [30, 31]. UHPC, which requires fewer materials and little maintenance, seems to be one of the best possible ways to reduce environmental impacts [32]. But the amount of cement in UHPC generally ranges from 800 to 1100 Kg/m^3, (which is about 3 times as much as that of regular concrete [5].

When it is stated that the cement content is large in UHPC, it is important to understand the durability aspect of UHPC. The durability of concrete may be defined as the ability of concrete to withstand weathering action, chemical attack, and abrasion while maintaining its desired engineering properties—the durability issues of concrete structures such as corrosion of reinforcement, Alkali-Silica Reaction, freeze-thaw action, etc. There are several research papers that studied the durability aspect of UHPC, where a series of durability tests were performed to determine its resistance to various environmental aggressors. These studies showed that UHPC exhibits enhanced durability properties over normal concrete regardless of the curing treatment applied. The higher durability in UHPC is the use of a low water-to-binder ratio(W/B) of approximately 0.2, their dense microstructure, and a higher proportion of fine particles [33]. The UHPC matrix is characterized by a very dense and minimal disconnected pore structure, which results in low permeability. The low permeability of UHPC prevents chloride ingress (Chloride ion diffusion is less than 0.02 x10^{-12} m^2/s), which yields superior durability characteristics and became commercially available in the USA in 2000. After that, FHWA (Federal Highway Administration) started investigating the applications of UHPC on highway infrastructure. This research led to the use of UHPC in several applications in bridge construction, including precast and pre-stressed girders for bridge decks [34].
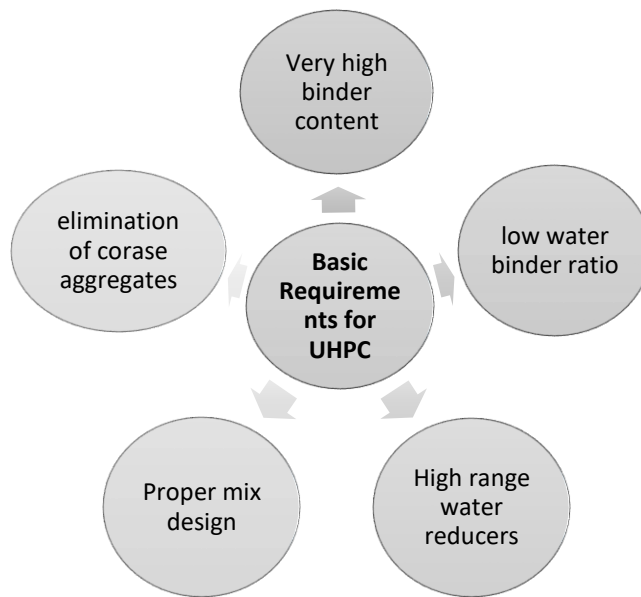
Figure 2.8 demonstrates the basic requirement of UHPC. The significant drawback of concrete without fibers is the reduction in ductility. This is improved with the addition of steel fibers without compromising the mechanical properties due to the crack bridging effect of fibers.

2.4 UHPC standards

No specific code or standards exist for UHPC material properties that provide a clear definition or guidelines for categorizing its material properties. Though technical guidelines and professional recommendations were previously available in countries such as the United States, Japan, France, and Switzerland, the standardizations are necessary to establish meaningful test results as those guidelines do not have official status. Moreover, standardization is necessary for structural engineers to use in the design of practices.

The following codes and standards with regard to UHPC are referred from various references and resources in various places all over the world [13].

- NFP 18 470:2016- (July 2016) Concrete – Ultra High-performance fiber reinforced concrete Specifications, Performance, Production, and Conformity. This is a self-supporting document; however, in line with NF EN206/CN, the French standard for normal structural concrete is consistent with European standards. Appendices to this document cover the standardized methods associated with the relevant UHPC characteristics. This document includes both structural and non-structural UHPC [36].

- NFP 18 710:2016 (April 2016)- This document is considered a national complement to Eurocode 2 and applies to the design of UHPFRC structures (buildings and civil engineering) [37]. This document includes the UHPC with metallic fibers, i.e., UHPFRC, which possess a compressive

strength greater than 150 MPa. This is basically the document that can be referred to for design rules for UHPFRC according to NFP 18-470 [37].

- NFP 18-451- This document basically deals with the UHPFRC structures -specific rules for UHPFRC that complement and suggest amendments or precisions to the executed standard NF EN 13670/CN. Though this document was prepared following NFP 18 470:2016, it provides more information to the contractors and engineers to use UHPFRC for new structures. This standard provides general indications based on relevant industry-level experiences, which could make the use of UHPFRC more widespread [38].

- ACI (American Concrete Institute) committee 239, ACI 239C 2018, Ultra-High Performance: An Emerging Technology Report, ACI committee 239 documented advancements in the testing, design, and specification of UHPC. This subcommittee of the ACI committee consisted of a set of industry experts who began the task of writing a Terms of Reference (TOR) for the new Emerging Technology Report (ETR) on the structural design of UHPC. However, this report was more focussed on structural applications for bridges, led by the Federal Highway Administration and primarily UHPC, made with metallic fibers that possess a compressive strength greater than 150 MPa.

  A part of the activities of this committee was in collaboration with the ASTM, American Society for Testing and Material (ASTM), intending to provide a new standard practice for fabrication and testing specimens of UHPC (ASTM C1856/C1856M, 2017), with metallic and non-metallic fibers. This standard can be applied to UHPC specimens having a compressive strength of at least 120 MPa, with the size of aggregate less than 5mm, and a flow diameter between 20 and 25 cm as measured by the modified flow table test method described in ASTM C1437 and ASTM C230/C230M[39]. These requirements could not include the scope of several architectural UHPC compositions possessing lower compressive strength(less than 120 MPa)and high spread values(25 to 30cm) that confer the ability for self-compacting, that guarantee efficient air removal and high surface quality for complex texture and shape [40].

- ASTM C1856/ C1856M, 2017, Standard Practice for Fabricating and Testing specimens of Ultra-High-Performance Concrete. This standard sets guidelines for measuring the properties of fresh UHPC and procedures for manufacturing and testing specimens of hardened UHPC. This standard is developed referring to the existing practices and test methods incorporating modifications to the referred standards for application to UHPC [41].

- Like ACI and ASTM committees, the National Precast Concrete Association (NPCA) made an effort to provide some guidelines for manufacturing architectural precast UHPC elements in their report released in 2013(NPCA,2013). This was documented to provide a guide for manufacturing

architectural precast UHPC elements and described the general handling and quality control procedures, including storage of raw materials, forming, batching, curing, and the plan requirements for architectural UHPC [42].

2.5 Environmental impacts of UHPC

As we have gone through several pieces of literature regarding UHPCs, it is understood that the strength and durability of UHPC are far way better than that of ordinary concrete, which classifies it as an extraordinary building material. However, now the construction industry focuses more on sustainable construction strategies, intending to reduce the embodied CO2 in building materials. Thus, it is relevant to assess the negative environmental impacts of UHPC and recommend solutions to produce it in a more sustainable way [43-45].

Generally, the mix proportion of UHPFRC contains a relatively lower w/b ratio and high cementitious content and steel microfibers. Even though the development of UHPC requires fewer materials and little maintenance seems to be one of the best possible solutions to minimize the environmental impacts, the higher amount of cement that generally ranges from 800 to 1100 Kg/m^3 (which is about 3 times as much as that of regular concrete) marks it as 'a less sustainable solution' [5].

A considerable amount of CO_2 is emitted during cement manufacturing; First of all, cement is made from limestone, clay, and sand. This mixture is ground into powdered form and heated in a Kiln, typically at 1500^{0}C, and forms pellets called clinker. The clinker is then mixed with a small amount of gypsum and powdered to form the Ordinary Portland cement [46].
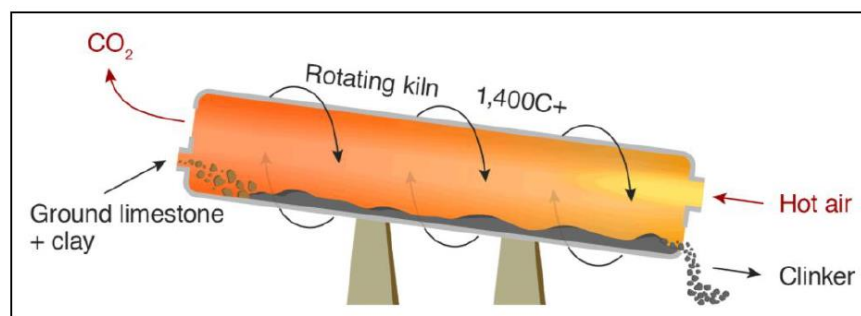
Figure 2.9:Manufacturing process of cement [47]

Limestone is a sedimentary carbonate rock mainly composed of minerals calcite and aragonite, which are different crystal forms of calcium carbonate ($CaCO_3$). When limestone is heated, a chemical process called calcination is initiated, where CO_2 is burned off, as shown in Figure 2.8 and its detailed chemical decomposition in Eq. 2.1.

$$CaCO_3 \rightarrow CaO + CO_2 \qquad\qquad (2.1)$$

A major portion of the emissions from the cement industry is drawn from the calcination process, the rest from heating furnaces and transportation. In cement production, large amounts of CO_2 are emitted, about 1 ton of CO_2 per ton of clinker. Around 40% of the CO_2 comes from the combustion of fuel, fine grinding, etc., and 60% from the decarbonization of limestone to form a clinker [48].

Unfortunately, Portland cement possesses a high environmental cost. Cement production could be the third-largest source of CO_2 in the world. According to think tank Chatham House, cement production is the major source of about 8% of the global emissions. Considering the cement industry as a country, it would be the third-largest emitter in the world after China and the US. For the cement industry to fall in line with the Paris agreement, its annual emissions must drop by 16%. There are a few reasons that cause cement production to be detrimental to the environment. Primarily, cement production consumes almost a 10th of the world's industrial water use, often in water-stressed areas.

Further, its production involves quarrying, which results in air pollution by generating dust and exacerbating respiratory diseases. The production also requires huge kilns, which need large amounts of energy. The production of portland cement expends about 0.33% of the annual energy consumed in the US, which corresponds to the amount of energy in around 13 million tons of coal [49].

Being the most popular material consumed on earth after water, concrete releases extreme amounts of Carbon dioxide (CO_2) each year. The environment will be exposed to over 4 billion tonnes of CO_2 annually due to the building industry until overall emissions are cut worldwide [50].

As we discussed in the introduction chapter, the environmental impacts of concrete are mainly due to the cement contained in it. The CO_2 is primarily released during the calcination process during cement manufacturing. Figure 2.10 represents the increase in CO_2 released by the cement industry during the past years.
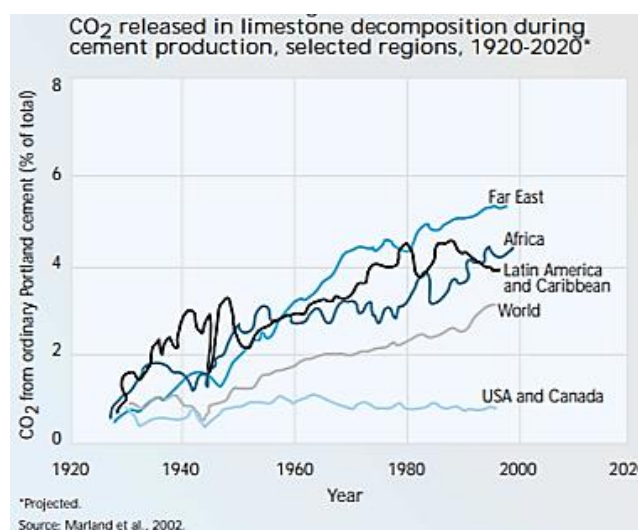
Figure 2.10:CO_2 released during cement production graph from 1920 till 2020 [51]

Based on the study conducted by the National Ready Mixed Concrete Association, each pound of concrete releases 0.93 pounds of CO_2. Since concrete is such a globally widespread material, the amount of CO_2 released in the industry grows. Thus, it is highly significant to design concrete more sustainably by limiting CO_2 [51].

As we understood, cement has a massive carbon footprint. However, it has a lower embodied energy (the sum of all the energy required to produce a material) than materials such as steel or aluminum, which indicates replacing it with another material would not be a simple solution. Significant research work has been done so far and still going on to develop more sustainable alternatives to Portland cement [52], which is where real change is needed. Since the world is now turning more towards sustainable construction, several studies have been conducted to develop strategies to reduce or replace cement content in concrete. The best and most straightforward method recommended is reducing or replacing the cement portions in concrete with secondary cementitious materials (SCMs) [50].

2.5.1 Major SCMs in UHPC

Secondary Cementitious Materials (SCMs) are materials used in conjunction with Portland cement and supplement the properties of hardened concrete through hydraulic and/or pozzolanic activity. Secondary cementitious materials include fly ash, ground granulated blast furnace slag (GGBS), limestone, silica fume, rice husk ash, etc. Fly ash and GGBS are the most commonly used of these materials, as they are valuable by-products of other industrial processes [53]. CEM II and other alternatives are the most common low carbon alternatives, as it substitutes clinker for different materials such as fly ash (FA) and Ground Granulated Blast Furnace Slag (GGBFS). Figure 2.10 represents the most widely used SCMs and their chemical compositions.
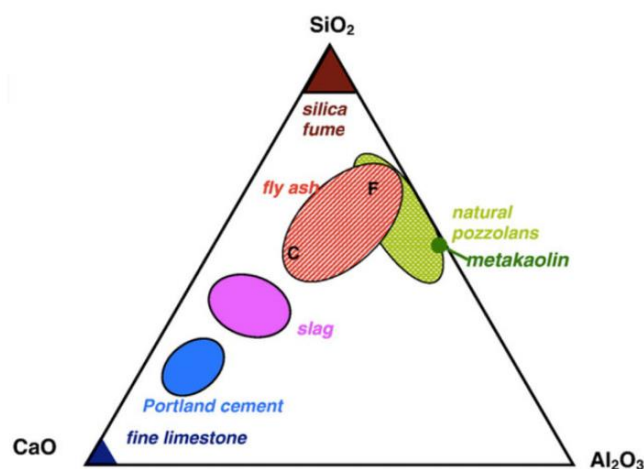
Figure 2.11:Ternary diagram for cementitious materials [46]

Fly Ash

Pulverized Fly Ash is a by-product of coal-burning power stations. In a typical modern coal-fired power station, approximately 80% of the ash is produced as a fine powder known as Pulverized Fuel Ash (PFA) (also known as "Fly Ash" in some countries). This powdered fly ash is carried in the gas stream out of the boiler, ultimately collected by mechanical arrestors and/or electrostatic precipitators as it is light and fine. The 'ash' is recovered from the gases and used, amongst other functions, as a cement substitute. PFA typically ranges in size from 0.5 to 150 microns [54].
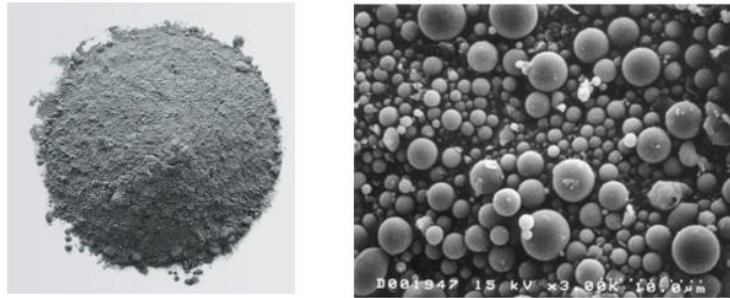
Figure 2.12:The image of powdered Fly ash Vs. Scanning Electron micrograph of Fly ash

Fly ash has the following benefits;

- The use of FA as a partial replacement for carbon-intensive cement indirectly helps to conserve more virgin resources like limestone and iron for steel production potentially, and thus the environmental impacts associated with the production of cement can be avoided [55].
- 1 tonne of Portland cement requires 1.6 tonnes of limestone and clay for its manufacture, the replacement of cement by SCMs reduces abiotic depletion
- The coal power plant that produces FA will benefit from the reduction of residue handling area, as well as health effects associated with the presence of FA
- FA is a by-product obtained during burning coal. Since these operations (burning of coal) would continue regardless of whether the by-products were used or not, the emissions associated with the primary product are assigned to the primary product.
- It can also help reduce deforestation, fuels, and the loss of biodiversity associated with the production of cement from limestones
- Finally, as discussed above, FA can improve the durability of concrete, thereby prolonging the lifetime of structures and reducing the environmental burden associated with repair and maintenance.

Ground Granulated Blast Furnace Slag (GGBFS)

Ground Granulated Blast Furnace slag is manufactured from blast furnace slag, a product of the iron-making process. The final product GGBFS has an amorphous/ glassy form, exhibiting cementitious properties. This potential of GGBFS enables it to be used at high volume replacement due to its self-cementitious properties [56].

This is a granular product with minimal crystal formation that is highly cementitious, powdered to the fineness of cement, and gets hydrated like Portland cement [57].

Figure 2.13:Ground granulated blast furnace slag [50**]**

Slag tends to decrease the compressive strength of UHPC at an early age because of the slow hydration of slag. Still, it increases the late age compressive strength through the pozzolanic reaction between slag and Ca $(OH)_2$ that enriches the packing density of the UHPC. The finer particle size of slag exhibits higher compressive strength. Thus, the slag powder is recommended for UHPC mixes. It also increases the workability of concrete because of its lower water absorption compared to cement.

2.5.2 Role of SCMs in reducing the carbon footprint

The carbon footprint and embodied energy consumption of the concretes with FA /Slag as SCMs from various reports are presented here. Table 2.5 provides the carbon footprint data taken from the fact sheet of the sustainable development report 2020 of MPA (The concrete Centre).

Indicative ECO_2 values for the main cementitious constituents of reinforced concrete are provided in the table, published by MPA cement, UK Quality Ash Association and Cementitious Slag Makers Association, and the British Association of Reinforcement. These values are derived using data from 2017/18 and represent 'cradle to -factory-gate 'values as they do not consider transport from the place of manufacture to concrete plants. As per the table, the embodied CO_2 in Fly ash and GGBFS is considerably low compared to that of Ordinary Portland Cement (which is 860kg/tonne) [58].

35

Material		Embodied CO$_2$ (Kg/tonne)
Portland cement CEM I		860
Secondary cementitious materials (SCMs)	Ground granulated blast furnace slag(ggbfs)	79.6
	Fly ash	0.1
	Lime stone	8
Aggregate		2.6
Reinforcement		412

Figure 2.13 is a graphical representation of the summary of embodied-CO$_2$ and the 28-day compressive strength of the UHPCs in a paper reviewed[59]. The bar graph corresponds to the 28-day compressive strength of the left Y-axis and the line plot to the e-CO$_2$ data of the right Y-axis, and the hatched ones mean that the specimen was thermally treated. The data are divided by the type of SCMs used and then sorted by the 28-day compressive strength in descending order. From the bar chart, we understand that UHPCs with FA and slag replaced with cement have lower e-CO$_2$, which substantiates the effect of FA and slag as SCMs in lowering the emissions of UHPC.
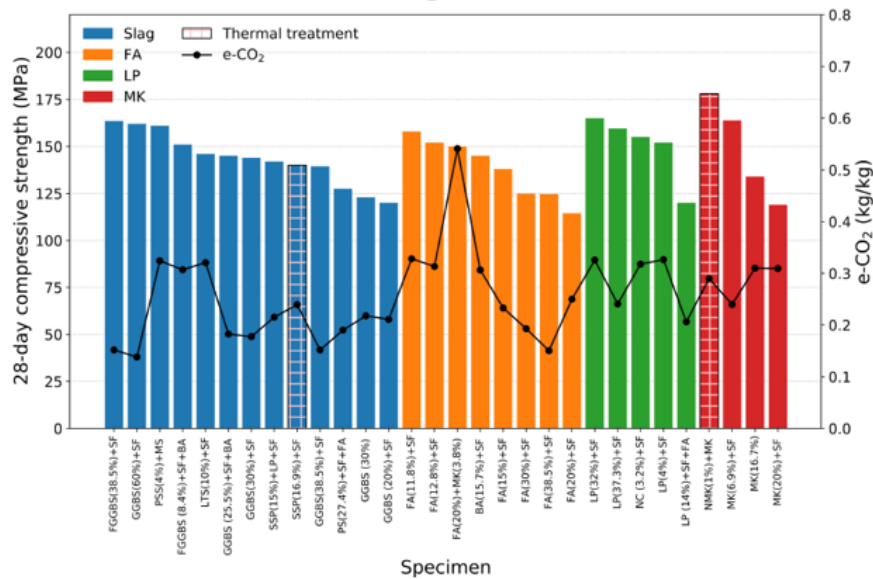
Figure 2.14:The 28th-day compressive strength and eCO2 of the concrete specimen using various SCMs [33]

The data represented by Table 2.5 and Figure 2.13 provided the environmental benefits of replacing the cement with secondary cementitious materials, without compromising the superior mechanical properties of UHPC.

2.6 Fibers in UHPFRC

Although cementitious materials have a plethora of usage in the construction industry, there are some unresolved defects, especially due to their low tensile strength. The integrity of the concrete can be challenged by the micro-scale defects in the internal structure that develop over the course of time. These micro and nano defects in concrete can be effectively treated with the incorporation of various fibers. The addition of fibers enhances the toughness, bond strength, ductility, and post-cracking tensile behavior of concrete [60].

Similarly, though UHPC possesses excellent compressive strength, the reduction in ductility has been considered one of the major drawbacks of UHPC as ductility decreases with an increase in compressive strength. The addition of steel fibers makes it UHPFRC, an improved version of UHPC with improved ductility and tensile and flexural strength. In theory, small steel fibers bridge micro-cracks and control the growth of these cracks, leading to the higher tensile strength of concrete, while the larger fibers control macro cracks, leading to enhanced load-bearing capacity and ductility.

According to the engineers, the fibers can be mainly classified into steel fibers and synthetic fibers. Steel fibers are typically used when crack control is the priority, whereas synthetic fibers reduce cracks due to shrinkage. The commonly employed synthetic fibers are carbon, glass, and polymeric fibers [61]. Fibers normally enhance the strength and toughness of the composites mainly through the fiber bridging mechanism, which facilitates a decrease in the net stress intensity with fiber pull out, fiber fracture, or plasticity [62].

The addition of fibers in the UHPC mixture can ascertain ductile behavior in tension and transform the brittle behavior into ductile in compression. UHPC without fibers, though they possess a higher tensile strength ranging from 7MPa -10MPa, exhibits very brittle behavior. Or in other words, UHPFRC poses higher strength varying from 7 MPa to 15 MPa and exhibits ductile behavior in the post cracking stage. However, several studies have proved that tensile performance characteristics of UHPC are primarily influenced by fiber characteristics, including fiber type, shape, aspect ratio, orientation and distribution, and percentage of fibers [63].

The steel fibers significantly improve many mortars and concrete engineering properties, notably impact strength and toughness. Flexural strength, fatigue strength, and resistance to cracking and spalling are also enhanced (ACI 544. 3R-2). The compressive strength is only marginally affected by the presence of the steel fibers. The addition of 1.5% by volume of steel fibers can increase the direct tensile strength by up to 40% and the flexural strength by up to 150% [40].

The volume of steel fibers normally added to the concrete ranges from 0.25 vol.% (20kg/m^3) to 2 vol.%(157Kg/m^3). The low end of the fiber percentage applies to lightly loaded structures, whereas

the upper end is used for security applications (safes, vaults). Volumes of more than 2% steel fibers usually reduce the flowability, workability, and dispersion of fibers. This scenario requires a special mix design or concrete placement techniques [64].

2.6.1 Benefits of steel fiber

The brittle failure of cementitious materials such as mortar and concrete at low tensile strength has always been a limitation that could be effectively overcome using steel fibers [65]. Among the commonly adopted fibers in cementitious composites, the performance of steel fibers has been found to be the most adequate as they exhibit superior tensile strength and stiffness that can significantly improve the mechanical properties of cementitious materials. The resistance and delay in developing crack propagation is the fundamental benefit of including steel fibers into the cementitious matrix, as it was generally understood that the addition of fibers could improve the crack resistance of concrete by upgrading its critical crack resistance. The contribution of fibers to the strength of the matrix starts during the crack initiation and also extends up the post-cracking stage by improving the post-cracking behavior. This is normally done by transferring the stress by the fibers bridging the cracked sections. This stress transfer between the fibers and the matrix depends upon the interfacial bond properties [65]. In case the interfacial bond is too strong, the ductile fibers break at some point even before fully de-bonded, and the majority of the embedded portions of the ductile elements could not develop plastic deformation and dissipate energy in this case. However, in the case of a weaker interfacial bonding instead, the fibers may be pulled out of the matrix, and only the frictional force could take limited energy out of the system [62].

The bond is the zone through which tensile forces are transmitted between the steel fibers and the cementitious matrix. The tensile strength of the SFRC mix can be varied according to the fiber-composite interfacial bond strength. If the bond is weaker, the pull-out of fiber can be easily done at lower loads; in other words, if the bond is stronger, the pull-out can only be possible at a higher load [66].

In general, two main types of bonds develop between the fiber and the matrix.

They are; i) physiochemical through adhesion and friction at the interface and mechanical through the anchor effect of interlocked fibers. The physiochemical bond through adhesion and friction is usually governed by the properties of the surface of fibers as well as the interfacial transition zone (ITZ). This bond is predominant in the case of straight fibers with no hooked ends, as this type of bond is first activated during the pull-out process and determines the pull-out resistance of the straight fibers. Mechanical interlock develops from the geometric deformation in the length of pre-deformed fibers and the transverse tensile strength of the concrete [67].

The efficiency of any reinforced composite (RC) is determined partly by the interfacial bond conditions between the reinforcement (rebar or fiber) and the composite mix as the stress transmission from the composite to the reinforcement, and vice versa, is achieved through the interfacial bond. Although the reinforcement in RC (reinforced concrete) and SFRC (Steel fiber reinforced concrete) balances the weakness in concrete under tension, there is a significant reduction in the physiochemical bond in SFRC for fibers as they are not continuous like the rebars. Another major difference is the collapse mechanism during bending. For the rebars, plastic hinge collapse is predominant during bending, whereas in the case of fibers, they usually get pulled out before the hinge formation happens [65]. Interfacial bonding can greatly influence the cracking that takes place in the cement matrix. In an uncracked matrix, the stress is typically transmitted from the composite to the longitudinal axis of the fibers mainly through friction at the interface.

The mechanical properties of steel fiber reinforced concrete (SFRC) are closely connected to the mechanical properties of the interface between the cementitious matrix and the fiber. Figure 2.15 explains how the bridging effect of the fiber at the matrix-fiber interface actively transmits the tensile load at the interface [68].
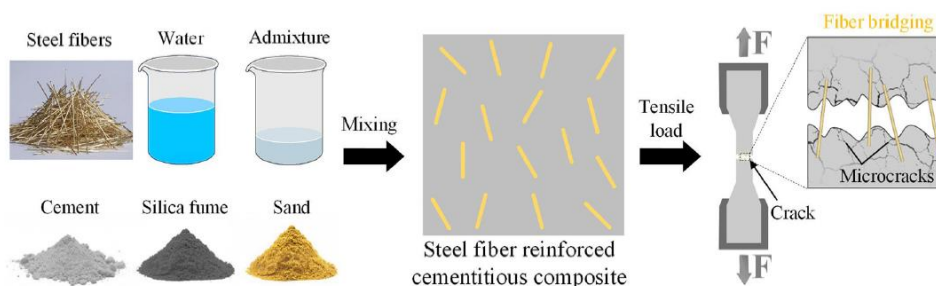
Figure 2.15:The bridging effect of the fibers at the matrix-fiber interface in SFRC

2.6.2 Bond strength

Steel fibers are added to improve the relatively low tensile strength of concrete. Significant improvements in ductility were observed as a result of the effect of reinforcement. During the occurrence of cracking, the load is transmitted to the fibers bridging the crack facilitating the stress to remain in the uncracked part of the matrix, provided the fibers are not getting pulled out of the matrix. Thus, the quality of the bond is a crucial factor in determining the mechanism and mode of failure of a composite. The fibers act as a stress transfer media, as their ends are anchored on each side of the crack during the occurrence of the crack [66]. The mechanisms in physiochemical bonds usually take place with the combined action of physical and chemical adhesion between the fibers and the cementitious composite. In contrast, mechanical bonding is developed through the fiber-fiber interlock and geometric deformations in the hooked-end, crimped, and twisted fibers. Consequently,

much research has been conducted to study more about each of the mechanisms responsible for bond-slip resistance. Bonds in steel fiber reinforced concrete can be classified based on the type of stress transferred across the interface. Figure 2.16 illustrates the tensile failure of concrete beams for; a) plain concrete without steel fiber reinforcement and b) with reinforcement. The steel fibers bridge the crack and prevent crack growth in the case of steel fiber reinforced concrete. A similar mechanism of bridging the cracks is possible with UHPFRC.
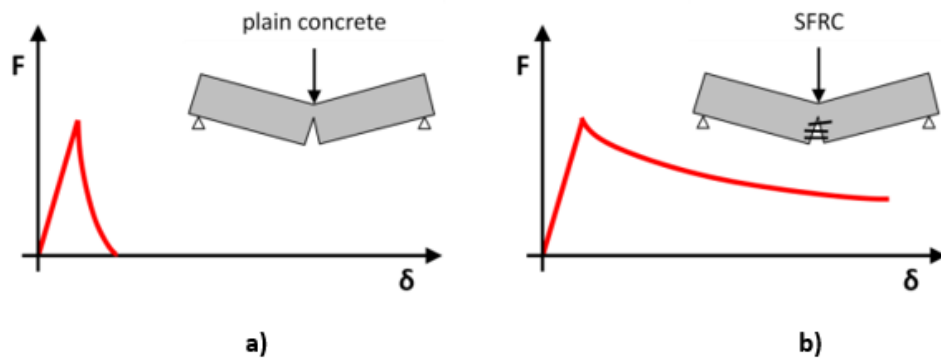
Figure 2.16:Schematic behavior of plain concrete (a) and SFRC (b)in a bending test [44]

The most significant effect of the addition of fibers in UHPC is reflected in their flexural and tensile strength values even though the compressive strength is also increased, which are almost more than double those obtained with the control UHPC without fibers. The short steel fibers added can be straight, hook-ended, or corrugated. The addition of steel fibers can reduce the flowability or workability of UHPC as it increases the frictional force between them and the concrete mix. The experiments show an inverse relationship between the fiber content and workability in UHPC. The length of the steel fibers plays a major role in the mechanical properties of UHPC. The compressive strength and durability are usually not affected by this. Generally, the steel fibers over 10 mm improve the tensile and flexural strength and increase the load capacity during fracture. This impact is mainly due to the increased bond area between the fiber and the matrix. Conversely, the excessive length of fibers can weaken the effective distribution of fibers in the matrix, leading to weakened behavior under flexure and tensile stresses [19].

As for most reinforced composites, a mutual interface is established between the fibers and the matrix by the adhesive chemical bond. The transmission of stress between fiber and the surrounding matrix is achieved when the bond acts as ITZ (inter-transition zone). The continuity of the ITZ facilitates the effectiveness of fibers in transferring the applied stress to the matrix. Thus, the strength of the bond within the ITZ is a key factor that significantly influences the composite's tensile response [66].

2.6.3 Type of fibers

Fibers in concrete are added to improve its structural integrity, including crack control. Fibers for concrete are available in different types, sizes, and shapes. The different types of fibers include steel fibers, synthetic fibers, glass fibers, carbon fibers, and natural fibers. In this paper, we study steel fibers in detail as they are used in the experimental part.

2.6.3.1 Steel fibers

The most common fibers used in concrete are steel fibers. They have a wide range of applications in the field of civil engineering [69]. Steel fibers used for reinforcing concrete can be defined as short, discrete fibers with an aspect ratio (ratio of length to diameter) ranging from 20 to 100 mm, with varying cross-sections. They are adequately small enough to be easily and randomly distributed in the fresh concrete through the conventional mixing procedure. An appropriate amount of steel fibers in the concrete can cause qualitative alterations in concrete properties, including increased resistance to cracking, toughness, impact, and bending with improved tenacity, durability, and blast loading properties[70]. The key characteristics of steel fibers are their higher tensile capacity, similar to the traditional reinforcement steel rebars. The incorporation of an appropriate amount of steel fibers into the fresh concrete can improve the bond between mortar matrix and aggregates, thereby boosting the toughness and energy absorption behavior. The significant contribution of steel fibers to the parent material is the enhanced ductility and improved strength properties such as tensile strength, compressive, and flexural strength.   Moreover, steel fibers can have a more significant influence in reducing the cost of construction as they can be used to substitute traditional reinforcement rebars, which are much heavier and require more energy, time, and resources for production [70].

A remarkable number of efforts took place to optimize the shape of steel fibers to achieve improved fiber-matrix bond characteristics and fiber dispersibility in the concrete mix. The classification of the general four types of steel fibers provided by ASTM 820 on manufacturing includes cut sheet, melt extracted, cold drawn wire, and other fibers. Figure 2.17 shows different types of fibers based on shape [71].
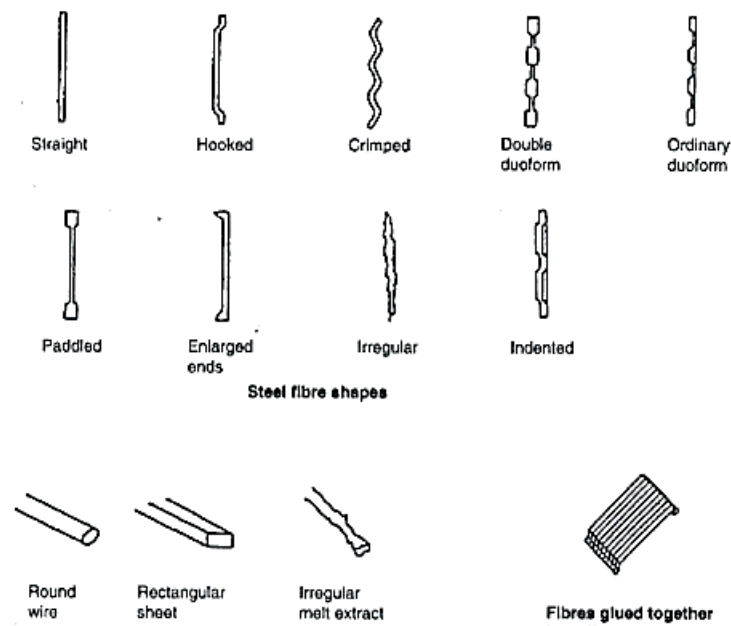
Figure 2.17:Different types of fibers based on shape [46]

The rounded and straight steel fibers, having a diameter between 0.25 -1.0mm, are usually produced by cutting and chopping wire. Moreover, the shearing sheet of flattening wire produces flat and straight steel fibers of 0.15-0.41 mm thickness by 0.25-1.14 mm width. The crimped and deformed steel fibers are produced based on the complete length crimping or bent or enlargement at each side of the fiber. The bending or flattening process used to deform fibers expands their bond and allows them to participate more in the mixing and handling. Generally, this mixing and handling are facilitated through fibers being collected into bundles. During the mixing process, these bundles are dispersed into single fibers. Young's modulus of steel fibers is 205 MPa, aspect ratio ranges from 30-100, ultimate tensile strength varies from 345-1700 MPa, and length varies from 19 to 60 mm for respective fibers [71].

2.7 New trends and applications of UHPFRC in the industry

The most significant application of UHPFRC is that it can be used for constructing lighter structures such as shells and walls. Another significant use is in the field of flooring and prefabrication. As UHPFRC is a reliable material with its higher toughness, it limits the crack propagation, providing high impact resistance. The use of UHRPRFC is directly aimed at certain specific applications. They are used in those situations where higher strength has to be provided along with higher safety. Since UHPRFC offers excellent durability, it makes that an ideal option to be used in structural elements that are exposed to aggressive environments. Furthermore, a great benefit with regard to its higher compressive and tensile strength is the possibility to reduce the dimensions of the structural elements in favor of a lower weight and better appearance. This possibility of reducing the sections and the mass paves a path in the right direction towards the perspective of new seismic-resistant buildings [72].

Figure 2.18:UHPFRC applications in the marine bridge (Extension of Haned airport) [65]

3   Response Surface Methodology (RSM)

Response surface methodology is a popular mathematical and statistical method for experimental design. The response of interest is affected by several variables, and the objective of this method is to optimize the response. RSM investigates to establish an appropriate relationship between input and output variables and understands the optimal operating condition for a system under research. Or in other words, this technique investigates the effect of the independent variables (Factors) over the response/output, either alone or in combination. The main idea of RSM is to use a sequence of designed experiments to obtain an optimal response. RSM, being a statistical approach, has been extensively employed to maximize the production of certain substances by optimizing the variables that participate in the operation. Design of Experiments (DOE) has been used extensively for this optimization using RSM.

3.1 Design Of Experiments, DOE

Design Of Experiment (DOE) is a multipurpose mathematical methodology that has been used for planning and conducting experimental programs. DOE (Design Of Experiments) is a branch of applied statistics that are used to perform scientific studies of a system, process, or product in which input variables (X_s) were manipulated to investigate its effects on measured response variables [73].

In Engineering and Research environment, experiments are often conducted to explore the relationship between the key input process variables (factors) and the output performance characteristics (that define the quality of the material), estimate the relationship, and confirm. Exploring includes understanding data from the process, whereas estimating refers to determining input variables' effects on the response characteristics. The confirmation step verifies the predicted results obtained from the experiments [73].

One of the very popular scientific methods employed by many engineers until the 19th century was OVAT-one variable at a time. In this method, one variable was varied, keeping all other variables fixed in an experiment. However, this approach was later considered inefficient, unreliable, and time-consuming as this largely depends on other factors such as guesswork, luck, experience, etc. [73, 74].

The statistical method has an essential place in planning, conducting, analyzing, and interpreting data in engineering experiments. It can help the engineers deal with the variability, fix the variables, measure the responses, and enable them to make the best decision. When several variables influence the character of a product, it is important to understand that not all variables affect the performance of the system in the same manner. Therefore, the objective of DOE is to identify the corresponding

variables that have a strong influence on the performance characteristics and thereby determine the optimal levels.

Table 3.1:Comparison of experimental designs based on the conventional and statistical method [75]

Experimental Design	
Conventional method	Statistical method
➢ OVAT-one variable at a time ➢ Time-consuming, unreliable, and inefficient ➢ Largely depend on other factors such as guesswork, experience ➢ Cannot interpret the interaction between 2 or more variables	➢ It is known as the Design of Experiment ➢ Modeling is used to predict the behavior of process variables ➢ Could predict the relationship/interaction between the values of some measurable response variable(s) and those of a set of variable parameters that can influence the response ➢ Can interpret the interaction between more than 3 process variables and can predict the response value at various process conditions ➢ Reduce time and improve efficiency ➢ Reduce the number of experiments ➢ Optimization: Could find the factors' values that produce the best value or values of the response(s).

Table 3.1 compares experimental designs based on the conventional and statistical methods and the advantages of the statistical method over the conventional method. The Design of Experiments (DOE) was first developed in the 1920s and 1930s by Ronald A Fischer. He conducted research in agriculture intending to increase crop yield in the U K. In the research, Fischer had to determine the effect of various fertilizers on different plots of the land, and the condition of crops was influenced by a number of factors other than the effect of fertilizers. Thus Fischer came up with a DOE that could differentiate the impact of each factor on the performance of the system [74]. In 1935 Fisher wrote a book on DOE, in which he detailed how convincing and valid conclusions can be made from experiments in the presence of nuisance factors. He analyzed these nuisance factors under the fluctuations of the weather conditions such as rainfall, temperature, and soil conditions [74].

Although DOE was developed primarily for agriculture purposes, this statistical method has been widely applied in various fields of science and industry, notably to support the design, development, and optimization of processes and products. DOE consists of a series of applied statistical tools used to categorize and quantify cause systematically- and effect relations between variables and responses in the studied phenomenon or experiment, which can result in finding the circumstances and conditions or combinations of the variables under which the process becomes optimized [76]. There exist well-established guidelines and procedures that support the implementation of DOE methods. Figure 3.1 presents the steps and components in DOE.

Objective
- screening
- Prediction
- opitmization

Factor
- Fixing the number of independant variables
- Fixing the levels of each variables
- Fixing the range of eah variable

Type of design
- Fixng the type of design
- full factorial,fcractional factorial
- CCD,Box-behnken
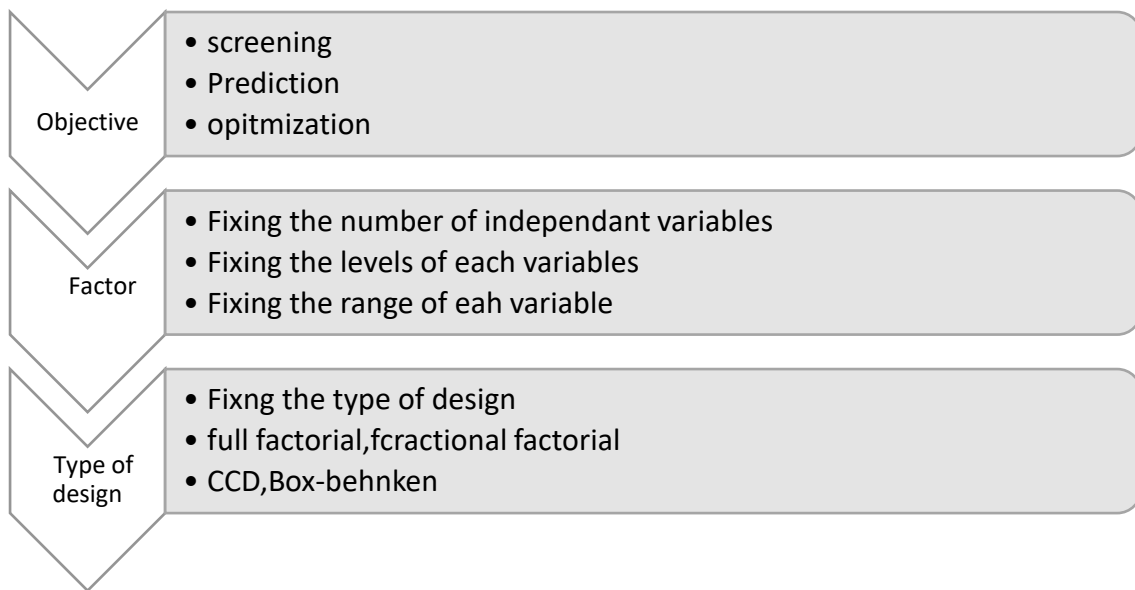
Figure 3.1:DOE steps and components

3.2 Major Steps in DOE

Design Of Experiments (DOE) consists of a number of steps that are elaborated in this chapter;

1)Defining the Objective and response variables: This step includes screening and optimization. The objective of the process or study is defined and the output or response of the process, which has to be optimized is determined in this step. The response should be a measurable quantity, the value of which is assumed to be affected by modifying the levels of the factors and can be optimized.

2) Selecting the parameters/factors: During this step, the significant factors that cause a potential impact on the response are carefully chosen. The factors should be process conditions that can influence the value of the response variable. These factors can be either quantitative or qualitative.

3) Determining the levels and range: Variables in the DOE and their levels and range are usually determined based on the type of investigation, process type, and available resources. There is Two-level(2^k), Three-level (3^k), and Five levels (5^k) are the levels normally used [75].

4)Selecting the experimental design type: The experimental design type is finalized based on the available guidelines that can facilitate finding the appropriate design from the available ones. The popular designs available are Full factorial design, fractional factorial design, CD, Box-Behnken design, etc. The most popular ones are CCD and Box-Behnken designs [77].

5) Execution of experiment: The last step after designing the experiment through the earlier steps is the actual execution of the experiment, which gives a response that can correlate with the response given by the experimental design.

6) Data analysis: This step can be performed using statistical methods or software such as regression or ANOVA

7)Practical conclusions and recommendations: This step includes a graphical representation of the results that can be generated using statistical software such as Minitab and validating the results.

Application of DOE in scientific research

Being a multipurpose tool, DOE can be used in a variety of situations to identify the critical input parameters (input variables) and how they are related to the output (response variables). Although DOE is not a recently developed tool, its application has been widely expanded over the last two decades in the scientific field, including product/process quality improvement, product optimization, and services. The application of DOE across various scientific fields during the period from 1920 to 2018 across the globe is shown in Figure 3.2. Though the application of DOE in research started in the 1920s, significant use of DOE was begun in the late 1960s and 1970s. Thus, it took around 50 years for the DOE to achieve substantial application in the research. The development of software in this connection was developed in the 1990s, and thereafter the popularity of DOE in research in the scientific field rose sharply.
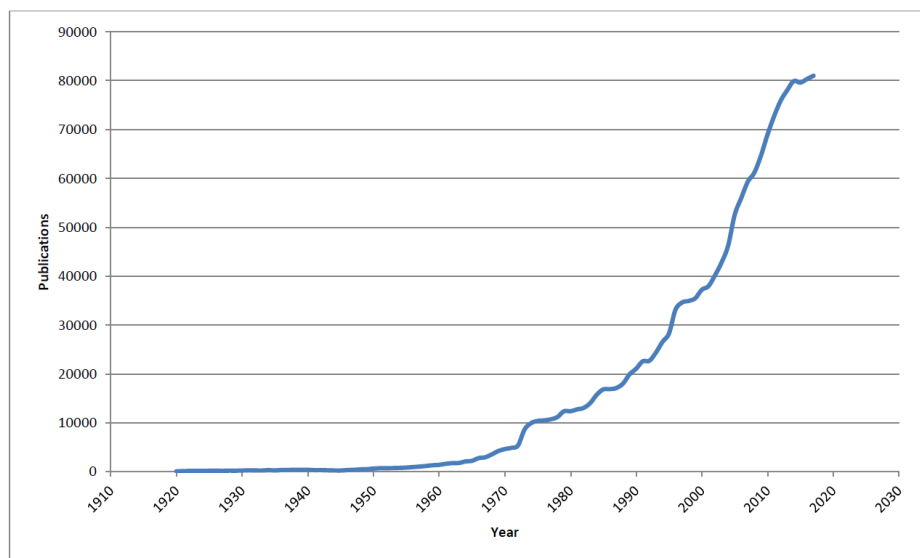
Figure 3.2:Application of DOE across various scientific fields during the period (1920-2018) [66]

DOE software

DOE can be swiftly designed and analyzed with the help of appropriate software. Some commercial and freeware software packages available to serve this purpose such as Minitab, Statistic, SPSS, SAS, Design-Expert, Statgraphics, Prisma, etc. In addition, the DOE design and analysis can also be done using Microsoft Excel using the guidelines and procedures given [74].
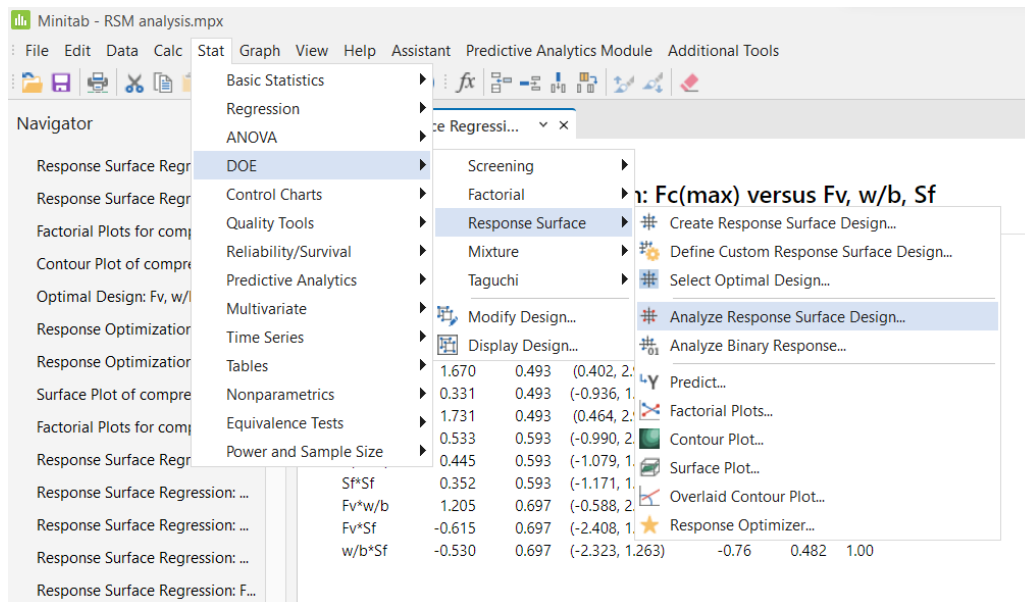
Figure 3.3:Response surface analysis using Minitab

The most popular commercial packages are Minitab and Design Expert, which facilitate user-friendly interface and excellent graphics output[78]. Minitab was used for the study of the response surface in this paper (as shown in Figure 3.3), which offered a free license for 30 days.

Response Surface Methodology; a useful research tool

RSM is a set of advanced DOE methodologies that enable the researchers better understand and optimize their response. DOE has the goal to obtain maximum information with the minimum number of experiments

The first and foremost step in RSM is to identify the factors, or in other words, the dependent variables that affect the response surface. After this step, the experimental design is done according to the factors determined, and regression and optimization techniques are modeled using one within another [79]. The parameters affecting the process are called independent variables, while the responses are dependent variables.

For example, consider the rainfall intensity of an area is affected by the depth of rainfall X_1 and the duration of the rain X_2. Therefore, the rainfall depth and duration of the rain can vary continuously. The rainfall intensity can be any combination of X_1 and X_2. Suppose these dependant variables are

from a continuous range of values (with defined intervals). In that case, RSM is a beneficial tool for developing, improving, and optimizing the response variables, a function of rainfall's depth and the rainfall duration, which can be mathematically represented as Eq.3.1.

$$Y = f(X_1) + f(X_2) + e$$

(3.1)

where Y- is the response (dependant variable) ;

X_1 and X_2-are the independent variables, and 'e' is the experimental error.

RSM is an efficient statistical tool for experimental design, model building, evaluation of the factor's effects, and the searching for optimum conditions. RSM is one of the DOE branches, and it uses a collection of mathematical and statistical techniques to produce a robust design for experiments [80].

Defining independant variables and levels

Choose the experimental design

Planning DOE based on the experimental design

NO

Performing regression analysis

Comparing of predicted and actual results

YES

Determining the optimal design
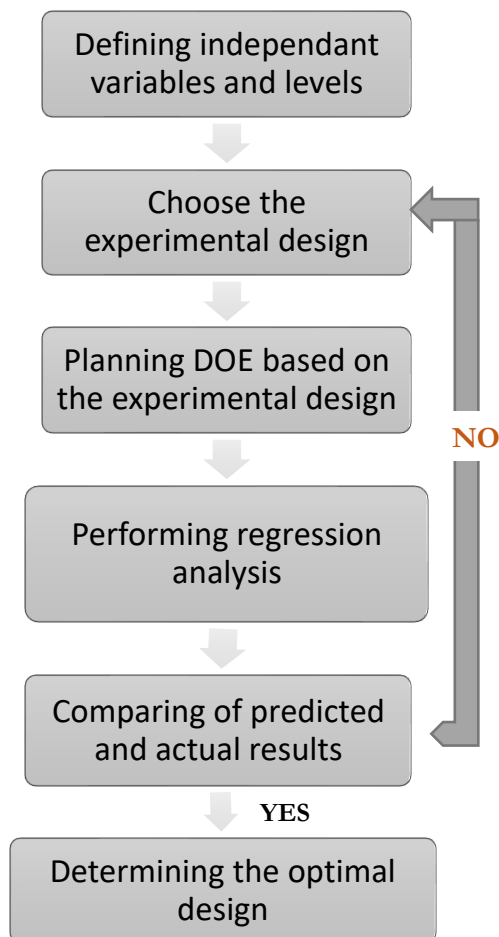
Figure 3.4:Various steps involved in the research using RSM as a research tool

Figure 3.4 demonstrates the various steps involved in the research using RSM as a research tool [80].

49

3.3 Statistical background of RSM

The response surface method was first introduced for the first time by Box and Wilson in 1951 and has been attained popularity over the years and still used as one of the efficient experimental design tools in the industry and science. RSM and linear regression analysis have a strong relationship with each other. In RSM, attempts are made to find ways to estimate interaction so the linear and quadratic effects and the local form of surface response using a quality experimental program. If the applied surface provides a desirable approximation of the actual response surface, the response surface analysis can be compared with a similar approximation of the actual system analysis. This was understood by carrying out a series of experiments involving various factors. The statistical basis of RSM is polynomial regression modeling [77].

The general setup of the method is; The response variable will be continuous quantitative variables (eg, capacity, yield, strength, etc.), and the mean response will be an unknown function of the levels of K factors (e.g., temperature, fiber percentage), where levels of these factors are real and can be controlled precisely. These factors can be arranged in a particular type of experimental design that allows for fitting that allows for second-order polynomials to the quantified response. After the analysis, the mean response, when plotted as a function of the combinations of the factors, will be known as the response surface as shown in Figure 3.5 [77].
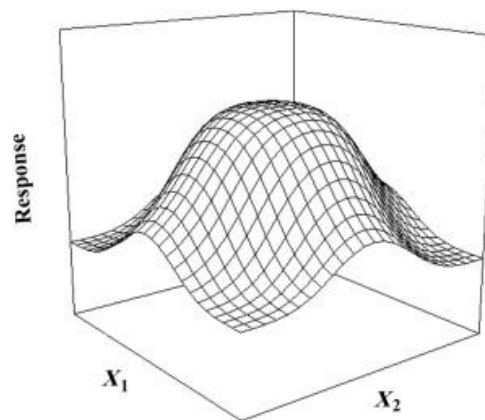
Figure 3.5:Example of response surface [72]

A response surface design can be defined as a set of advanced DOE techniques that are capable of better analysis and optimization of the response. Response surface methodology is generally used to refine the models after determining important factors using screening designs or factorial designs, especially considering the curvature in the response surface. The response surface models may involve either main effects and interactions, or they may have quadratic or cubic terms to account for curvature, as shown in Figure 3.6.
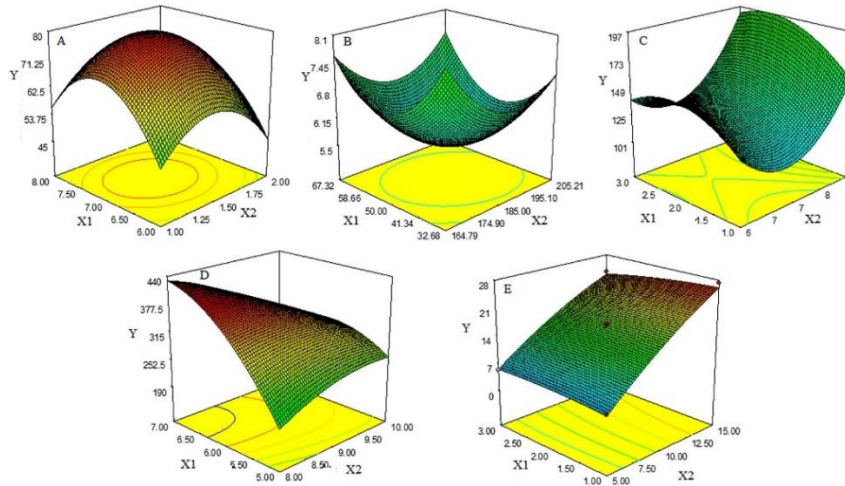
Figure 3.6:Different response surface plots and relative 3D for the second-order model. (A: maximum, B: minimum, C: saddle, D: maximum outside the experimental region, and E: plateau) [75]

The difference lies between the equation for response surface design and the equation for factorial design. The addition of the cubic or quadratic terms that enable the modeling curvature in the response has the following advantages.

- Response surface equations can model how changes in the variables affect the response of interest.

- Response surface equations can find out the levels of the variables that optimize the response.

- It can also determine the operative conditions for the optimal design that meets the required specifications [78]

3.4 Types of RSM Designs

Response surfaces can be employed to determine the settings of factors that produce the desired (maximum, minimum, or optimum) response, satisfy the specification requirements, and model the relationship between the factors and the measured response.

Although there are several models exist for the experimental design using RSM, Box Behnken designs (BBD) and Central composite designs) CCD) is the most popular experimental design used.

3.4.1 Central Composite Design (CCD)

A Box-Wilson Central Composite Design, commonly called CCD, was first explained by Box and Wilson (1951) and, in practice, is the most commonly used response surface design.

The CCDs shown in Figure 3.7 consist of:

- 2K factorial points in (Fig 3.7) are also called cube points, where 'K' is the number of factors in two levels (both a and b). The factorial points considered are 4 and 8 for k=2 and 3, respectively.

- Axial points, also known as star points, are located at a given distance α from the design center in each direction and on each axis that allows curvature estimation. Therefore, there are 2K axial points if there are K factors. Though the choice of α depends on the type of design, the common

value used is $\alpha=(2K)^{1/4}$. The axial points are 4 and 6 with $\alpha =1.414$ and 1.682 for k=2 and k=3, respectively. The axial points are usually outside the cube, as shown in the figure below, but those points could be at the cube's interior, on the cube, for $\alpha=1$, or for $\alpha<1$. A special type of CCD with $\alpha=1$ is the face-centered design, where the axial points are at the center of each face of the factorial space.

- CCD designs should have enough possibility of replication, often at the center points, that enable checking the model's accuracy. The default number of center points is 5 and 6 for K=2 and three designs, respectively [77, 81].
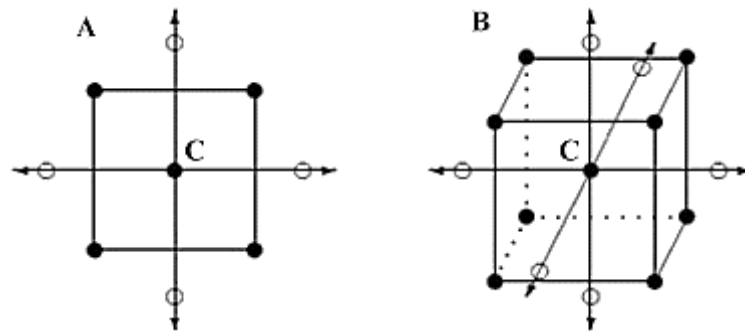
Figure 3.7:CCD with a) two factors (b) three factors. Shaded circles are factorial points, unshaded circles are axial points, and the shaded circle in the middle labeled with C is the center point [69].

The total of factorial points, axial points, and center points determines the total number of experimental runs that should be executed, which are 13 (4+4+5) and 20(8+6+6), respectively.

In a response surface design, the high level and low level should be defined for each factor: the low level of all factors is coded to -1 and the high level to +1, then the center point is the average of the two levels and coded to 0. For instance, if a CCD with two factors (water-cement ratio; 0.5 and 1: steel fiber content in % ;2 and 3), the factor combination coded as (-1+1) corresponds to w/c= 0.5 and steel fiber content= 3%. The center point is coded as w/c= 0.75 and steel fiber content=2.5%; then, the axial points are at a distance from $\pm\alpha$ from the design center [77].

A second-order polynomial should be fitted for the data analysis. The standard second-order polynomial model is given as equation (3.2) for K factors.

$$Y_{x,t} = b_0 + \sum_{i=1}^{K} b_i x_i + \sum_{i=1}^{K} b_{ii} x_i{}^2 + \sum_{i<j} b_{ij} x_i x_j + \varepsilon_{x,t}$$

(3.2)

where $Y_{x,t}$, is the tth response observed for the combination of factors (X_1, X_2, ..., X_K); the random variable $\varepsilon_{x,t}$, , is independent with N (0, σ^2) distribution. The parameter b_i characterizes the linear effect of the ith factor, the parameter b_{ii} represents the quadratic effect of the ith factor, and b_{ij} indicates the cross-product effect, or interaction effect, between the ith and j[th] factors [82].

The polynomial equation (Eq.3.2) is subjected to the scrutiny of variation to test the significance of the linear, quadratic, and interaction terms. Validation of the final model consisting of significant terms against the observed responses should be carried out using statistical measures. This validated regression model is a powerful tool for deciding factor levels for achieving the desired response depending on the demarcated specifications. Since each of the responses is significant for determining a system's desirability, all responses are to be considered simultaneously.

Response optimization is an approach that enables trade-offs among various responses and recognizes the combination of factor settings that optimize a set of response variables [77]. Central Composite designs have the desired properties of orthogonal blocks and rotatability.

Orthogonal blocks: CCD is usually done in more than one block. Those blocks can be orthogonal, allowing the model terms and block effects to be estimated independently and minimizing the variation in the regression coefficients.

Rotatability: CCD can provide rotatable designs that provide constant prediction variance at all equidistant points from the design center [78].
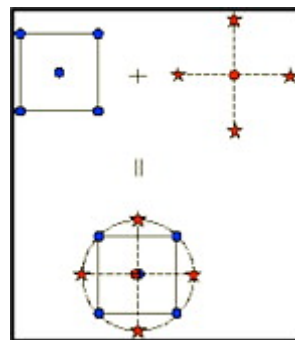
Figure 3.8:Generation of a CCD model [73]

For a factorial design, the levels of the points of a are ±1, and the start designs are ±α, where $|\alpha| \geq 1$[81]. CCD consists of 2^k factorial points with n_F factorial runs, 2k axial (star) runs, and n_c central runs. These factorial runs are usually used for fitting the first-order model and the axial runs for the fitting of second-order sentences. The value of α decides the distance between the axis and the center points. Rotationality is another judicious factor in choosing the response surface design [80]. Figure 3.8 demonstrates the generation of a CCD model.

Face-centered design: Face cantered designs are the type of central composite design with *α=1.* In this design, the axial points are the center of each face of the factorial space. The FCCD consists of axial points located on the cube's five-sided surface.

The number of experiments to be performed in a central composite design is decided by the following formula when the factorial design is full: $N = 2^k + 2k + N_0$. Table 3.2 represents the number of experimental runs using CCD.

Number of experimental runs in a CCD					
Number Of factors	2	3	4	5	6
Number of coefficients to estimate	6	10	15	21	28
Number of experimental runs	9	15	25	43	77

Specialized software such as MINITAB, SAS, and Design Expert can provide CCD based on fractional factorial designs that limit the number of tests; for instance, it is possible to process six factors with 30 tests (rather than 77 tests).

Figure 3.9 displays the Minitab screen, that generated 15 experimental runs for our experimental work using RSM, as 15 is the minimum experimental runs for 3 factors using the CCD model. This endorses the application of statistical software to limit the number of tests which could save time and materials.
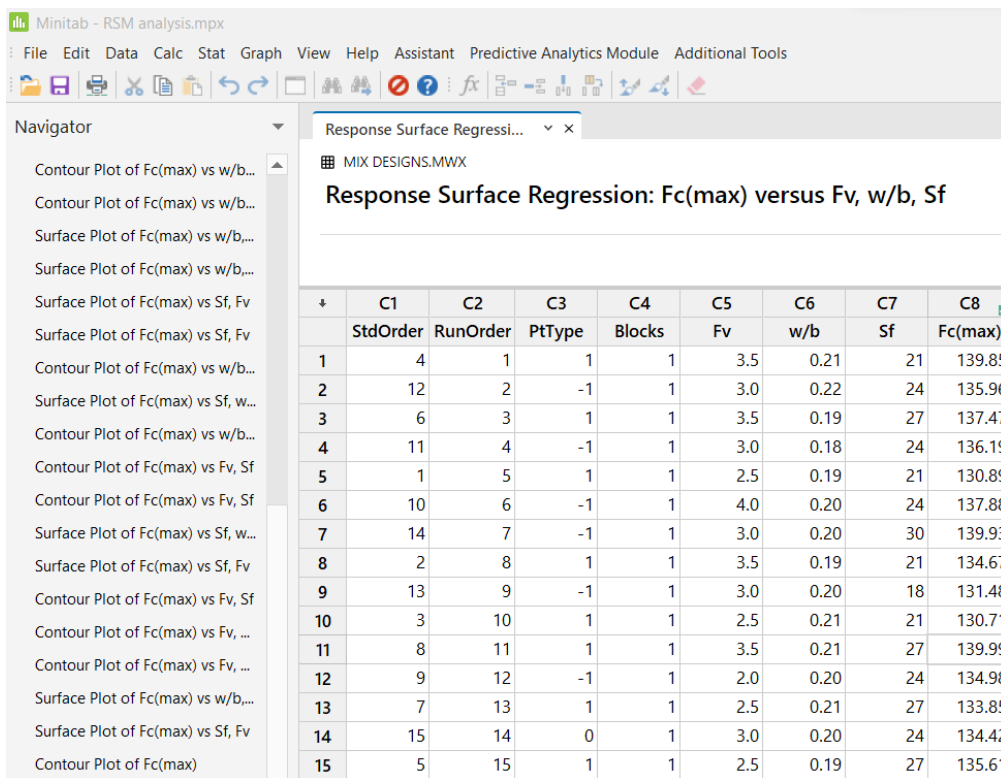
Figure 3.9:Experimental runs (15 no) generated by Minitab

As the target of RSM is optimization, while the position of the optimal point is unknown prior to testing, a design that is capable of delivering equal accuracy for estimation in all directions is advantageous.

3.4.2 Box Behnken Designs (BBD)

The Box Behnken Designs (BBD) can also facilitate modeling the response surface. However, these designs are not based on full factorial or fractional factorial designs. These designs can generate higher-order response surfaces using fewer required runs than the normal factorial technique. Box

Behnken designs use the twelve middle edge nodes and three center nodes to fit a 2nd order equation. The design points are located in the middle of the sub-areas of the dimension k-1. For instance, if three factors are considered, the points are positioned in the middle of the edges of the experimental domain, as shown in Figure 3.10 [81].
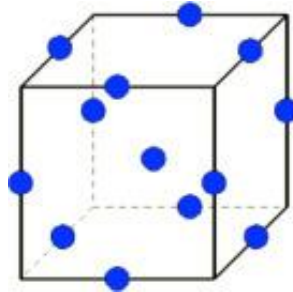
Figure 3.10:Example of three factors Box Behnken Design [73]

Box-Behnken Designs generally have fewer design points than CCD, classifying them as less expensive to execute than CD with the same number of factors. However, since they do not have an embedded factorial design, they are not the right choice for designing sequential experiments. BBD has been useful primarily when the safe operating process of the zone is known.

CCD usually have axial points outside the cube, which may not be in the region of interest or impossible to conduct as they may be beyond the safe operating limit. Since BBD does not have axial points, it can be ensured that all the points fall within a safe operating zone. BBD also confirms that all the factors are not set to their high levels simultaneously [78].

BBD often requires three levels per factor. But BBD for three factors does not comply with the iso-variance per rotation criteria. In contrast, the BBD with factors above three can comply with the criteria of iso-variance criteria if the points are added to the center. Table 3.3 represents the number of experimental runs in BBD.BBD can also respect the criteria for orthogonality [81].

Table 3.3:Number of experimental runs in a BBD

Number of trials in a BBD				
Number Of factors	3	4	5	6
Number of coefficients to estimate	10	15	21	28
Number of experimental runs	13	25	41	49

3.5 Application of RSM in civil Engineering

It has been reported that RSM has a great application in industrial processes, as it can be widely used for optimizing the product and processes. There are several models and methods used in optimizing the field of concrete technology. RSM provides statistically validated models that can be deployed for establishing optimal process configurations. It is typically useful in those situations where several parameters influence one or more responses or performance characteristics and to optimize more

than one response to meet specific requirements. This method also facilitates sufficient experimental interpretation of the non-linear response surfaces of the experimental results. In RSM, several parameters that vary simultaneously are fitted to the polynomial function. Moreover, it proportions the constituent materials to achieve optimum mix proportions used as a mathematical model for predicting the desired responses.

RSM has the predictive capacity to determine the concrete properties such as compressive strength, tensile strength, slump, water absorption capacity, etc. This method enables the researchers to design the experiment to reduce time and drudgery associated with the repetitive number of experiments to be performed. The accurate and speedy determination of the properties through this method can considerably reduce construction time, especially when there is a demand for faster project execution. The application of such an innovative experimental design facilitates opportunities to carry out appropriate changes in the mix-proportions of concrete ingredients to attain the design objectives. This approach prevents the circumstances in which concrete's aimed design strength is met, or concrete with excessive strength is produced.

The optimization of mix-design using RSM can invariably result in the utilization of raw materials cost-effectively and can indirectly result in reduced construction failure and reduced construction cost. RSM has also been used as research a method in numerous research regarding cement and concrete, including damage detection, non-destructive testing (NDT), etc.

History of RSM application in the design of cement-based materials

RSM has been employed to choose the better response region from the response surface by defining the response surface of the response on the parameters so as to establish the optimization method of the optimal experimental condition. In fact, RSM has been applied in the design of cement-based materials in the past. For instance, Linoshka et al. used RSM to design cement-based materials with compressive strength as the response and establish a model, considering the effect of chosen parameters(w/b, fly ash content, and nano-iron oxide content) on the response [83]. In 2017, Fedosian et al. developed a statistical model based on RSM aimed at producing eco-efficient UHPC with improved workability [84]. In 2018, Mohammed et al. applied RSM in their research to establish a statistical model regarding the mechanical and post-cracking properties aimed at improving the performance of engineered fly ash-based geopolymer composites[85]. In 2019, Yu Sun et al. studied the effect of porous aggregates carrier in effectively reducing autogenous shrinkage of UHPC without compromising durability, using the application of RSM [86]. T F Awolusi et al. in 2019 used RSM to predict and optimize the properties of concrete containing steel fiber extracted from waste tires with lime stone as filler[87].In 2020, Hou et al. developed a statistical model for optimizing magnesium phosphate cement-based rapid materials via RSM [88].

The above papers referred highlighted the successful application of RSM in establishing appropriate and accurate modeling and optimization of concrete mixes that are stronger, workable, durable, and sustainable.

Kioumarsi et al.[89] evaluated the nonlinear behavior of a reinforced concrete bridge pier wall by nonlinear finite element analyses (NLFEA) method and RS; prediction models were developed for thermal conductivity of cementitious composites [90]; a statistical model was developed to predict the maximum shear load capacity of SPSW with a rectangular opening and analyzed using the NLFEA [82].

Considering the previous studies with regard to the application of RSM in concrete and cement, it can be ascertained that adopting RSM would be an efficient and accurate approach to optimize the performance of UHPRFC. In light of the above studies, RSM is applied to establish a statistical relationship between the variables, I,e w/b, F_v(steel fiber %), and S_f (silica fume content) and the compressive strength as the response in this study.

4   Method

The study was conducted preliminarily by literature review, followed by experimental work. The literature review provided insights into carrying out the experimental work. A significant part of the experimental design was done using Response Surface Methodology (RSM). In addition to the experiments in connection with the application of RSM to establish a statistical relationship between the variable parameters and the compressive strength of UHPFRC, a number of additional experiments were also performed to analyze the effect of a higher dosage of steel fibers in the mechanical properties of UHPFRC.

The method adopted for this study consists of several stages and procedures. The first and foremost step was to formulate the research objectives. A thorough literature review followed this step, and the tools for carrying out the study were identified as an experimental program, which further bifurcated for achieving the desired objectives. The results from the experiments conducted at the laboratory and the analyzed data using the Minitab software were discussed and interpreted with the previous studies to arrive at the conclusions and examine the scope for further work. An overview of the method, the steps, and the procedures implemented; in this study is illustrated in Figure 4.1.

4.1 Literature review

As the literature review provides an overview of the current knowledge, relevant theories, methods, and research objectives, the primary step of this thesis was a literature review through which the research gaps were identified and proposed the research objectives. Even though literature review is presented here as a method used for the thesis, the other methods to investigate the research objectives were discovered after reviewing several papers regarding UHPFRC[5, 6, 8, 10, 13, 14, 17, 29, 32, 37, 53, 60, 66, 72, 84, 91-97]. Since the thesis is a continuation of the previous project report prepared last semester, the literature search also progressed accordingly.

As mentioned earlier, the thesis mainly focused on applying RSM and investigating the effect of higher fiber dosages. The experimental design for accomplishing each task was devised separately. As the experimental design using RSM needed further insight, we reviewed several papers [9, 75-77, 79, 80, 82, 84, 85, 87-89, 98, 99] regarding the application of RSM in scientific research generally and in cement and concrete specifically. This gathering of detailed information and procedures is reflected in the further process of the thesis. The influential parameters and responses for the RSM investigation were selected and finalized after referring to several papers [9, 79, 82]. Also, the higher fiber dosage range and mechanical properties were fixed based on the previous papers reviewed [14, 60, 97].
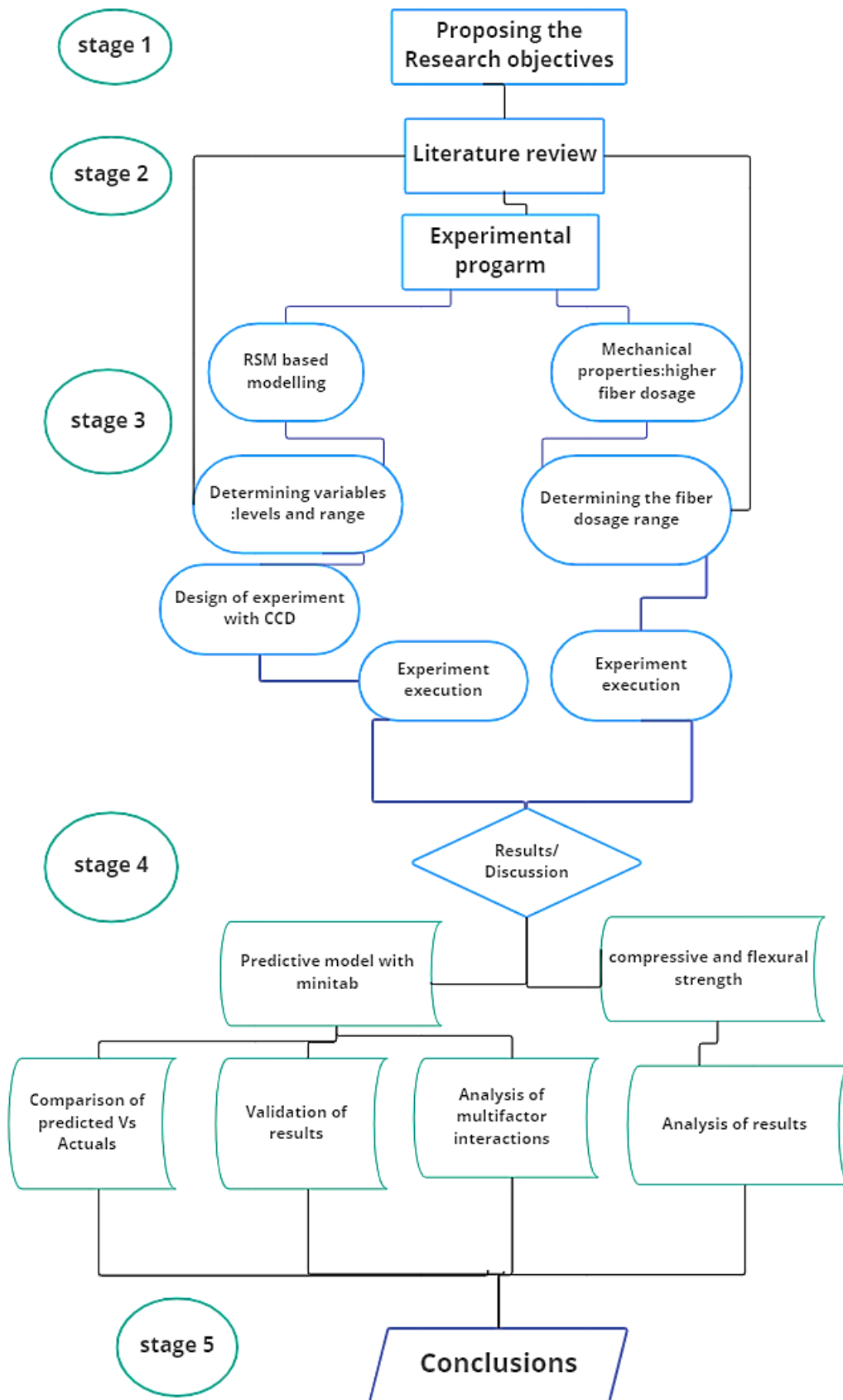
Figure 4.1:Flow chart illustrating the method used

4.2 Experimental program

The experimental program consisted of; i) RSM-based optimization and modeling, where 15 runs of experiments were carried out to optimize the results, and ii) additional 4 experiments, where the mechanical properties of UHPFRC with higher fiber dosage were analyzed.

In response surface methodology (RSM), the models are developed based on the data in experimental design, explaining the relationship between the factors (independent parameters) and response (dependent parameters). These models can evaluate the influence of each parameter and the influence of interactions of combinations of the parameters on response and process optimization [98].

The application of response surface methodology as a modeling and optimization tool requires many stages that primarily involve factors chosen, design of experiment, appropriate model selection, validation of the model, graphical representation of the models, and optimization, as explained in Figure 4.2.

Choice of parameters
- The variables that can influence the response most have to be selected
- Silica fume (Sf), Steel fiber (Fv) and w/b are considered

Experimental deisgn
- Range and levels are judiciously fixed(5 levels for each variable)
- The design type is chosen is CCD
- 15 experimental runs to be performed for 3 variables
- 45 spceimens casted and the 28th day compressive stregth tested

Analysis
- Statistical relationship between variables and response is obtained from Minitab
- Actual test results and predicted values are compared
- validation of the propoesed regression model is done
- Response surface anlaysis is done with contours and 3D plots to understand intearcation effects of variables with response

Figure 4.2:Steps involved in RSM

The basic UHPC recipe used for the experimental program (provided in chapter 4.2.3) is obtained from the Master thesis (Sirak & Ahmed 2022) developed at the OsloMet laboratory. After testing various mix designs, this optimal UHPC mix was finalized to achieve maximum compressive strength without compromising flowability [100]. The choice of the right recipe was made based on the flowability and the 7th-day compressive strength test done without steel fibers.

4.2.1 Materials used in the experimental program

Figure 4.3 provides an overview of the major materials used for preparing the UHPFRC mix to perform experiments.

Figure 4.3:Materials used for the experimental program

The physical and chemical details of each component used for the experiment are explained in the following.

Cement: The cement used for the experiment was Portland composite cement EN197-1 CEMII/B-M. The physical and chemical properties of the cement are given in Table 4.1 and Table 4.2;

Table 4.1:Physical properties of cement used

Physical properties of cement used		
Fineness	450 m2/kg	
Soundness	1 mm	
Initial setting time	140 minutes	
Compressive strength	2 days	31 MPa
	28 days	55 MPa

Table 4.2:Chemical composition of cement

Chemical Composition	%
CaO	57
SiO_2	24
Al_2O_3	6.5
Fe_2O_3	2
MgO	5.3
SO_3	3
K_2O	0.65
Na_2O	0.3
Alkali equivalent(Na_2O eq)	0.73
C_3A	5.3
Cl^-	0.05
Cr(VI)	< 2

Sand (Sand A and B): Two types of sand are used in the mix. The finer sand used in the mix is hereafter named Sand A, having a size of 0.1-0.4mm, and the coarser sand, named Sand B, has a size of 0.4-0.8mm; Mapei AS supplies the sand.

sand A (0.1-0.4mm)   sand B (0.4-0.8mm)

Figure 4.4:Sand used for the experiment

Silica fume/Micro silica: The micro-silica provided by Elkem is used here. This consists of spherical primary particles, having an average diameter of 0.15 micron. The particles' specific gravity is about 2.3 and doesn't have any internal porosity.

Figure 4.5:Silica fume used for the experiments

Water: The water used throughout the experiments was normal water maintained at room temperature (around 20^0C).

Superplasticizer (HRWRA): The superplasticizer used in the experiments is Master Ease 2050, supplied by Master Builders; this is a super plasticizing additive that enables low viscosity to concrete and provides optimal rheological properties. The active component in this SP is polycarboxylates. The pH value is 10.0±1.5 and the density is 1,05 ± 0,02 kg/l .

Figure 4.6:Superplasticizer used for the experiments

Steel fibers: The steel fibers used in this study are Dramix ® OL 13/.20 straight steel fibers. The material properties and geometry are given in table 4.3 (EC Declaration of Performance DRAMIX® OL 13/.20 [101]).

Figure 4.7:Dramix OL 13/.20 steel fiber from Bekaert

Table 4.3:Material properties of straight steel fiber[101]

Material properties	
Fiber shape	straight
bundling	loose
tensile strength (N/mm2)	2750
Young's modulus (GPa)	200
Length(mm)	13
diameter(mm)	0.21
Aspect ratio	62

4.2.2 Spread test

The spread test is conducted to find the flowability of freshly mixed UHPC. This test is considered a versatile test for checking the quality of freshly mixed UHPC. The test is based on ASTM C1437, "Standard Test Method for Flow of Hydraulic Cement Mortar." The freshly mixed UHPC is spread into a spreading cone (Figure 4.8). This test should be done with special care to keep the humidity level of the spread cone and base plate at the same level. This has to be ensured before testing. The mix need not be compacted in the mould as the UHPC paste has high inherent flowability. The spread cone has to be filled up to the rim and then lift it with a constant speed. The leftover mix sticking to the interior surface of the cone is scraped off and added to the paste on the baseplate as it spreads. The diameter of the mix's spread (circular in shape) is measured along with two orthogonal directions after 2 minutes ± 5 seconds, and the average diameter is calculated and recorded as the spread value.

Figure 4.9 demonstrates different stages of the flow test conducted in chronological order (from left to right). The spread value (the measured spread diameter) is a measure of flowability. The acceptable spread values range between 175 mm and 300 mm, and the spread values beyond this range indicate

that the mixture should be rejected [102]. Previous studies found a linear decrease in the compressive strength by increasing the flow diameter but keeping the flow diameter between 150 mm and 185 mm for initial flow and between 180mm and 210 mm after 20 drops in 20 s, fulfilling the self-compacting capability of UHPC [102].

Figure 4.8:Cone used for the spread test

Figure 4.9:Various stages of the flow test

4.2.3 UHPC recipe

The UHPC recipe used in the experimental program is given in Table 4.4, and the ratios adopted for developing the recipe are shown in Table 4.5; This basic recipe is followed throughout the experimental program, incorporating variations as per the experimental design.

Table 4.4:The basic UHPC recipe without steel fibers [100]

Component	Quantity - [kg/m3]
Cement - OPC	783.6
Sand A (100-400 microns)	951.6
Sand B (400-800 microns)	237.6
Silica Fume	196.2
Water(w/c=0.25)	195.6
HRWRA(SP)	93.9
Steel fibers	0

Table 4.5:Major ratios for UHPC recipe

Water cement ratio W/C	0.25
Water Binder ratio W/B	0.22
Silica fume(Sf)	25%
HRWRA (SP)	5.5 %

The experimental program progressed through the following general steps.

Weighing the ingredients: The dry ingredients were weighed using the bigger weighing machine, water, and SP with the graduated cylinders and beakers(Figure 4.10 [103, 104]. The room temperature of the ingredients is kept at 20^0C. The water used for the experiment was normal (neither cold nor hot) and kept at room temperature, at 20^0C.

Figure 4.10:The devices and equipments used for weighing the ingredients

Mixing: A pan mixer (Figure 4.11) with a capacity 50 kg (40 ltr) and a high-speed whirler,1.5KW was used to mix the UHPC constituents.

Figure 4.11:Pan mixer used for mixing Zylkos

For the mixing part, the dry ingredients such as coarse sand, fine sand, and silica fume are first mixed for 3 minutes. Thereafter cement was added and mixed for another 5 minutes. After 5 minutes, half of the water and half of the superplasticizer (SP) were added to the hole made in the middle of the mixture. This is mixed for 1 minute, and then the remaining water and SP are poured through the top-notch of the mixer into the mix gradually. The mixture is kept under mixing for 15 minutes.

Finally, steel fibers were added, and mixing continued until fibers were fully dispersed for 5 minutes. The mixing procedure is tabulated as per Table 4.6. As we planned to cast beams as well as cubes from each mix, the mixes were large batches within the capacity of the mixer to carry out the mixing.

Ingredients	Mixing time (in minutes)
Sand A (fine sand) , Sand B (coarse sand) and silica fume	3 min
cement	5 min
water and SP	15 min
steel fibers	5 min

Casting: The fresh UHPC mix was poured into the moulds right after the flow test without any compaction process as UHPC is considered a self-compacting concrete. The cubical moulds used are plastic moulds of 100 mm side, and the beam moulds were steel with a size of 100x100x500mm, as shown in Figure 4.12.
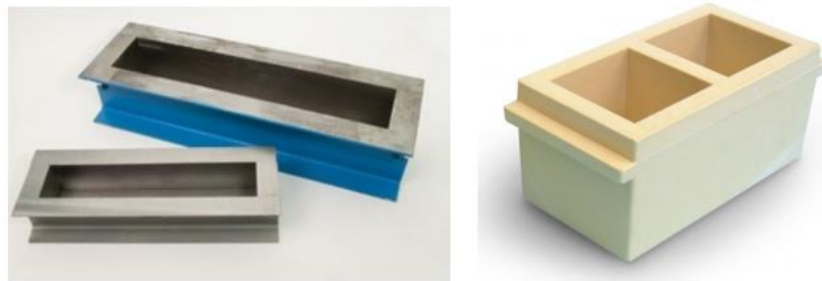
Beams moulds 100x100x500 mm   plastic cube mould 100mm

Figure 4.12:Moulds used for casting

For the RSM part, we had 15 runs, and thus we cast 45 cubical specimens in total (15*3 for each mix). For the other part of the experimental work, we cast 33 specimens (24 cubes and 9 beams) so that 3 of the cubes from each mix could be tested for compressive strength on 7th day and the remaining 3 on 28th day. The specimens were covered by plastic cover immediately after casting to avoid moisture evaporation and kept for 24 hours until taken out for curing. The cubes and beams were removed from the mould after 24 hours and kept for curing in a curing tank filled with water, maintained at a temperature of 20^0c for 28 days.
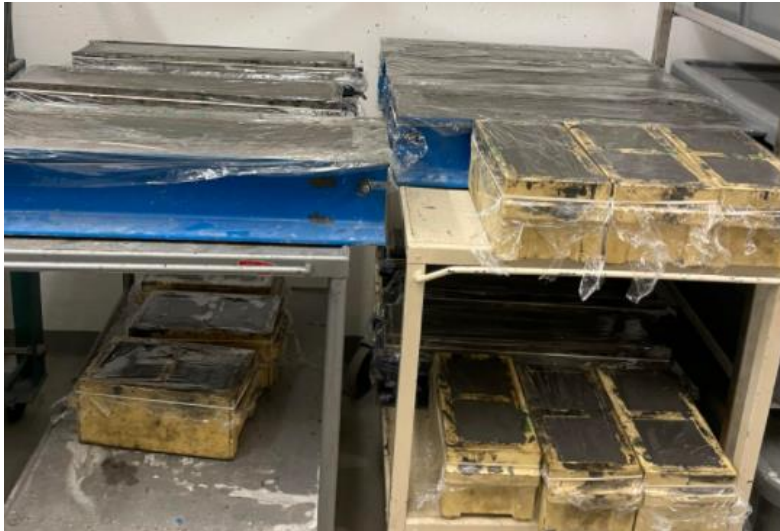
Figure 4.13:Freshly cast specimens wrapped with moist covers

Curing: The specimens were carefully taken out of the moulds after 24 hours and kept in the curing tank. The curing tank (as shown in Figure 4.14) was filled with water and maintained a temperature of 20^0C.

Figure 4.14:Curing tank in the laboratory

Testing: In this study, the mechanical properties of UHPFRC, such as compressive strength and flexural strength, are tested with the corresponding machines available in the laboratory.

4.2.4 Investigated characteristics

The mechanical properties of UHPFRC investigated in this study are elaborated on the following.

Compressive strength: Concrete's compressive strength is a major mechanical property defining the concrete mix. It can be defined as the capacity of concrete to withstand loads before failure. The compressive strength of concrete is measured by crushing cubical or cylindrical specimens in a compression testing machine. The compressive strength can be calculated by the failure load divided by the cross-sectional area and reported in Megapascals (MPa) in SI units. The compressive strength test is regarded as the most important among many tests applied to concrete, as it provides an overview of the characteristics of the concrete [105].

The standards used for the compression testing of specimens in this paper are NS-EN 12390-3:2019, the European standard for testing hardened concrete, as no standards exist for UHPC separately, and the machine in the laboratory is calibrated with the loading rate and other specifications as per the European standards.

The test was performed in 100x100x100 mm^3-sized cubes. The specimens were placed centrally in the machine over the loading platform, and the rate of loading was 0.600 MPa, which complies with NS-EN 12390-3:2019 [12].

The formula gives the compressive strength:

$$f_c = F/ A_{c,}$$

(4.1)

where,

f_c is the compressive strength in MPa (N/mm2).

F is the maximum load at failure in N.

'Ac' = cross-sectional area of the specimen on which the compressive force acts, calculated from the designated size of the specimen (EN 12390-1). The compressive strength shall be expressed to the nearest 0,1 MPa (N/mm2) [12].
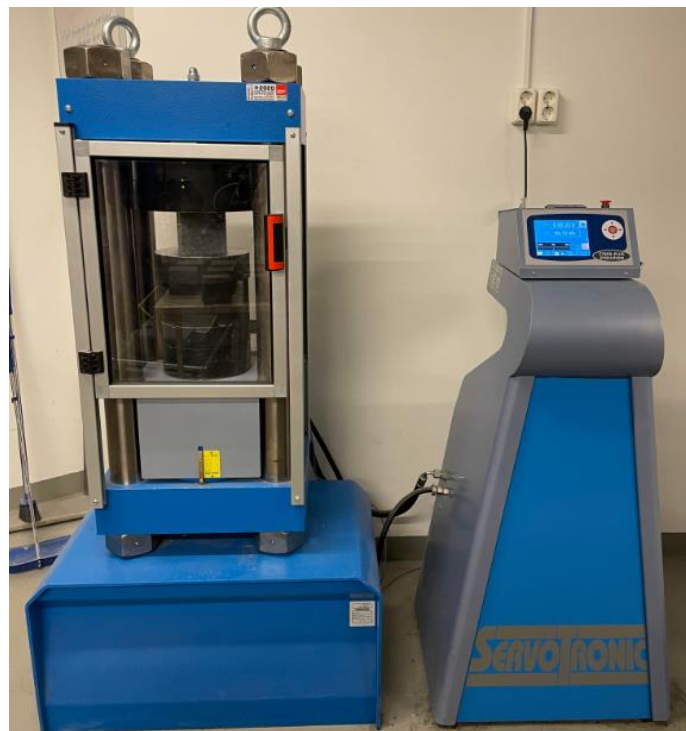
Figure 4.15:Compressive strength test machine

A major part of this thesis relied upon testing the compressive strength of UHPFRC cubes. The cubes were prepared according to the mixing and casting procedure (as explained in chapter 4.2.3) and tested at twenty-eight (28) days. Compressive strength values obtained were determined by taking the average of three specimens. The cubes were tested using a compression testing machine available in the laboratory, as shown in Figure 4.15. The contact surface of the supporting and loading rollers was wiped clean before and after placing each specimen. Positioning the specimen was done so that the load was applied on the uppermost surface of the specimen as cast in the mould. Adequate care was taken to ensure that the specimen was aligned with the loading device.

Loading was done slowly and continuously increased until the specimen cracked with a sound and the recording device stopped after recording the maximum load. The compressive strength of the specimen is expressed as the maximum crushing load in Newton (N) divided by the effective surface area of the sample considered for testing (cube in tour case) in millimeters (mm).

The machine can be configured with the loading rate and area of loading before starting the test so that it directly gives the compressive strength in MPa along with force in KN, as shown in Figure 4.16.
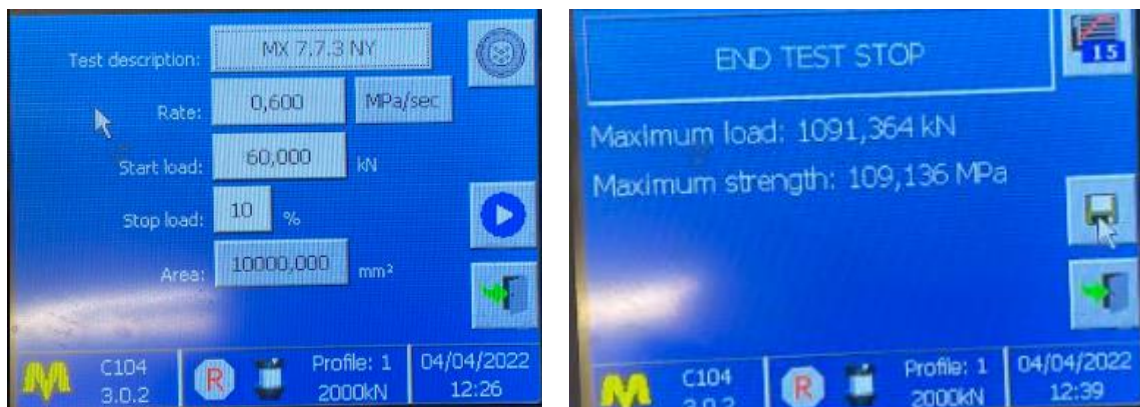
Figure 4.16:Configuration settings and display of results in compression testing machine

Flexural strength: Tensile strength is the ability of concrete to resist tensile forces or tensile stresses applied to it. It determines the load-bearing behavior of concrete as compressive strength, which is usually taken as a parameter depending on the tensile strength of concrete in a mesoscale. The tensile strength of concrete is measured in N/mm2 or MPa. Unlike steel, concrete is a solid composite material that is weak in tension. Concrete is usually reinforced with steel bars to compensate for this weak behavior during tension [106].

The flexural strength of concrete, also known as the modulus of rupture, can be defined as an indirect measure of the tensile strength of concrete. It is a measure of the maximum stress on the tensile zone of an unreinforced concrete beam or slab at the failure point during bending. The flexural strength is expressed as the modulus of rupture in MPa and is determined by standard test methods ASTM

C78(third point loading) or ASTM C293 (center point loading). The specimen size and the type of loading greatly influence the flexural strength [106].

ASTM C293: Centre-Point Loading   ASTM C78: Third- Point Loading
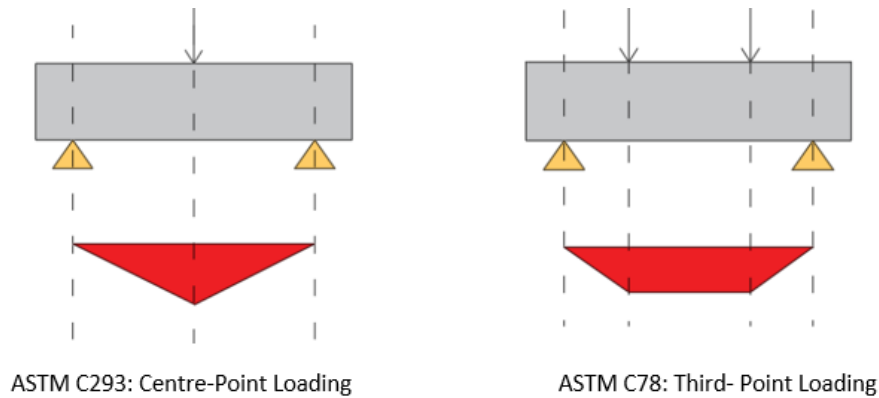
Figure 4.17:Test configurations for flexural test [55]

When a simply supported beam is subjected to loading under bending, tensile stresses develop at the bottom of the beam; once these tensile stresses exceed the flexural strength of the beam, cracks start to occur at the point of maximum bending moment. The load applied and the pattern of crack can be used to calculate the flexural strength of the beam. The determination of flexural strength is a significant factor in the design of concrete members. The flexural strength testing machine available at the laboratory is shown in Figure 4.18.
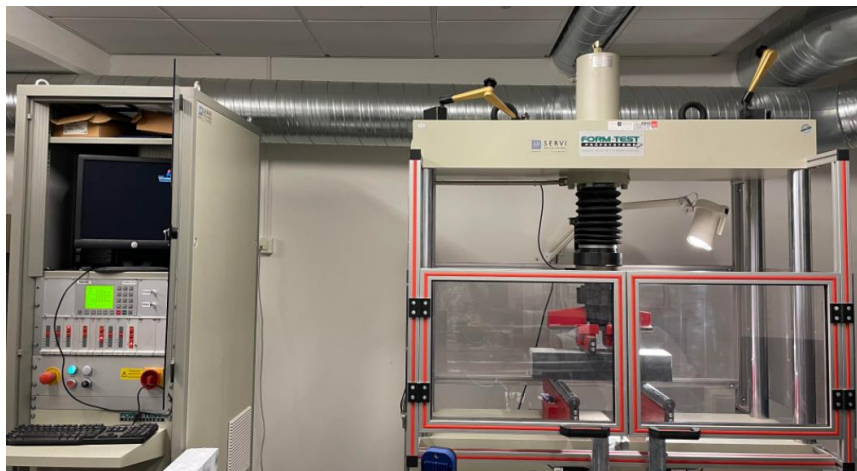
Figure 4.18:The machine for testing flexural strength at the laboratory

As per NS-EN 12390-5:2019 [11], the flexural strength is given by the formula;

$$f_{ct,fl} = \frac{F \times l}{d_1 \times d_2^2}$$

(4.2)

where,

$f_{ct,fl}$ = The flexural strength , in MPa(N/mm^2);

F   = Maximum load in;

l   = The distance between the lower rollers; in mm and,

d_1 and d_2 = lateral dimensions of the cross-section in mm.

Figure 4.19:Beams marked for three-point bending test

Considering the beam dimensions,

The total length of the beam = 500 mm

The length of the loading span (l) = 300 mm

d_1 and d_2 = 100 mm

Figure 4.19 shows the beam marked with a loading span of 300 mm (in the middle) and 100 mm on both sides.

4.3 RSM based modeling and analysis

The second part of the experimental program was designed with RSM, one of the DOE branches.

In this study, the predicted responses will be estimated using a second-order polynomial function, including the two-factor interactions between the parameters for 'k' variables as given as Eq. 4.3 [82, 89, 107].

$$Y = \beta_0 + \sum_{i=1}^{k} \beta_i X_i + \sum_{i=1}^{k} \beta_{ii} X_i^2 + \sum \sum_{i<1}^{k} \beta_{ij} X_i X_j$$

(4.3)

Where 'Y' is the predicted response, which is maximum compressive strength, X_i is the coded level of a design variable, where i, k indicates the total number of variables, coefficient β_0 is a constant in the equation, and β_i, β_{ii}, and β_{ij} are the regression coefficients for the linear, quadratic and interaction effects, respectively [82].

Central Composite Design (CCD) can be used to predict dependent variables, also known as responses, using a relatively small number of experimental data, with all the selected parameters varied in a preferred range. The most common design type that fits a second-order model is CCD. In this study, CCD is used to fit the Eq. 3.2 with the obtained response (maximum compressive strength). The

number of design points in CCD for k variables is 2k factorial points, 2k axial points, plus one center point. This is represented in Figure.4.20 for three variables. In the half fractional factorial points design, the number of fractional points is limited to 2^{k-1}[82]. The coded distance of the axial points from the center point can be obtained by applying the Eq. 4.4:

$$\alpha = \sqrt[4]{2^k} \qquad\qquad (4.4)$$
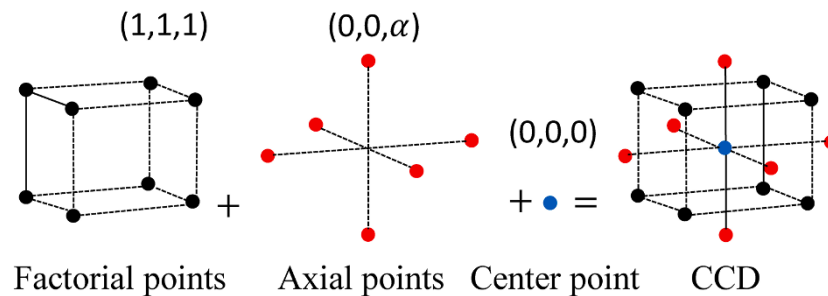
Figure 4.20: Experimental design for the fitting of a second-order model when the number of variables is 3 (k = 3), using central composite design (CCD) [78]

RSM based modeling consisted of the following steps

   I. Selecting parameters and levels

  II. Experimental design with CCD

 III. Analysis of results

Selecting variables and levels: The major goal of RSM is to predict the maximum compressive strength of UHPFRC by considering the interaction effects of influencing variables on the compressive strength of UHPFRC. The effect of these parameters was investigated using RSM and experimental analysis. The studied three parameters, also called independent variables for the experimental design, are water-to-binder ratio, silica fume content, and steel fiber content. They are symbolized by w/b, S_f, and $F_\%$ (the independent variables) and are in coded terms; Fc (max) indicates compressive strength (dependent variable or response). Fiber dosage is the percentage by volume of the mix. Silica fume content is calculated as the % of cement.

In order to study the combined effects of these variables, experimental analysis was carried out with various combinations of the selected variables. Each numerical factor or variable is chosen must be considered for five levels in CCD: the factorial zero level (Xi = 0), the one level (Xi = ±1), and the axial points (*Xi* = ±α), where α equals 2 for all variables. Table 4.7 is the representation of the above description of the factorial points.

No	Variables	Unit	Notation	Axial	Factorial			Axial
				(-2)	Low(-1)	Centre(0)	High(1)	(+2)
1	Steel fiber content	%	F_v	2	2.5	3	3.5	4
2	Water binder ratio		w/b	0.18	0.19	0.20	0.21	0.22
5	Silica fume content	%	S_f	18	21	24	27	30

The range and level of each variable were judiciously selected. It includes both the lower and upper levels from the basic UHPC recipe, as we know that the basic UHPC recipe was finalized after obtaining the results from a number of experiments that optimized maximum compressive strength and acceptable flowability.

For instance, the w/b ratio chosen for the ideal recipe was 0.2. Thus, we considered the levels above and below 0.2 (starting from 0.18 and ending at 0.22). Similarly, for the silica fume content, the ideal recipe uses 25%; therefore, we fixed a range from 18 to 30. However, the steel fibers were selected from the normal range of 2% and increased to 4% with an interval of 0.5. These ranges and levels were fixed accordingly.

Designing experiment with CCD: According to central composite design, RSM with three variables requires 15 experimental runs. Table 4.8 demonstrates the 15 experimental runs, which must be performed with UHPFRC in the laboratory according to CCD with three variables i.e., $F_{\%}$, w/b, S_f, and levels specified. Minitab 21.1.0 (Pennsylvania State University in conjunction with Triola Statistics Company in 1972) was employed for data analysis as well as the design of the experiments[78]. The experimental runs generated with CCD from Minitab are given in Table 4.8.

Table 4.8:Experimental runs for the possible combinations of the factors generated by Minitab

Run order	F_v	w/b	S_f
1	3.5	0.21	21
2	3	0.22	24
3	3.5	0.19	27
4	3	0.18	24
5	2.5	0.19	21
6	4	0.20	24
7	3	0.20	30
8	3.5	0.19	21
9	3	0.20	18
10	2.5	0.21	21
11	3.5	0.21	27
12	2	0.20	24
13	2.5	0.21	27
14	3.0	0.20	24
15	2.5	0.19	27

The 15 mixes, as per Table 4.9, were designed, taking into account the three parameters. The mix designs for the 15 experimental runs were developed based on the basic UHPC recipe and the run orders generated by Minitab.

Table 4.9:Mix designs used for the experimental runs

Mix Designs -for the experimental work based on RSM									
Mix design	w/c	w/b	Cement (g)	Sand A (100-400 Microns) (g)	Sand B (400-800 Microns) (g)	Silica Fume (g)	Water (ml)	SP(ml)	Steel fiber(g)
1	0.25	0.21	3056	3711	927	642	764	229	1072
2	0.25	0.22	2812	3402	843	675	703	229	918
3	0.25	0.19	3209	3883	963	866	802	229	1072
4	0.25	0.18	3514	4252	1054	843	879	229	918
5	0.25	0.19	3362	4068	1008	706	840	229	765
6	0.25	0.20	3056	3711	927	733	764	229	1225
7	0.25	0.2	2903	3513	871	871	726	229	918
8	0.25	0.19	3362	4068	1008	706	840	229	1072
9	0.25	0.20	3362	4068	1008	605	840	229	918
10	0.25	0.21	3056	3711	927	642	764	229	765
11	0.25	0.21	2873	3476	862	776	718	229	1072
12	0.25	0.20	3056	3711	927	733	764	229	612
13	0.25	0.21	2873	3476	862	776	718	229	765
14	0.25	0.20	3056	3711	927	733	764	229	918
15	0.25	0.19	3209	3883	963	866	802	229	765

Based on the 15 mix designs (as shown in Table 4.9), 45 cubic specimens were cast. Figure 4.21 represents a set of cube specimens prepared for testing. We did not conduct a flow test for each mix as the fresh properties were not the main focus in this part. The casting of 45 specimens took three days. All the specimens were kept in the water tank for curing (the temperature at 20^0C) for a period of 28 days.

Figure 4.21:A set of cubes prepared for the experiments

Obtaining the results and analysis: The experimental results obtained from the tests performed in the laboratory after 28 days are used as the input data for analysis in Minitab. The cube specimens were taken out of the curing tank, kept for drying, and tested for compressive strength. Consecutively, the predicted second-order regression model using the coded variables is obtained in the form of an equation from Minitab. This regression equation can be used to explain the statistical relationship between the independent variables and the responses. The statistical model is presented along with the experimental results and the analysis done with RSM in the Results chapter.

4.4 Analyzing mechanical properties of UHPFRC with higher fiber dosage

This section includes testing the mechanical properties of UHPFRC specimens with higher fiber dosages. The range of fiber dosage is considered from 2.5 to 4 (% by volume of the mix). The mechanical properties; such as compressive strength and flexural strength, were tested in cube and beam specimens. The mixes made accordingly are illustrated in Table 4.10.

Table 4.10:Mixes and the steel fiber content

Mix	Amount of steel fiber (%)
Mix I	2.5
Mix II	3
Mix III	3.5
Mix IV	4

The flow test for assessing the workability of UHPC was conducted immediately after mixing each mix. The test was conducted based on ASTM C1437 standards using the cone mould and following the guidelines. The SP amount was adjusted to each mix to keep the flow diameter constant. For Mix I , 6% SP was added, and the flow diameter observed was 220 mm.

For Mix II and Mix III, SP 6.5% and 7% were added, respectively. The amount of SP was decided based on the strategy of keeping the constant flow diameter in the range of 210 ± 10 mm. And an amount of 0.5% of SP was increased each time as the fiber percentage was increased by 0.5%, and this strategy was successfully adopted in the first three mixes (Mix I , Mix II and Mix III) .
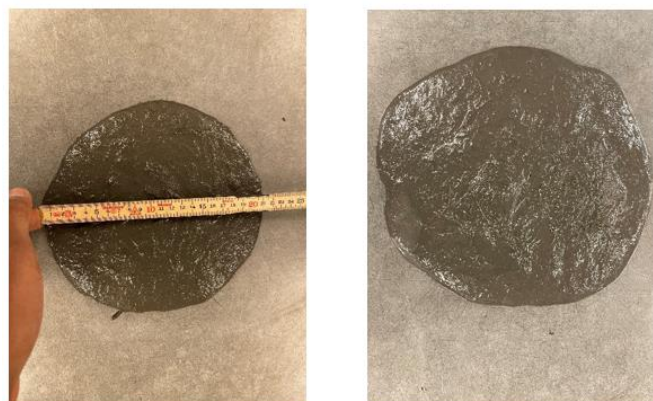
Figure 4.22:Flow test for Mix I

The plan for including the mix Iv (with 4% steel fibers by volume) later came on to the plan after testing the 7 days' compressive strength of the earlier mixes(Mix I, II, and III) to understand the trend of the compressive strength of UHPFRC on adding one more increment of fibers. However, considering the limited availability of materials and time constraints, we prioritized cast cubes to assess the compressive strength and withdrew the plan of casting beams with this mix. Therefore we cast 6 cubes (3 for 7 days and 3 for 28 days of testing) with the mix IV. Since we didn't include the beams, mix IV wasn't large enough, unlike the previous mixes. The SP added was 7.5%.

Figure 4.23:Mix with 4% steel fiber (the highest dosage of steel fiber considered in the study)

Even though the mixing procedure and the approach to adding SP were similar to the previous mixes, the flow diameter was around 140 mm during the flow test. Flowability is a measure of flowability. The acceptable spread values range between 175 mm and 300 mm, and the spread value outside this range indicates that the mixture should be rejected. The obtained flow value was not within the acceptable range. This may be due to the presence of a larger volume of steel fibers(4%) and a smaller batch of the mix.

However, we continued with the casting, without adding extra SP to improve the flow, in order to keep up with the strategy of 'increment of 0.5% SP with the addition of 0.5% steel fibers in each mix'. This was done to understand how the fresh properties of UHPC are influenced by the addition of fibers and how they can be regulated with the addition of Superplasticizers. Moreover, the compressive strength of the cubes can be tested to understand the trend of variation of compressive strength. The results could be thus interpreted as we know the conditions of the test.

Figure 4.24: flow test done for Mix I

5 Results and Discussions

For achieving the research objectives, we depend primarily on literature review, and the insights grasped from the literature were unutilized for developing further methods to accomplish the desired goals. As mentioned in the method chapter, the experimental program succeeded in the literature review. In order to develop predictive models for establishing statistical relationships between influential parameters and compressive strength of UHPFRC, the response surface methodology was adopted. Besides the mechanical properties of UHPFRC, specimens with higher dosages were also investigated through experimental analysis. The experimental results and the results of data analysis performed with Minitab are presented.

The results are discussed based on the previous studies, significant interpretations made, and areas, where further investigation is required are identified and proposed for future work.

5.1 RSM based modeling

This section presents the experimental results, regression equation, predicted responses, and the parameters' influence on the response using RSM.

The experimental results for the compressive strength of 45 cube specimens prepared with the 15 mix designs (as per the experimental design) were obtained. Three cubes from each mix were tested, and the average of this three was recorded as the compressive strength. According to CCD, with three control factors, a total of 15 experiments were performed.

The CCD for the selected three variables, experimental results obtained, and the RSM predicted responses are presented in Table 5.1.

Table 5.1: The used CCD for three variables, experimental results for the FC(max) and the RSM predicted responses

CCD	Run order	Uncoded variables			Fc(max)	
		F_v%	w/b	Sf%	Experimental (MPa)	RSM predicted(MPa)
Factorial	1	3.5	0.21	21	139.85	138.12
	2	3	0.22	24	135.96	136.61
	3	3.5	0.19	27	137.47	137.28
	4	3	0.18	24	136.19	137.29
	5	2.5	0.19	21	130.89	131.83
	6	4	0.20	24	137.88	139.65
	7	3	0.20	30	139.93	139.04
	8	3.5	0.19	21	134.67	133.99
Axial	9	3	0.20	18	131.48	132.12
	10	2.5	0.21	21	130.71	131.14
	11	3.5	0.21	27	139.99	139.30
	12	2	0.20	24	134.98	132.97
	13	2.5	0.21	27	133.85	134.78
	14	3.0	0.20	24	134.42	134.17
Centre	15	2.5	0.19	27	135.61	137.58

The experimental results obtained are given as the input for Minitab for analyzing the data and generating the response surface. Minitab provided the predicted values for each combination of the independent variables. Experimental values and the RSM predicted values are compared to assess the fitting of the predicted model.

5.1.1 Regression equation

The predicted second- order response function for maximum compressive strength F_c **(max)**, obtained from the RSM regression model using the coded variables, is presented as Eq.5.1;

Fc (max) = 354 - 47.8 Fv - 2044 w/b + 3.46 Sf + 2.13 Fv*Fv + 4446 w/b*w/b + 0.0391 Sf*Sf

(5.1)

As previously mentioned, the variable parameters are steel fiber content (F_v) in percent (%), water binder ratio(w/b), and silica fume content (S_f) in percent (%). Consequently, the compressive strength obtained is in MPa. This equation describes the relationship between independent variables and the response. The regression equation (Eq 5.1) can be used for predicting the compressive strength for any possible combination of the three variables considered.

The experimental results and the RSM predicted results presented in Table 5.2.

Table 5.2:Comparison of Fc (max)obtained from experiment and RSM

Run order	Experiment	RSM	R_{factor}*
1	139.85	138.123	1.013
2	135.96	136.614	0.995
3	137.47	137.283	1.001
4	136.19	135.289	1.007
5	130.89	131.831	0.993
6	137.88	139.647	0.987
7	139.93	139.044	1.006
8	134.67	133.991	1.005
9	131.48	132.119	0.995
10	130.71	131.143	0.997
11	139.99	139.296	1.005
12	134.98	132.967	1.015
13	133.85	134.776	0.993
14	134.42	134.173	1.002
15	135.61	137.583	0.986

*R_{factor}= Experiment/RSM

R_{factor} is the ratio of experimental values to the RSM predicted values, indicating that the regression coincides well with the test data. Figure 5.1 represents the normal probability distribution diagram of the residuals (the difference between the obtained Fc $_{(max)}$ by experiment and the predicted Fc $_{(max)}$ by Eq.5.1). For the predicted model, the residuals are normally distributed on both sides of 0. as shown in the plot.
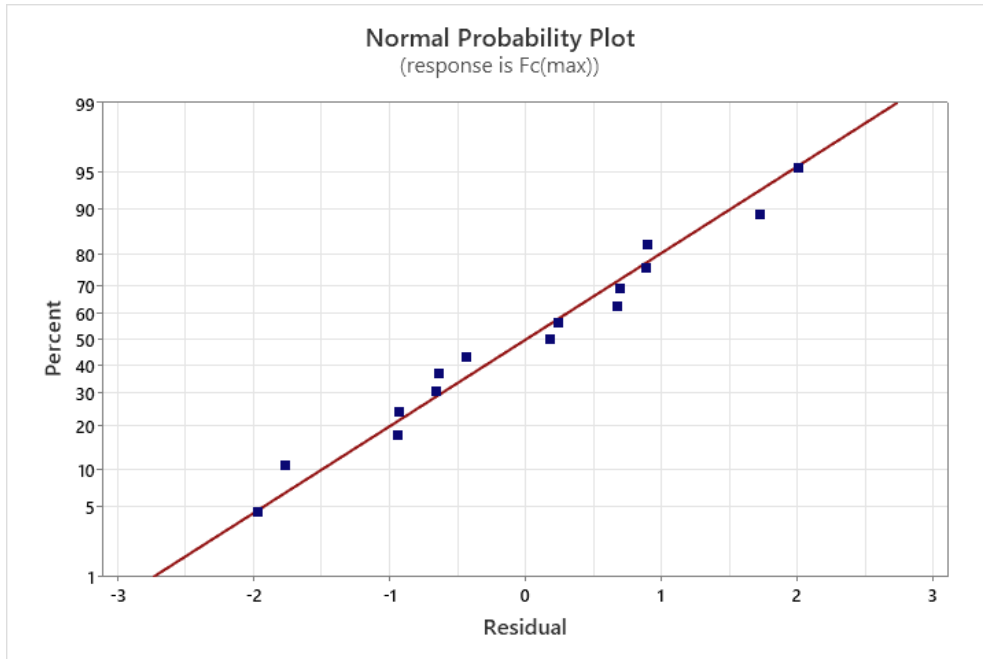
Figure 5.1: Normal probability plot

Table 5.2 and Figure 5.1 ascertain that the experimental results and the RSM predicted values are in good agreement with each other.

5.1.2 Validation of results

Even though the predicted values and actual values are in close proximity to each other, we verified the validity of the regression equation (Eq.5.1) obtained by RSM with a set of experiments (four experiments considering the availability of time and materials) with random values of parameters within the defined levels.

Table 5.3: characteristics of the selected random specimens for validating the results

Specimens	Fv	w/b	Sf
S1	2.5	0.2	25
S2	3	0.2	25
S3	3.5	0.2	25
S4	4	0.2	25

Then, the obtained results from the experiment were compared with the results obtained from RSM equations. For our study, we performed four experiments for the part of this thesis to analyze the influence of higher fiber dosage on mechanical properties. The experimental results obtained for this part were used for the validation of RSM results here. The sets of the parameters chosen for the validation are illustrated in Table 5.3. Table 5.4 presents a comparison of the obtained results of Fc(max) from experiments and RSM equations.

Table 5.4:Comparison of the results of the experiment and RSM to verify the validity of the equation obtained by RSM

Specimen	Experiment	RSM	*R^f
S1	134.368	133.960	1.003
S2	137.361	134.852	1.019
S3	138.392	136.808	1.012
S4	140.899	139.830	1.008

*R^f= Experiment/RSM

The results validate that RSM can accurately predict the Fc(max) of the specimens. This proves that the RSM model has good prediction capability, and the actual experimental test value is surprisingly superior to the predicted value. This establishes that our results are in conformity with the previous research based on the CCD design of RSM in cement and concrete [82],[99].

As the predicted values are generated using the regression equation, validated as per Table 5.4, this equation can be used to predict the compressive strength of any combination of the factors considered without conducting the actual experiment, highlighting the application of RSM in the research field.

5.1.3 Effect of each parameter on the response

For better clarity and understanding of the impact parameters on the response, the effect of each parameter on the compressive strength (28th day) is presented in this section.

Effect of water binder ratio: The effect of the w/b ratio on the compressive strength is obtained from the regression equation by keeping the other two variables constant (Fv=3, Sf=24) is illustrated in Figure 5.2.
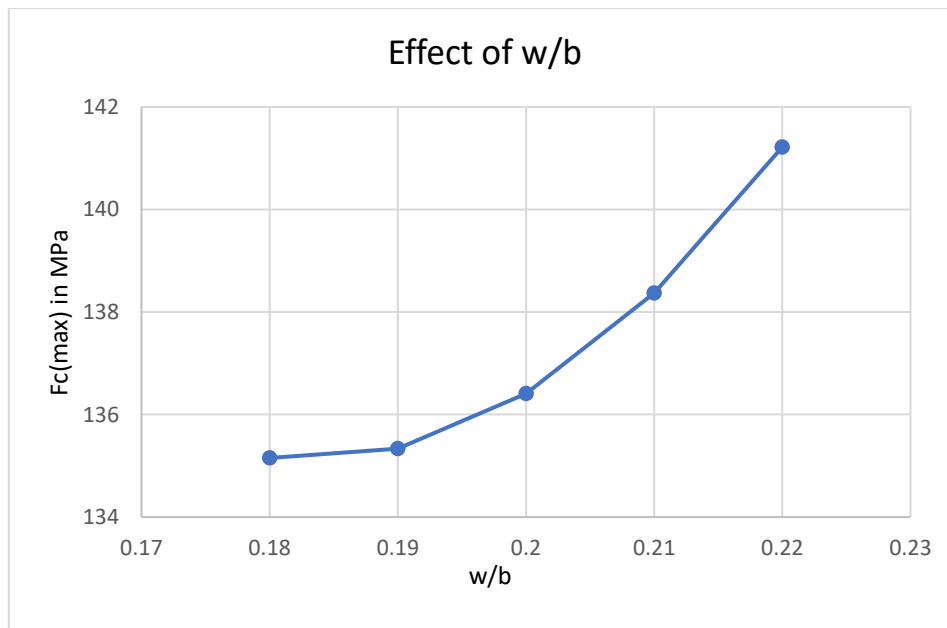

Figure 5.2:Effect of w/b on Fc(max) keeping Fv=3.5 and Sf=24

It can be observed from the regression equation that w/b has the greatest influence on compressive strength as (w/b)^2 has the highest constant (Refer to Eq.5.1). Figure 5.2 shows that the compressive

strength increases with the increase in w/b from 0.18 to 0.22(range considered). This result agrees with the design principle of UHPC that w/b should be in the range of 0.16-0.2. However, in some papers, the highest compressive strength was achieved for w/b=0.21 and decreased thereafter for w/b 0.22 and 0.23 [108].

The previous studies observed the mix's fluidity increases with an increase in w/b. When w/b is less than 0.19, the mixture is sandy. On the contrary, when the w/b ratio reaches 0.23, the concrete mix will be in a slurry state, which can improve the fluidity of UHPC obviously. With the lesser water content of concrete mixtures with a low w/b, a denser hydration film was formed on the surface of the cementitious particles after the hydration reaction, which could further hydration reaction and maintain the homogeneity of UHPC by bonding cementitious materials and fine aggregates. The porosity will also be low when the w/b ratio is low, which is beneficial to improve the compressive strength. For our study, the mean w/b is 0.2; however, w/b up to 0.22 improves the compressive strength as per our findings.

When the w/b is lower than 0.2, the compressive strength decreases slightly as this can cause low viscosity to the mixture [108]. This result is inconsistent with the findings of a previous study. However, the reviewed literature and the experimental result shows that w/b alone cannot determine the maximum compressive strength as some studies obtained an ultimate compressive strength of 150 MPa with a w/b = 0.25 [108]. Considering this, we recommend continuing the experiments with a w/b ratio above 0.22 until 0.27 as future work.

Effect of steel fiber dosage (Fv)

The influence of steel fiber content on the compressive strength obtained from the regression equation and keeping the other two variables constant (w/b=0.2, Sf=24) is illustrated in Figure 5.3.
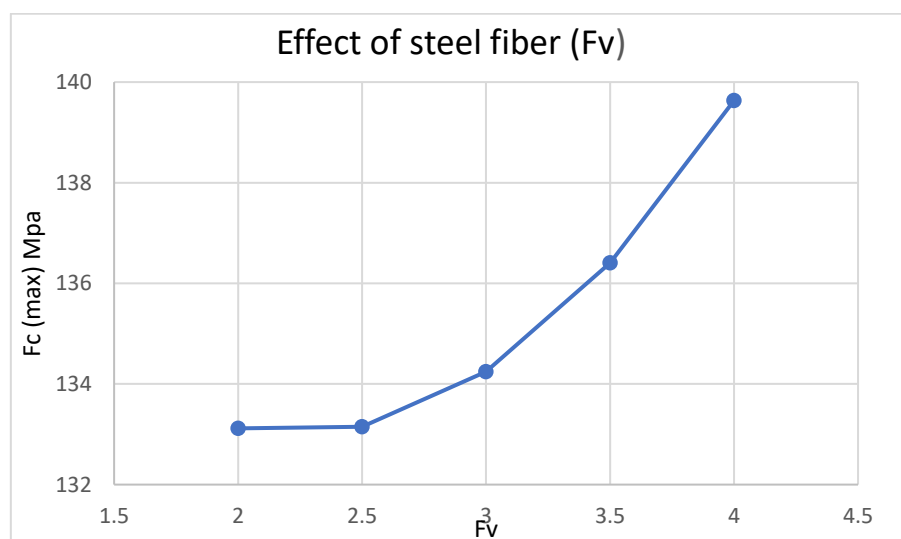

Figure 5.3: Effect of Fv on Fc(max) keeping w/b=0.2 and Sf=24

The graph clearly indicates that the compressive strength steadily increases with the increase in steel fibers. An increase of 5% in compressive strength is observed from mixes with 2% to mixes with 4%. According to the previous studies, the compressive strength increases with steel fiber addition [96, 109]. The previous studies explored the mechanical properties of UHPFRC with a 5% volume fraction of steel fibers. It was observed that the addition of steel fiber from 2 to 5% led to a gain in compressive strength by 3.7 to 25% compared to the mixtures without fibers [109]. Besides, the UHPC mixtures with higher fiber dosage exhibited relatively improved durability [95].

Effect of steel fiber dosage (Fv)

The effect of silica fume content on the compressive strength keeping the other two variables constant (w/b=0.2, Fv=3) is shown in Figure 5.4. The results show that there is an upright increase in the compressive strength when the Sf is between 20% and 30%. The previous research in this regard recommended that silica fume dosages of 20%-30% of the total binder material achieve denser particle packing and pozzolanic activity in UHPC, leading to higher durability and strength [18].

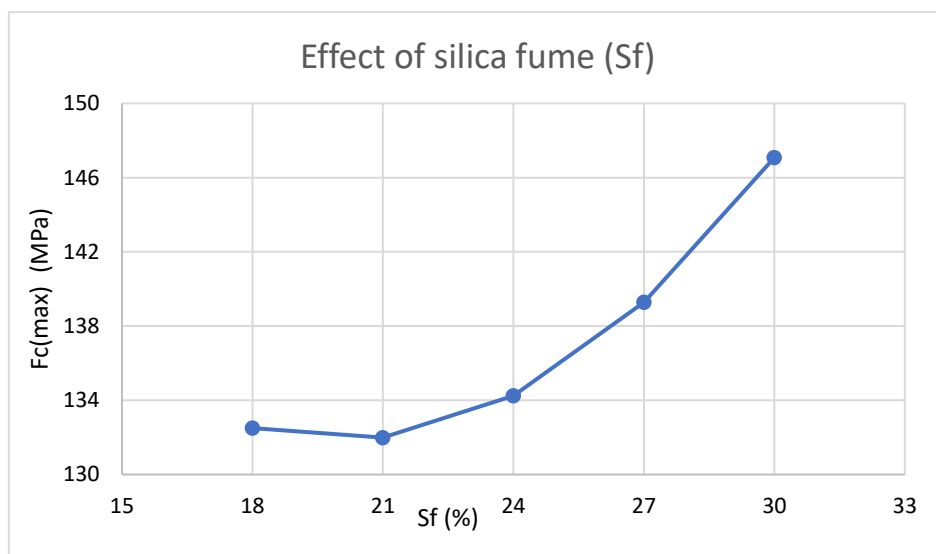Figure 5.4: Effect of Sf on Fc(max) keeping w/b=0.2 and Fv=3%

Also, previous studies observed that the compressive strength of UHPC increases with the increase of silica fume content. The increase in compressive strength for 15% silica fume content was 60% larger than the mix without silica fume content [110]. The results obtained are in compliance with the previous studies and recommendations.

5.1.4 Effects of multi-factor interactions on the response

According to the regression equation and data obtained through the RSM analysis, the 3D response surface and 2D graphs have been generated that exhibit the relationship between compressive strength of UHPFRC (as a response) and the interaction effects of the parameters such as w/b, S_f and F_v on the response. The response is expressed graphically in the three-dimensional space that can reveal the response surface's shape. Two dimensional graphs are generated using the regression equation by varying two variables and keeping the third variable as a constant (usually the mean of the range selected) which can disclose the effects of the multiple factor interactions on the response. Minitab holds the value of the third variable if we consider three variables simultaneously while calculating the fitted response values.

Interactive effects of Sf and w/b: The interaction influences of Sf with various water binder ratios (w/b=0.18,0.2 and 0.22), keeping Fv=3, is presented in Figure 5.5. The interactions show that the compressive strength is highest while the Sf=30 and w/b=0.18. There is a steady increase in compressive strength with the increase in Sf for w/b=0.18, while there gain in compressive strength is remarkably low for w/b=0.22. Similar sets of graphs can be produced by changing the holding value. This graph can be used to change the parameters appropriately to maximize the compressive strength. The 3D plot showing the response surface (Figure 5.6) also suggests an approximate linear dependency of Fc(max) on Sf and w/b for a fixed value of Fv.
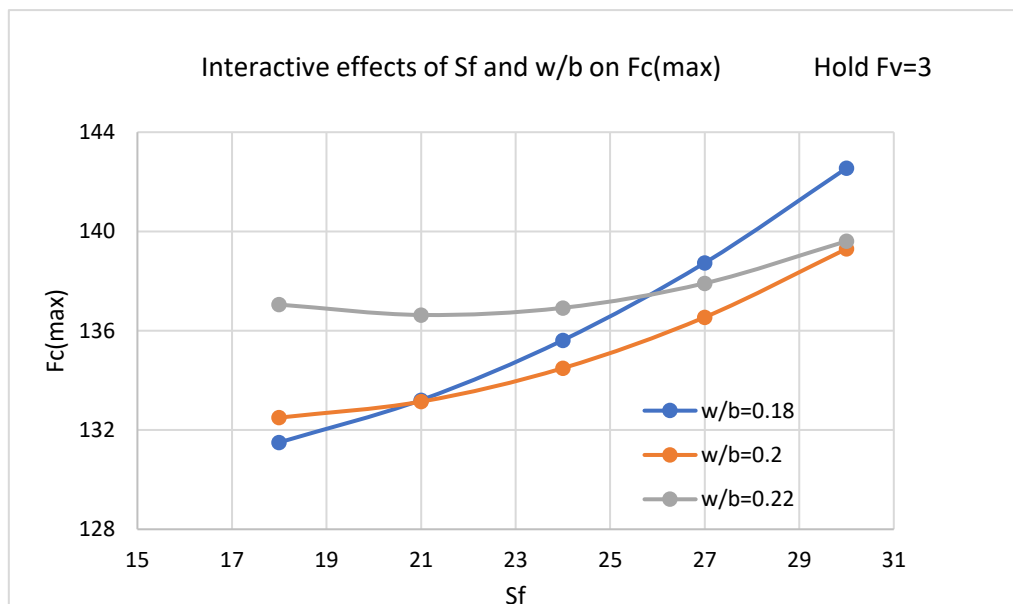
Figure 5.5: Interactive effect of Sf and w/b on Fc(max). The holding value is Fv=3

Figure 5.6:3D response surface showing interaction effect of S_f and w/b

Interactive effects of Fv and Sf: The interaction influences of Fv and SF by holding the value of the third variable, w/b=0.2, are demonstrated in Figure 5.7. The interactions suggest that the compressive strength has approximate linear dependency on Fv and Sf except for Sf=30. The compressive strength is inconsistent with Sf=30, while there is a steady increase in compressive strength with the increase in steel fibers for Sf=18 and Sf=24. However, the highest Fc(max) is achieved with Sf=30 and Fv=4, which reinstates the observations from previous studies that the compressive strength effectively improves with binder content and steel fiber. Our observations in this regard suggest that the combination of higher silica fume content (30%) with a higher steel fiber content (4%), keeping the w/b=0.2, can maximize the compressive strength of the UHPFRC mix.

The 3D plot that shows the response surface (Figure 5.8) generated based on the interactions of the variables endorses the above findings.

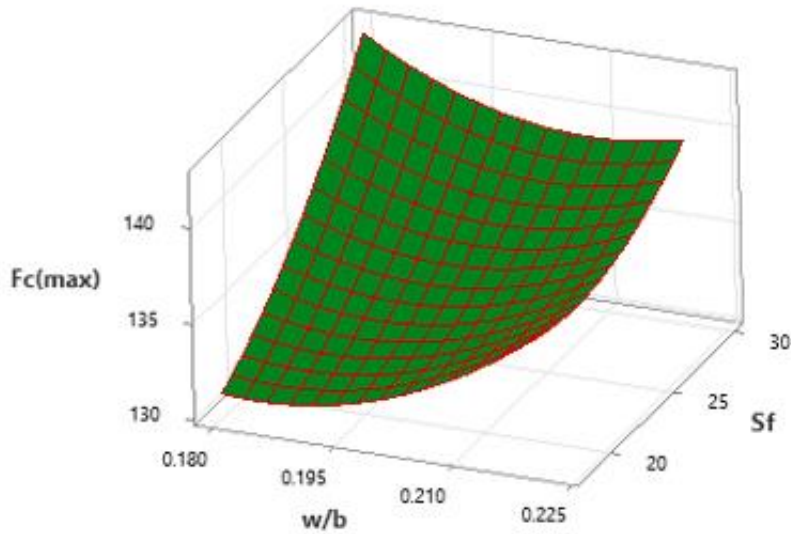Figure 5.7:Interactive effect of Fv and Sf on Fc(max). The holding value is w/b=0.2
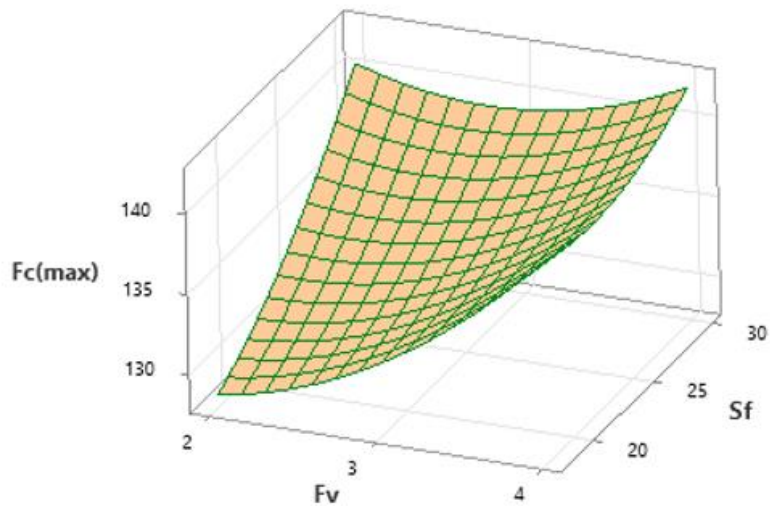
Figure 5.8: 3D surface showing interaction effects of Fv and Sf

Interactive effects of w/b and Fv: The interaction influences of w/b and Fv by holding the value of the third variable, Sf=24(mean of the range selected), are presented in Figure 5.9. There is a clear negative relationship between compressive strength and w/b for Fv=2, which is inconsistent with the previous studies. However, the dependency of compressive strength on w/b for Fv=3 and Fv=4 is approximately linear. However, the highest Fc(max) is achieved with Fv=4and w/b=0.22(the highest levels of the parameters considered), which are in line with the recommendations from previous studies[97].

The response surface 3D plot (Figure 5.10) shows that the highest response was obtained for the interactions of the variables with their highest value considered.
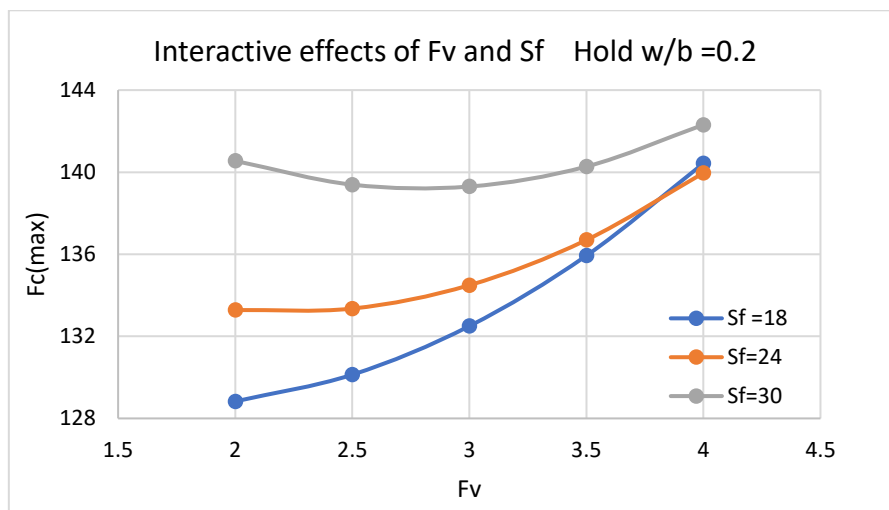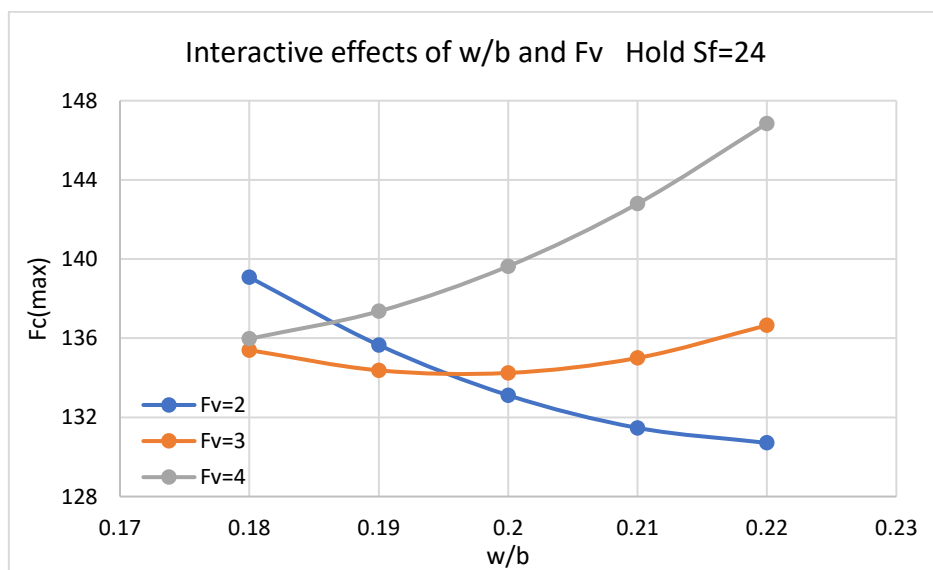

Figure 5.9: Interactive effect of w/b and Fv on Fc(max). The holding value is Sf=24
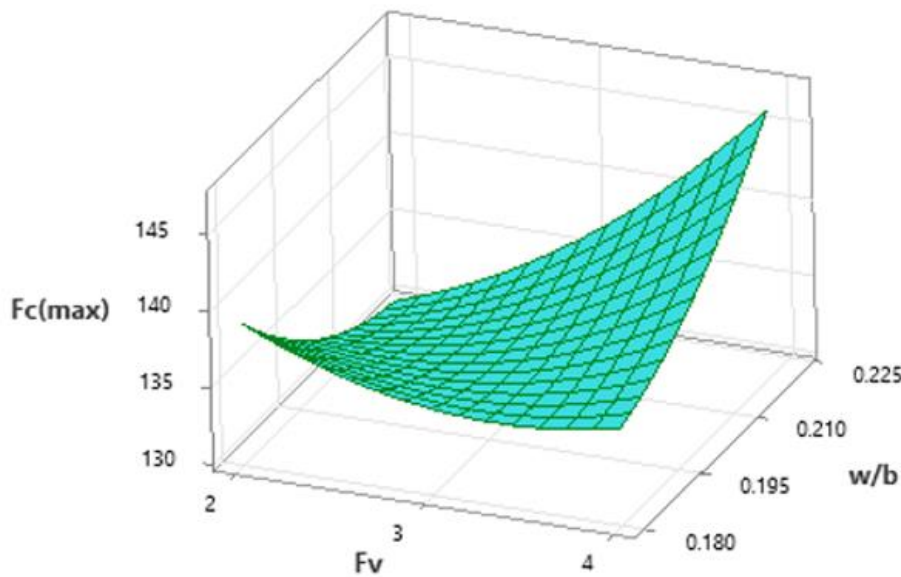
Figure 5.10:3D surface showing interaction effects of w/b and Fv

The analysis of the above graphs and 3D plots provided insights into the interaction effects of the variables on the compressive strength, which could be helpful in optimizing UHPFRC for maximum compressive strength. As previous studies suggest, an appropriate selection of the parameters such as w/b, S_f, and F_v can constructively impact the mechanical properties and durability of UHPC remarkably [111].

5.2 Mechanical properties of UHPFRC with higher fiber dosage

The experimental results obtained concerning the mechanical properties of UHPRFC in the fresh and hardened stage are presented in this chapter. An overview of the flow and mechanical properties obtained from the experiments is shown in Table 5.5. The analysis and interpretation of each development are discussed based on the experimental results and interpreted with previous studies.

Table 5.5:Flow and mechanical properties of UHPFRC mixes

Fiber dosage(%)	Flow diameter(mm)	*Compressive strength(MPa)	*Flexural strength (MPa)
2.5	220	134	27
3	218	137	15.55
3.5	225	138	18.6
4	138	141	-

*-28th day Compressive and flexural strength

5.2.1 Fresh properties

The flow test explained in chapter(4.2.2) was conducted to find out the flow diameter of the UHPC mix. For the mixes I, II, III, and IV, the amount of SP was adjusted to maintain a constant flow diameter.

The amount of SP was increased at a steady rate for each mix according to the increase in fiber amount, as given in Table 5.6.

Table 5.6:Steel fiber content and SP added on each mix

Mix	Steel fiber(%)	SP (%)
Mix I	2.5	6
Mix II	3	6.5
Mix III	3.5	7
Mix IV	4	7.5

Figure 5.11 shows the relationship between the percentage of steel fiber added and the amount of Superplasticizer used for each mix. Figure 5.12 presents an overview of the relationship between the flowability and steel fiber dosage, provided SP is increased at a constant rate.

Figure 5.11:Relationship of steel fiber dosage and amount of Superplasticizer used

Figure 5.12:Relationship between steel fiber dosage and Flowability

It can be observed from Table 5.6 that for the mixes I, II, III, and IV, the amount of superplasticizer was 6%, 6.5%, 7%, and 7.5 % (The percentage by volume of the mix), respectively. The increment of SP was
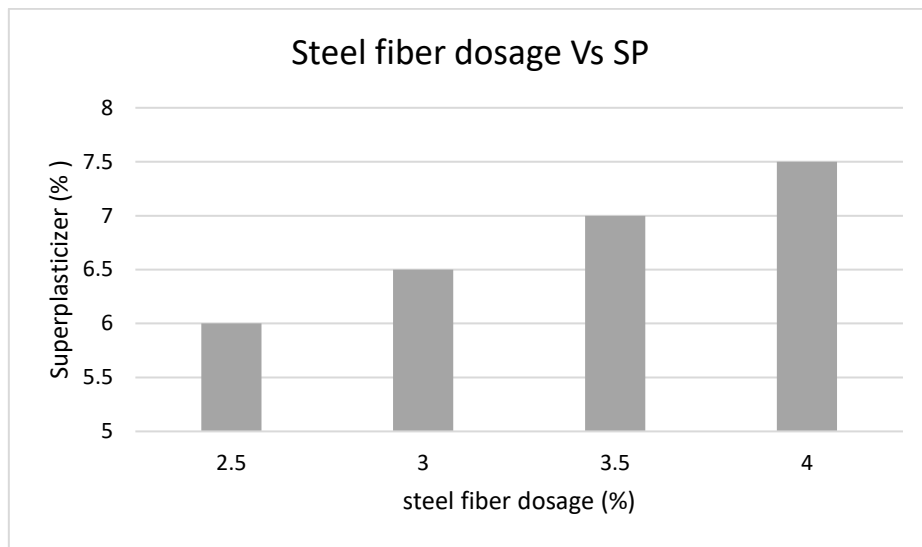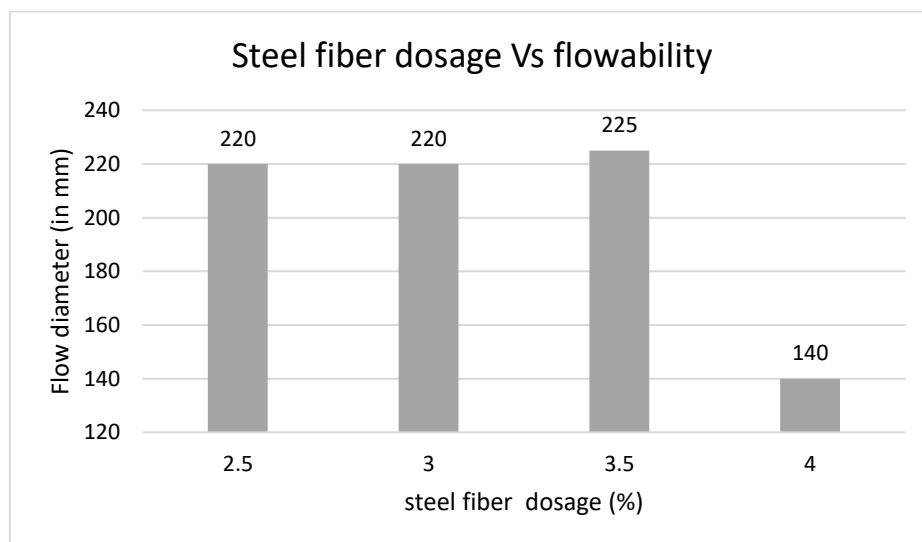
kept at 0.5% to maintain the flow diameter at 210 ± 10mm. This effect indicates that the amount of superplasticizer can influence the flow diameter, which is considered the measure of workability in UHPC. As for each mix, the fiber ratio was incremented by 0.5%, and so was SP, and this strategy could also keep the flow in a constant range, as demonstrated in Figure 5.12. It can be observed that the flow diameter for mix IV is 140 mm, which is relatively poor and unacceptable as per the standards[102]. It is equally important to produce workable concrete that can be easily placed and be self-compacted while focussing on the excellent mechanical properties as a result. The relatively poor workability of the mix can be the presence of a higher dosage of fibers.

Moreover, because the mix wasn't large enough, unlike the other mixes since we only cast cubes (not beams); therefore we realize that the mix IV cannot be recommended for practical use, though the 28th-day compressive strength of the mix was the highest among all the mixes with a value of 141 MPa(as per Table 5.8), considering the poor workability. However, we also understand that the workability could have been improved by adding more superplasticizers, and thus, the target of superior compressive strength could have been achieved without compromising workability.

It is important to note that the compressive strength alone does not determine the quality of the concrete. Good concrete should be workable even though it possesses superior mechanical properties for practical use.

As we observed that the flowability of UHPC decreased slightly with increased fiber dosage, our experimental results in this regard agree with the previous studies [96]. It is well ascertained that steel fibers can hinder the velocity of mixtures under free-flowing. Similar reflections were reported in previous studies[95, 112].We also noticed from the previous studies that the dosage of superplasticizers increases with the increase of fibers content, which can be endorsed again with the results and experience of our experiment [14].

5.2.2 Compressive strength

The 7th-day compressive strength was tested for sets of 3 cubes from each mix on the 7th day, and the results obtained are presented in Table 5.7 and Figure 5.13

Table 5.7: 7th-day compressive strength

Mix	Average Compressive strength (MPa)
Mix I	110
Mix II	113
Mix III	109
Mix IV	108
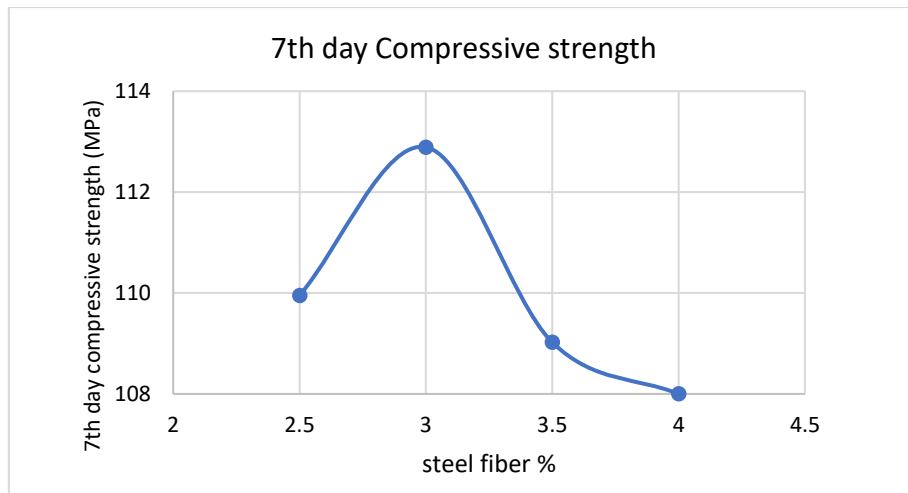
Figure 5.13:Relationship between steel fiber dosage and 7th-day compressive strength

The experimental results show that mix II(with 3% steel fibers) has the highest compressive strength, 113 MPa, and slightly decreases thereafter, with an increase in steel fibers**.

Figure 5.13 indicates that the compressive strength increases initially with the increase in fiber content from 2.5 to 3 (%) and thereafter shows a declining trend with the increase in fiber from 3% to 4%. However, 7th-day compressive strength is not the precise indicator of the compressive strength and is often considered the early strength gain and is approximately 64-70% of the 28-day compressive strength.

The fiber content significantly contributes to the compressive strength, as we studied from the literature. Thus, it was expected from the test that the increased fiber content should be accompanied by increased compressive strength. But it got reduced for the mixes III and IV. However, we may consider that the curing time develops different compressive strength levels, and a more accurate estimation of the compressive strength can be achieved on the 28th-day test. The previous research in this regard validates our results that the compressive strength of UHPFRC specimens increased with the increase in fiber dosage and age [92].

28th-day compressive strength: The compressive strength of the cubes was tested on the 28th day. Three cubes from each mix were tested, and the average compressive strength was calculated, as presented in table 5.8, Figure 5.14.

Table 5.8 : Experimental results for 28th day compressive strength

Mix	28th day-Average Compressive strength (MPa)
Mix I	134.4
Mix II	137
Mix III	138
Mix IV	141

28th Day compressive strength
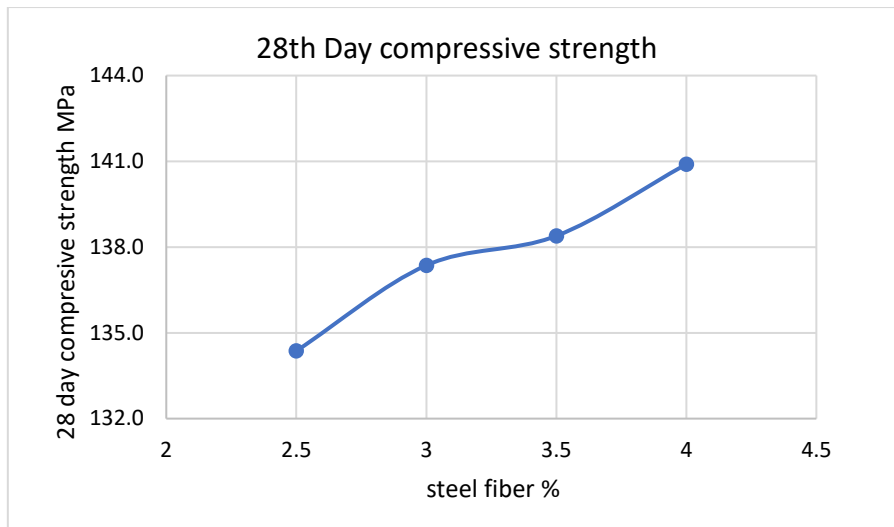
Figure 5.14: 28th-day compressive strength and steel fiber content
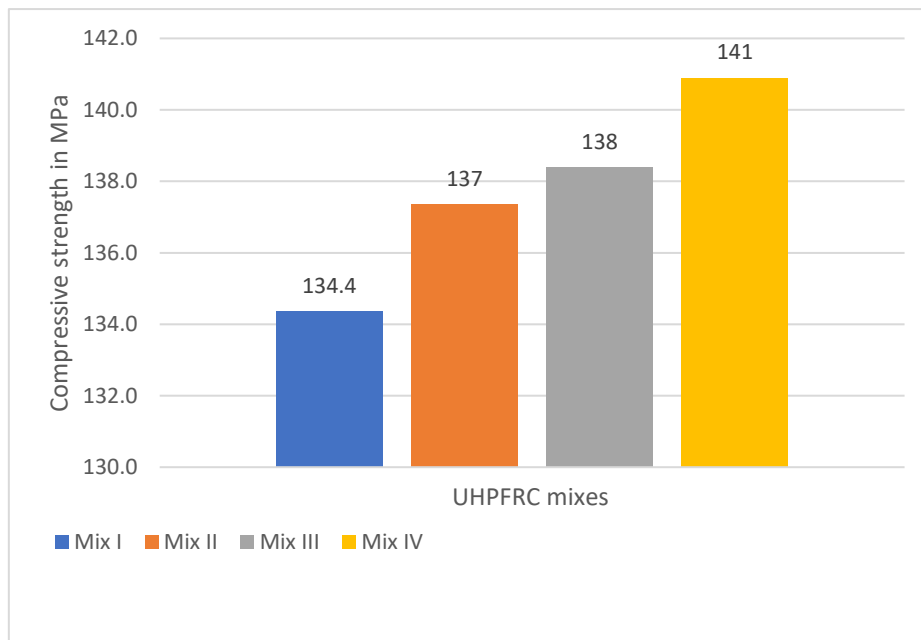
Figure 5.15: Overview of the compressive strength tested for the mixes with varying steel fiber content by volume (Mix I=2.5%, MixII=3%, Mix III=3.5%, and Mix IV=4%)

Figure 5.15 provides an overview of the 28th day compressive strength tested for the mixes with varying steel fiber content by volume (Mix I=2.5%, Mix II=3%, Mix III=3.5%, and Mix IV=4%). The results show that the compressive strength increases steadily with the increase in steel fiber content. Earlier studies reported the positive influence of steel fibers on compressive strength. The highest compressive strength observed in our study is 141 MPa, which corresponds to 4% steel fibers. As compressive strength is defined as the capacity of concrete to withstand loads before failure, the gain in compressive strength with the increased fiber content might be explained by the ability of fibers to delay and limit the crack formation and propagation.

Figure 5.16 exposes the crack patterns observed during compressive failure of the cube specimens. The crack patterns indicate that specimens with higher steel fiber contents remained relatively intact while sustaining loads with minimal fracture signs during compressive strength testing. The hairline cracks generated on the surface are controlled more in the specimens with higher fiber content. Moreover, it was observed that the time taken for the failure was more for the specimens with higher fiber content, which characterizes its ability to withstand the loads for a longer duration without failure.

2.5% steel fiber   3% steel fiber

3.5% steel fiber   4% steel fiber
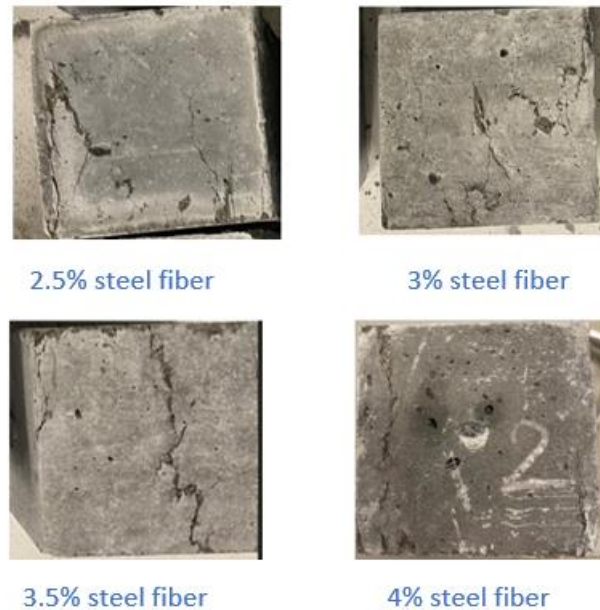
Figure 5.16:Failure of specimens from the compression tests

Moreover, compressive strength does not depend on the steel fibers alone; it depends more on the volume of hydration products and particle packing density. However, since all other parameters, materials, mixing procedure, casting method, and curing regime remained unchanged for this experiment, we may interpret the results as the effect of a higher dosage of fiber improves the compressive strength in UHPFRC and is in line with the observations made in previous studies [10].

The increase in compressive strength due to steel fiber addition in UHPC agrees with previous studies. The homogeneity of the distributed fibers can restrict the internal material deterioration and the propagation of cracks by absorbing the stresses developed at the tip of the fiber and thereby providing enhanced compressive strength. It should be noted that fiber reinforcement is primarily used in concrete to improve the tensile behavior and toughness characteristics of cementitious composites and not to increase compressive strength. However, since superior compressive strength is a significant aspect of UHPC, the effect of fibers on improved compressive strength merits further research.

The previous studies revealed that steel fibers in concrete structures could limit the axial and lateral deformations, thereby improving load-carrying capacity. Further, it was also observed that UHPC specimens without steel fibers experienced failure in an abrupt manner with a blast where a detachment of concrete occurred. However, the UHPC specimens reinforced with steel fibers could remain intact without breakage or detachment [95].

The failure pattern of the UHPC specimens in the order of increase in steel fiber shows the severity of damage load decreases with an increase in steel fiber. The fiber addition improved the failure pattern of UHPC from an abrupt sudden blasting to ductile behavior [96]. The results obtained are in agreement with the previous analyses in this regard.

In general, the compressive strength of UHPFRC increases with the increase in fiber dosage. However, in some cases, a decreasing trend for the gain in compressive strength, especially for higher fiber contents, was detected, which can be attributed to rather poor dispersion of fibers, inconveniences in the mixing process in mixes with higher fiber dosages which causes clumps of steel fibers in some instances[92]. As we investigated up to 4% fibers, the results obtained showed an increasing trend; however, the effect of fiber dosage above 4% on the compressive strength merits further research.

5.2.3 Flexural strength of beams

We tested a total of 9 beams (3 beams from each mix) for the mixes mix I, II, and III. We did not cast beams for the Mix IV considering the lack of availability of materials and time, as mentioned previously.

The first-crack flexural strength is used to indicate the maximum tensile stress for UHPC [97]. For our study, we measured the failure load from the flexural testing machine for three beams from each mix (total 3 mixes), and the average was recorded. The first cracking flexural strength for the recorded load was calculated using Eq.4.2. The flexural strength of the beams calculated in MPa (N/mm^2)) is presented in Table 5.9.

Table 5.9:Flexural strength tested for each

Group	Failure load(KN)	Flexural Strength (MPa)
1	89.85	26.96
2	51.83	15.55
3	62	18.60
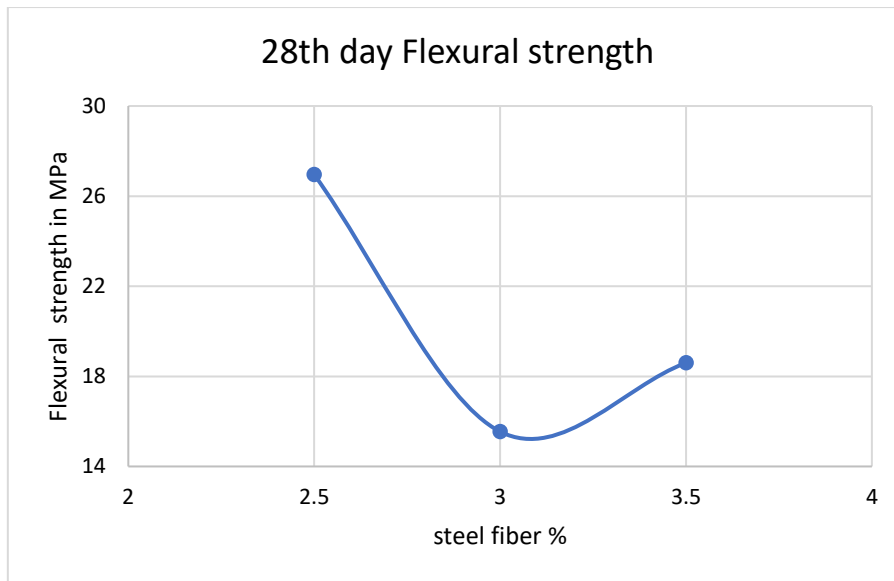
Figure 5.17:Relationship between 28th day flexural strength and steel fiber dosage
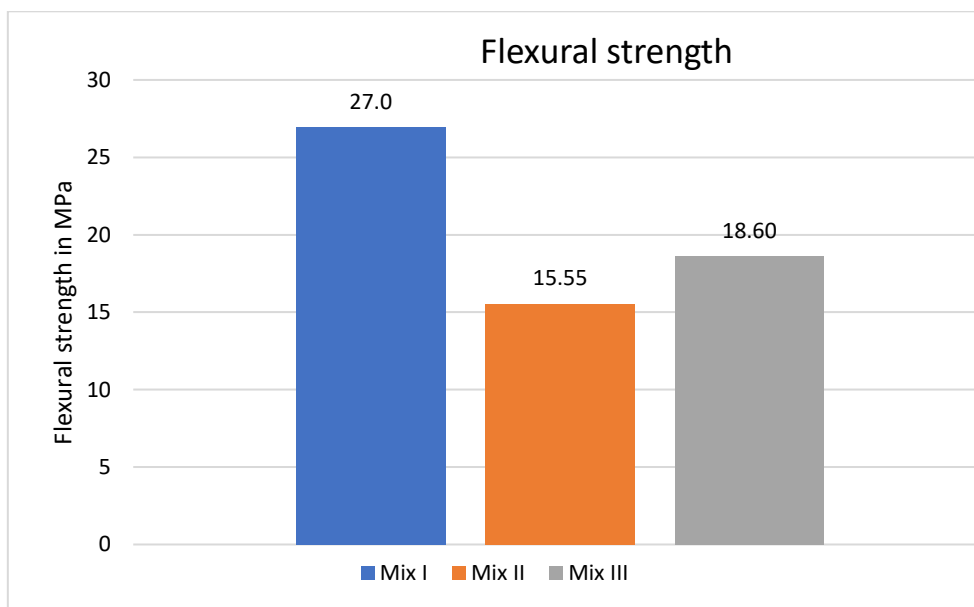
Figure 5.18: Overview of the flexural strength tested for the mixes with varying steel fiber content by volume (Mix I=2.5%, MixII=3%, and Mix III=3.5%)

Figure 5.18 presents an overview of the 28th-day compressive strength tested for the mixes with varying steel fiber content by volume (Mix I=2.5%, Mix II=3%, and Mix III=3.5%). The results show that the first cracking flexural strength is highest for the mix I(containing 2.5% steel fibers), 27 MPa. The flexural strength for mix II (3% fibers) declines to 15.55 MPa and slightly increases to 18.6 MPa for mix III (3.5% fibers). The results obtained are inconsistent with the previous recommendations, as many papers reported an improvement in flexural strength and the addition of more fiber content [10].

The close distribution of fibers can contribute to better bonding between fibers and matrix, and the fibers can also bridge the cracks. Fibers enable the concrete to uphold the structural integrity towards tensile load after the crack initiation by bridging cracks and transferring the load across the crack[10]. The initiation of the crack is highlighted in Figure.5.18 and its post-cracking behavior in Figure 5.19.

Figure 5.19:Initiation of the crack in beam (Mix I with 2.5% steel fibers)

Figure 5.20:Crack propagation (post cracking)

For our study, the first cracking flexural strength calculated for the mix I was 27 MPa, and it was lowered to 15.55 MPa for mix II. However, the flexural strength for mix III was slightly improved to 18.60 MPa (as per Figure 5.17). The fiber agglomeration might explain the reduction in flexural strength for mix II and III for higher fiber contents(>3%). However, the least strength found for mix II can be explained by the improper fiber distribution inside the mix even though we followed similar mixing procedures and strategies throughout the mix. There have been papers that observed that the fiber content did not significantly influence the first cracking flexural strength. The fibers are mainly activated after the first cracking strength is reached. However, some papers identified improved flexural strength and increased fiber volume up to 3%, and a plateau was identified after that [10].

Our results are inconsistent with the previous studies since we obtained the highest first cracking flexural strength for the lowest fiber content (2.5%), where it declined steadily with the 3% fibers (3%) and increased slightly with 3.5% fibers. As we selected the range of steel fiber content from 2.5%-3.5% for our study, it is challenging to draw conclusions on the flexural strength trend, which requires further thorough research with fiber content ranging from 0-to 4%.

The beam's post-cracking behavior (crack propagation) highlighted in Figure 5.21 shows the fibers' bridging effect, according to the crack pattern studied in in Figure 2.16 (chapter 2.6.2).

As per the previous research, the flexural stiffness of the beams before the occurrence of the first crack was not influenced significantly by the presence of steel fibers, while the post-cracking stiffness and peak load were improved considerably by the addition of fibers [113]. Accordingly, our results can be interpreted as we considered only the first-cracking flexural strength. However, an experimental study considering a wider range of fiber content with a major focus on the analysis of the first-crack and post-cracking flexural strength could have provided a more conclusive inference on the effect of fiber content.

6   Conclusions

In this study, the compressive strength of UHPFRC was investigated using Response Surface Method, in which actual experimental results were done on 45 cubes as input data and proposed a statical relationship between the influential parameters and the maximum compressive strength. This study also explored the effects of the higher steel fiber dosage (2.5% to 4% by volume) on the mechanical properties of UHPC through an experimental study done on 33 specimens.

The parameters considered were water to binder ratio(w/b), silica fume content (S_f), and steel fiber dosage (F_v). A statistical model was obtained using RSM results, which provided a good correlation between the parameters and the response. The influence of using higher steel fiber dosage on UHPFRC was also presented in this thesis. The results prove that the fiber addition improved the compressive strength and failure pattern from sudden explosive to ductile behavior. However, the effect of the increase in fiber content in flexural strength seems uncertain and merits further research.

The major conclusions of the study can be summarised as follows.

- The effects of multiple factors on the compressive strength of UHPFRC were investigated using the Response Surface Methodology (RSM) and determined the most significant factors and the influence of multi-factor interaction

- Comparing the results of experiments and RSM in terms of the Fc (max) indicated a negligible difference between the values of the two methods. Results demonstrated that RSM could accurately predict the compressive strength of the specimens.

- The combination of range analysis and variance analysis of factors using the graphs and contour plots found that the response's sensitivity is moderately higher for w/b than Fv and Sf.

- Response surface methodology (RSM) is a valuable tool for developing mathematical models (correlation) that predict the output variable (response) depending on the combinations of parameters level. In addition, it provides the opportunity to investigate the parameters that affect the response as well as demonstrate the relative magnitude and interactions between them. In fact, this technique facilitated optimization and modeling studies on UHPFRC.

- In general, the compressive strength of UHPFRC increased with the increase of fiber dosage and concrete age. But the flowability of UHPC decreased slightly with increased fiber dosage, which could be counteracted with an increased quantity of superplasticizers (SP).

- An additional parametric study should be conducted to generalize the results by expanding the range of parameters, for instance, including UHPFRC without fibers until those with higher dosages.

7 Future work

The experimental and modeling study conducted in connection with this thesis confirms the benefits of applying the Response Surface methodology in developing statistical models for optimization and prediction in cement and concrete, which can reduce the time and effort of research. However, the study can be continued by varying the levels and range of the parameters, especially w/b, being the most significant parameter, to arrive at a more reliable conclusion. The range and level chosen in the study were close to the recommended range, and it would be interesting to increase the intervals of the levels and see the effects.

The experimental results on the flexural capacity of beams showed a decreasing trend in the gain of flexural strength for the specimens with 3% fiber and thereafter increased by 3.5%. These results need to be examined experimentally more deeply in the future.

Furthermore, we could not perform the experiments replacing the cement content with fly ash or slag considering the time and availability of materials. There is a scope of future work, with the application of RSM, considering fly ash content as one of the parameters can analyze whether the mechanical properties can be maintained the same as with that using cement and how the emissions can be minimized by appropriately replacing cement with the SCMs, so as to attain a greener UHPC without compromising its superior mechanical properties. This can be highly relevant research as the world is looking forward to sustainable solutions in the construction industry to reduce emissions.

Therefore, it is recommended to continue the research into this choice which can potentially improve the use of UHPFRC and the application of RSM to be more accepted in many different construction applications.

8 References

1.	*Re discover concrete*. Available from: http://rediscoverconcrete.com/en/sustainability/a-better-building-material/concrete-innovations-en.html.
2.	manufacturer, P.-A.s.c. *How Concrete is made*. Available from: https://www.cement.org/cement-concrete/how-concrete-is-made.
3.	Ben Guida, D., *CO2 reduction from cement industry: Proceedings of the 2nd International Conference of Advanced Materials, Mechanical and Structural Engineering (AMMSE 2015), Je-ju Island, South Korea, September 18-20, 2015*. 2016. p. 127-130.
4.	*Rediscover Concrete*.
5.	Du, J., et al., *New development of ultra-high-performance concrete (UHPC).* Composites Part B: Engineering, 2021. **224**: p. 109220.
6.	Akhnoukh, A.K. and C. Buckhalter, *Ultra-high-performance concrete: Constituents, mechanical properties, applications and current challenges.* Case Studies in Construction Materials, 2021. **15**: p. e00559.
7.	Camões, I.F.a.C., *Eco-efficient ultra-high performance concrete development by means of response surface methodology.* Cement and Concrete Composites, 2017. **84**.
8.	Hisdal, M.B.E.a.J.-M., *Ultra High-Performance Fibre Reinforced Concrete (UHPFRC)– State of the art* SINTEF Building and Infrastructure-COIN Project report 44-2012, 2012.
9.	Ghafari, E., H. Costa, and E. Júlio, *RSM-based model to predict the performance of self-compacting UHPC reinforced with hybrid steel micro-fibers.* Construction and Building Materials, 2014. **66**: p. 375-383.
10.	Larsen, I.L. and R.T. Thorstensen, *The influence of steel fibres on compressive and tensile strength of ultra high performance concrete: A review.* Construction and Building Materials, 2020. **256**: p. 119459.
11.	Standard, N., *NS-EN 12390-5:2019*. 2019: Norway.
12.	Standard, N., *NS-EN 12390-3:2019; European standard for testing of hardened concrete* 2019.
13.	Bajaber, M.A. and I.Y. Hakeem, *UHPC evolution, development, and utilization in construction: a review.* Journal of Materials Research and Technology, 2021. **10**: p. 1058-1074.
14.	Chen, Y., et al., *Study on the mechanical and rheological properties of ultra-high performance concrete.* Journal of Materials Research and Technology, 2022. **17**: p. 111-124.
15.	Luo, Q., et al., *Improving flexural strength of UHPC with sustainably synthesized graphene oxide.* Nanotechnology Reviews, 2021. **10**(1): p. 754-767.
16.	Hoang, A.L., *Evaluation of the Splitting Tensile Strength of Ultra-High Performance Concrete*. Fibre Reinforced Concrete: Improvements and Innovations. 2021.
17.	Aziz, O. and G. Ahmed, *Mechanical Properties of Ultra High Performance Concrete (UHPC)*. Vol. ACI SP 289. 2012. 1-16.
18.	Safeer Abbas, M.L.N., and M. A. Saleem, *Ultra-High Performance Concrete: Mechanical Performance, Durability, Sustainability and Implementation Challenges.* International Journal of Concrete Structures and Materials, 2016. **10.1007/s40069-016-0157-4**.
19.	Lopez Gayarre, F., et al., *2 - Waste for aggregates in ultrahigh performance concrete (UHPC)*, in *Waste and Byproducts in Cement-Based Materials*, J. de Brito, et al., Editors. 2021, Woodhead Publishing. p. 29-51.
20.	Wang, C., et al., *Preparation of Ultra-High Performance Concrete with common technology and materials.* Cement and Concrete Composites, 2012. **34**(4): p. 538-544.
21.	Aïtcin, P.C., *1 - The importance of the water–cement and water–binder ratios*, in *Science and Technology of Concrete Admixtures*, P.-C. Aïtcin and R.J. Flatt, Editors. 2016, Woodhead Publishing. p. 3-13.

22. http://www.buildingresearch.com.np/newfeatures.php, *superplasticizers or high range water reducers*.

23. Xue, J., et al., *Review of ultra-high performance concrete and its application in bridge engineering.* Construction and Building Materials, 2020. **260**: p. 119844.

24. El Helou, R. and B. Graybeal, *The Ultra Girder: A Design Concept for a 300-foot Single Span Prestressed UHPC Bridge Girder*. 2019.

25. SELÇUK MEMİŞ, A.A.R., Department of Materials Science and Engineering, Institute of Science, Kastamonu University,Kastamonu, Turkey, *INVESTIGATION OF THE IDEAL MIXING RATIO AND STEEL FIBER ADDITIVE IN ULTRA HIGH PERFORMANCE CONCRETE (UHPC).* Romanian Journal of Materials 2020, 2020. **50**(3): p. 403 - 410.

26. Valcuende, M., et al., *Corrosion resistance of ultra-high performance fibre- reinforced concrete.* Construction and Building Materials, 2021. **306**: p. 124914.

27. Wu, C., J. Li, and Y. Su, *1 - Introduction*, in *Development of Ultra-High Performance Concrete Against Blasts*, C. Wu, J. Li, and Y. Su, Editors. 2018, Woodhead Publishing. p. 1-21.

28. Chengquing Wu, J.L.a.Y.S., *Development of Ultra-High Performance Concrete*. 2018: Woodhead publishing.

29. Ding, M., et al., *Possibility and advantages of producing an ultra-high performance concrete (UHPC) with ultra-low cement content.* Construction and Building Materials, 2021. **273**: p. 122023.

30. Burroughs, J.F., et al., *Potential of finely ground limestone powder to benefit ultra-high performance concrete mixtures.* Construction and Building Materials, 2017. **141**: p. 335-342.

31. Shi, C., et al., *A review on ultra high performance concrete: Part I. Raw materials and mixture design.* Construction and Building Materials, 2015. **101**: p. 741-751.

32. Habert, G., et al., *Lowering the global warming impact of bridge rehabilitations by using Ultra High Performance Fibre Reinforced Concretes.* Cement and Concrete Composites, 2013. **38**: p. 1-11.

33. Sohail, M.G., et al., *Durability characteristics of high and ultra-high performance concretes.* Journal of Building Engineering, 2021. **33**: p. 101669.

34. Technology, F.H.A.R.a., *Ultra-High Performance Concrete: A State-Of-The-Art Report for The Bridge Community*

CHAPTER 5. DURABILITY AND DURABILITY TESTING. 2013.

35. Mishra, S. and R. Mistry, *Reviewing Some Properties of Ultra High Performance Concrete.* International Journal of Engineering Research and, 2020. **9**.

36. Normalisation, A.F.d.,

NFP 18 470 : 2016, in *CONCRETE - ULTRA-HIGH PERFORMANCE FIBRE-REINFORCED CONCRETE - SPECIFICATIONS, PERFORMANCE, PRODUCTION AND CONFORMITY*. 2016.

37. Normalisation, A.F.d., *NFP 18-710*, in *National addition to Eurocode 2 — Design of concrete structures: specific rules for Ultra-High Performance Fibre-Reinforced Concrete (UHPFRC)*. 2016.

38. Normalisation, A.F.d., *NF P18-451*, in *Concrete - Execution of concrete structures - Specific rules for UHPRFC*. 2018.

39. Institute, A.C., *Ultra-High-Performance Concrete: An Emerging Technology Report-ACI 239R-18*, in *Emerging Technology Series*. 2018.

40. (ACI), A.C.I., *Guide for Specifying, Proportioning, Mixing,Placing, and Finishing Steel Fiber Reinforced Concrete*. 1998.

41. International, A., *ASTM C1856/C1856M-17 Standard Practice for Fabricating and Testing Specimens of Ultra-High Performance Concrete*. 2017.

42. George Quercia([Director of Research, T.L., PhD Kevin Gannon, RA ([Director of Program Development, TAKTL LLC], *Classification + Reference Standards for UHPC in Architectural Applications*

43. Imam, A., et al., *A review study on sustainable development of ultra high-performance concrete.* AIMS Materials Science, 2022. **9**(1): p. 9-35.

44. Yang, R., et al., *Low carbon design of an Ultra-High Performance Concrete (UHPC) incorporating phosphorous slag.* Journal of Cleaner Production, 2019. **240**: p. 118157.

45. Randl, N., et al., *Development of UHPC mixtures from an ecological point of view.* Construction and Building Materials, 2014. **67**: p. 373-378.

46. UK, G., *Green building design & products for sustainable construction UK*. 2020.

47. brief, C.H.C. *How cement is made*. 2018.

48. Norway, N.-C.m.i. *Cement productions and emissions*.

49. House, C., *Innovation in low carbon cement and concrete*.

50. Chen, Y., et al., *Ultra-High-Performance Concrete: Development of On-Site Fresh Mix Rheology Test Methods.* 2019. **55**: p. 1-11.

51. Assocation, N.R.M.C. *CO2 released during cement production graph from 1920 till 2020*. 2017.

52. Mindess, S., *1 - Sustainability of concrete*, in *Developments in the Formulation and Reinforcement of Concrete (Second Edition)*, S. Mindess, Editor. 2019, Woodhead Publishing. p. 3-17.

53. Ahmed, T., et al., *Development of ECO-UHPC with very-low-C3A cement and ground granulated blast-furnace slag.* Construction and Building Materials, 2021. **284**: p. 122787.

54. S, F.H.A.U., *Fly ash as a an engineering material*.

55. Giergiczny, Z., *Fly ash and slag.* Cement and Concrete Research, 2019. **124**: p. 105826.

56. Yuksel, I., *12 - Blast-furnace slag*, in *Waste and Supplementary Cementitious Materials in Concrete*, R. Siddique and P. Cachim, Editors. 2018, Woodhead Publishing. p. 361-415.

57. Administration, U.S.D.F.H., *Blast furnace slag*.

58. centre, T.C., *Sustianable Developemnt Report 2020 of MPA*, U.Q.A.A.a.C.S.M. Association, Editor. 2020: United Kingdom.

59. Park, S., et al., *The Role of Supplementary Cementitious Materials (SCMs) in Ultra High Performance Concrete (UHPC): A Review.* Materials (Basel, Switzerland), 2021. **14**(6): p. 1472.

60. Dehghanpour, H., et al., *Investigation of fracture mechanics, physical and dynamic properties of UHPCs containing PVA, glass and steel fibers.* Construction and Building Materials, 2022. **328**: p. 127079.

61. Nieuwoudt, P.D. and W.P. Boshoff, *Time-dependent pull-out behaviour of hooked-end steel fibres in concrete.* Cement and Concrete Composites, 2017. **79**: p. 133-147.

62. Tsai, J.H., A. Patra, and R. Wetherhold, *Finite element simulation of shaped ductile fiber pullout using a mixed cohesive zone/friction interface model.* Composites Part A: Applied Science and Manufacturing, 2005. **36**(6): p. 827-838.

63. Haidar Hosamo, P.S., *Experimental and finite element analysis of the shear behaviour of UHPC beams*. 2019, University Of Agder.

64. SINTEF, *COIN-Concrete workability and fibre content -State of the art* 2007: Trondheim,Norway.

65. Rees3, S.A.M.F.a.D.W.A., *Bonding Mechanisms and Strength of Steel Fiber–Reinforced Cementitious Composites: Overview.* Journal of Materials in Civil Engineering 2018. **30**(3).

66. Deng, Y., et al., *Steel fiber–matrix interfacial bond in ultra-high performance concrete: A review.* Engineering, 2022.

67. Abdallah, S., M. Fan, and X. Zhou, *Pull-Out Behaviour of Hooked End Steel Fibres Embedded in Ultra-high Performance Mortar with Various W/B Ratios.* International Journal of Concrete Structures and Materials, 2017. **11**(2): p. 301-313.

68. Zhou, A., et al., *Interfacial technology for enhancement in steel fiber reinforced cementitious composite from nano to macroscale.* Nanotechnology Reviews, 2021. **10**(1): p. 636-652.

69.   Panzera, T.H., A.L. Christoforo, and P.H. Ribeiro Borges, *15 - High performance fibre-reinforced concrete (FRC) for civil engineering applications*, in *Advanced Fibre-Reinforced Polymer (FRP) Composites for Structural Applications*, J. Bai, Editor. 2013, Woodhead Publishing. p. 552-581.

70.   Elma Akter, M.S.S.o.C.E.a.A.U.o.S.a.T.J., Changhui Road, Dantu District, Zhenjiang, Jiangsu, China and P.A. from:, *Study of fibers application in construction materials.* American Concrete Institute(ACI), 2022.

71.   Labib, W.L., *Fibre Reinforced Cement Composites*. 2018.

72.   Micelli, F., et al., *7 - Fiber-reinforced concrete and ultrahigh-performance fiber-reinforced concrete materials*, in *New Materials in Civil Engineering*, P. Samui, et al., Editors. 2020, Butterworth-Heinemann. p. 273-314.

73.   Jiju Antony, H.-w.U., Edinburgh,Scotland,UK, *Design of Experiments for Engineers and Scientists*. Vol. II. 2014: Elsevier.

74.   Benjamin Durakovic, I.U.o.S., *Design of Experiments Application, Concepts, Examples:*

State of the Art. Periodicals of Engineering and Natural Sciences, 2017. **5**.

75.   Omar, W.N.N.W. *Design Of Experiment (DOE)& Response Surface Methodology (RSM)*. Academia, 2015.

76.   Jankovic, A., G. Chaudhary, and F. Goia, *Designing the design of experiments (DOE) – An investigation on the influence of different factorial designs on the characterization of complex systems.* Energy and Buildings, 2021. **250**: p. 111298.

77.   Nassiri Mahallati, M., *Chapter 9 - Advances in modeling saffron growth and development at different scales*, in *Saffron*, A. Koocheki and M. Khajeh-Hosseini, Editors. 2020, Woodhead Publishing. p. 139-167.

78.   Minitab, *Minitab18 support*, in *What are response surface designs, central composite designs, and Box-Behnken designs?*

79.   Şimşek, B., Y.T. İç, and E.H. Şimşek, *A RSM-Based Multi-Response Optimization Application for Determining Optimal Mix Proportions of Standard Ready-Mixed Concrete.* Arabian Journal for Science and Engineering, 2016. **41**(4): p. 1435-1450.

80.   Aziminezhad, M., M. Mahdikhani, and M.M. Memarpour, *RSM-based modeling and optimization of self-consolidating mortar to predict acceptable ranges of rheological properties.* Construction and Building Materials, 2018. **189**: p. 1200-1213.

81.   Ait-Amir, B., P. Pougnet, and A. El Hami, *6 - Meta-Model Development*, in *Embedded Mechatronic Systems 2*, A. El Hami and P. Pougnet, Editors. 2015, Elsevier. p. 151-179.

82.   Bypour, M., M. Kioumarsi, and M. Yekrangnia, *Shear capacity prediction of stiffened steel plate shear walls (SSPSW) with openings using response surface method.* Engineering Structures, 2021. **226**: p. 111340.

83.   Soto-Pérez, L., V. López, and S.S. Hwang, *Response Surface Methodology to optimize the cement paste mix design: Time-dependent contribution of fly ash and nano-iron oxide as admixtures.* Materials & Design, 2015. **86**: p. 22-29.

84.   Ferdosian, I. and A. Camões, *Eco-efficient ultra-high performance concrete development by means of response surface methodology.* Cement and Concrete Composites, 2017. **84**: p. 146-156.

85.   Zahid, M., et al., *Statistical modeling and mix design optimization of fly ash based engineered geopolymer composite using response surface methodology.* Journal of Cleaner Production, 2018. **194**: p. 483-498.

86.   Yu Sun, R.Y., Zhonghe Shui, *Understanding the porous aggregates carrier effect on reducing autogenous shrinkage of Ultra-High Performance Concrete (UHPC) based on response surface method.* Construction and Building Materials 222(7):130-141, 2019. **222**.

87.   Awolusi, T.F., et al., *Application of response surface methodology: Predicting and optimizing the properties of concrete containing steel fibre extracted from waste tires with limestone powder as filler.* Case Studies in Construction Materials, 2019. **10**: p. e00212.

88.   Hou, D., et al., *RSM-based modelling and optimization of magnesium phosphate cement-based rapid-repair materials.* Construction and Building Materials, 2020. **263**: p. 120190.

89.   Hooshmandi, S., et al., *Application of response surface method (RSM) on sensitivity analysis of reinforced concrete bridge pier wall*. 2017.

90.   Baghban, M.H., M. Kioumarsi, and S. Grammatikos, *Prediction models for thermal conductivity of cement-based composites.* Nordic Concrete Research, 2018. **58**(1): p. 163-171.

91.   Jacques Resplendino (1), F.T., *THE UHPFRC REVOLUTION IN STRUCTURAL DESIGN AND CONSTRUCTION.* THE UHPFRC REVOLUTION IN STRUCTURAL DESIGN ANDCONSTRUCTION, October 1-3, 2013, Marseille, France, 2013.

92.   Pourbaba, M., et al., *Effect of age on the compressive strength of ultra-high-performance fiber-reinforced concrete.* Construction and Building Materials, 2018. **175**: p. 402-410.

93.   Resplendino, F.T.a.J., *Designing and building with UHPFRC- State of the art and development*. 2009: Wiley.

94.   SINTEF, *Ultra High Performance Fibre Reinforced Concrete (UHPFRC) – State of the ar*, in *SINTEF Building and Infrastructure*, M.B.E.a.J.-M. Hisdal, Editor. 2012.

95.   Abbas, S. and M.L. Nehdi, *Mechanical Behavior of Ultrahigh-Performance Concrete Tunnel Lining Segments.* Materials (Basel, Switzerland), 2021. **14**(9): p. 2378.

96.   Abbas, S., A.M. Soliman, and M.L. Nehdi, *Exploring mechanical and durability properties of ultra-high performance concrete incorporating various steel fiber lengths and dosages.* Construction and Building Materials, 2015. **75**: p. 429-441.

97.   El-Din, H., et al., *Effect of Steel Fibers on Behavior of Ultra High Performance Concrete*. 2016.

98.   Breig, S.J.M. and K.J.K. Luti, *Response surface methodology: A review on its applications and challenges in microbial cultures.* Materials Today: Proceedings, 2021. **42**: p. 2277-2284.

99.   Li, K., et al., *Raw material ratio optimisation of magnesium oxychloride cement using response surface method.* Construction and Building Materials, 2021. **272**: p. 121648.

100.   Omar, S.j.a.A., *UHPC recipe* 2022, Oslomet.

101.   Bekaert, *EC Declaration of PerformanceDRAMIX® OL 13/.20*. NV BEKAERT SA Bekaertstraat 2, B-8550 Zwevegem, Belgium.

102.   Sherif El-Tawil, Y.-S.T.J.A.B., II and R. Dewayne, *Open-Recipe Ultra-High-Performance Concrete.* Concrete International. **42**(6).

103.   www.gz-supplies.com/digital-electronic-weighing-scale-a-12-300kg/. *weighing scale for cement*.

104.   https://www.scientificglassservices.co.uk/scientific-glass-benefits-vs-plastic/. glass beakers and test tubes.

105.   Jaya, R.P., *14 - Porous concrete pavement containing nanosilica from black rice husk ash*, in *New Materials in Civil Engineering*, P. Samui, et al., Editors. 2020, Butterworth-Heinemann. p. 493-527.

106.   forum, C.E., *FLEXURAL STRENGTH OF CONCRETE*. 2019.

107.   Kioumarsi, M.M., M. Hendriks, and M.R. Geiker, *Quantification of the interference of localised corrosion on adjacent reinforcement bars in a concrete beam in bending.* Nordic Concrete Research (NCR), 2014. **49**: p. 39-57.

108.   Zhang, X. and H. Zhang, *Experimental Research on Ultra-High Performance Concrete (UHPC).* IOP Conference Series: Materials Science and Engineering, 2019. **562**: p. 012045.

109.   Kazemi, S. and A. Lubell, *Influence of Specimen Size and Fiber Content on Mechanical Properties of Ultra-High-Performance Fiber-Reinforced Concrete.* Aci Materials Journal, 2012. **109**: p. 675-684.

110.   Shihada, S. and M. Arafa, *Effects of silica fume, ultrafine and mixing sequences on properties of ultra high performance concrete.* Asian Journal of Materials Science, 2010. **2**(3).

111.   Sun, Z., et al., *Optimization design of ultrahigh-performance concrete based on interaction analysis of multiple factors.* Case Studies in Construction Materials, 2022. **16**: p. e00858.

112. Wu, Z., et al., *Static and dynamic compressive properties of ultra-high performance concrete (UHPC) with hybrid steel fiber reinforcements.* Cement and Concrete Composites, 2017. **79**: p. 148-157.

113. Yoo, D.-Y. and Y.-S. Yoon, *Structural performance of ultra-high-performance concrete beams with different steel fibers.* Engineering Structures, 2015. **102**: p. 409-423.